DISSERTATION

WILDFIRE-WATER SUPPLY RISK IN MONTANE WATERSHEDS OF COLORADO: BASELINE ASSESSMENT AND EVALUATION OF MITIGATION STRATEGIES

Submitted by

Benjamin Michael Gannon

Department of Forest and Rangeland Stewardship

In partial fulfillment of the requirements

For the Degree of Doctor of Philosophy

Colorado State University

Fort Collins, Colorado

Fall 2020

Doctoral Committee:

Advisor: Yu Wei
Co-Advisor: Antony Cheng

Stephanie Kampf
Matthew Thompson

ABSTRACT

WILDFIRE-WATER SUPPLY RISK IN MONTANE WATERSHEDS OF COLORADO: BASELINE ASSESSMENT AND EVALUATION OF MITIGATION STRATEGIES

This is a multi-part dissertation examining wildfire-water supply risks and the mitigation effectiveness of land and fire management solutions. Chapters 2, 3, and 4 were prepared independently for publication elsewhere. Chapters 1 and 6 provide brief bookends to discuss the motivations for this research and conclusions drawn from the three independent but related research chapters. Chapter 5 discusses common limitations of the risk models used in the research chapters and opportunities for improvement.

(CHAPTER 2) In fire-prone watersheds, concern over wildfire impacts to water supplies has motivated efforts to mitigate risk by reducing forest fuels. Methods to assess fuel treatment effects and prioritize their placement are needed to inform risk mitigation. We introduce a fuel treatment optimization model to minimize risk to multiple water supplies based on constraints for treatment feasibility and cost. We quantify risk as the expected sediment impact costs to water supplies by combining measures of fire likelihood and behavior, erosion, sediment transport, and water supply vulnerability. We demonstrate the prioritization framework on two watersheds in the Colorado Front Range. Our results suggest wildfire risk to water supplies can be meaningfully reduced by treating dense, fire-prone forests on steep slopes near water supplies. However, we found that the cost of fuel treatment outweighs the expected cost savings from reduced sediment by a considerable margin due to the high cost of thinning forests and the low expected fuel treatment-wildfire encounter rate. This highlights the importance of expanding the

use of more cost-effective treatments, like prescribed fire, and identifying fuel treatment projects that benefit multiple resources.

(CHAPTER 3) Water supply impairment from increased contaminant mobilization and transport after wildfire is a major concern for communities that rely on surface water from fire prone watersheds. We introduce a Monte Carlo simulation method to quantify the likelihood of wildfire impairing water supplies beyond limits for treatment by combining stochastic representations of annual wildfire and rainfall activity. Water quality impairment is evaluated in terms of turbidity limits for treatment by modeling wildfire burn severity, post-fire erosion, sediment transport, and suspended sediment dilution in receiving waterbodies. Water supply disruption is analyzed at the system level based on the impairment status of water supply components and their contributions to system performance. We use this approach to assess wildfire-water supply impairment and disruption risks for a system of water supply reservoirs and diversions in the Front Range Mountains of Colorado, USA. Our results show that wildfire may impair water quality in a concerning 15.7-19.4% of years for diversions from large watersheds. Reservoir impairment should be extremely rare for large, off network reservoirs (at most 0.01% of years) but occur in as many as 2.8% of years for smaller, on network reservoirs. System redundancy meaningfully reduced disruption risk for alternative conveyance routes (4.3-25.0% reduction) and almost eliminated disruption risk for a pair of substitutable terminal sources (99.9% reduction), whereas dependency among conveyance reservoirs nearly doubles risk of conveyance disruption. Our results highlight the importance of considering water system characteristics when evaluating wildfire-water supply risks.

(CHAPTER 4) In many fire-prone watersheds, wildfire threatens surface water drinking supplies with post-fire contaminant mobilization and transport. We evaluated the potential to

mitigate this risk by limiting fire sizes and watershed effects with a containment network of manager-developed Potential fire Operational Delineations (PODs) using wildfire risk transmission methods to partition the effects of many stochastically simulated wildfires to within and out of POD burning. We assessed water supply impacts with two metrics – total sediment load and water quality impairment above suspended sediment concentrations for treatment – using a linked fire-erosion-sediment transport model. Our results suggest that improved fire containment could substantially reduce wildfire risk by 13.0 to 55.3% depending on impact measure and post-fire rainfall. Containment based on the manager-developed PODs had greater potential in our study system to reduce total sediment load than it did to avoid water quality impairment because fires within many of the larger PODs resulted in impairment even when contained. Much of the residual impairment risk after containment originated from less than 20% of the PODs, suggesting strategic investments to further compartmentalize these areas of the landscape could improve the effectiveness of the containment network. Similarly, risk transmission occurred most frequently across control features in certain parts of the network, indicating that efforts to increase containment probability with fuels reduction would have a disproportionate effect if prioritized in these areas.

ACKNOWLEDGEMENTS

I would like to thank all who supported me in my graduate studies. I am especially grateful to my advisor, Yu Wei, for encouraging me to pursue a PhD alongside my professional work and to my work supervisor and co-advisor, Tony Cheng, for allowing me flexibility in my work schedule to fulfill the coursework requirements. I am also in debt of my committee members, Stephanie Kampf and Matt Thompson, for providing subject area guidance and for integrating me into their scientific communities. A special thanks is also due to Lee MacDonald for the substantial mentorship he provided on watershed science and writing. I would also like to thank my parents and extended family members for all the support they provided that set me on a track of academic success. I am also grateful for the various forms of support that funders and managers provided to my professional work that inspired the content of this dissertation. I also owe thanks to Karen Short and Joe Scott for sharing the fire modeling results used in Chapter 3 and for providing critique of the chapter.

TABLE OF CONTENTS

LIST OF TABLES

LIST OF FIGURES

CHAPTER 1 – PROBLEM STATEMENT AND FRAMING

Growing awareness of wildfire threats to drinking water supplies (Bladon et al. 2014; Martin 2016; Hallema et al. 2019) has spurred efforts to quantify wildfire-water supply risks and evaluate the effectiveness of mitigating actions. At global and regional scales, coarse measures of wildfire activity, watershed response, and water utilization have been combined to map relative measures of risk (Thompson et al. 2013; Robinne et al. 2018, 2019) that are well-suited for high-level policy making and planning. To better quantify water supply risks for local decision-making, linked wildfire and watershed models are increasing used to characterize post-fire hazards to water supplies such as sediment load from hillslope erosion or debris flow (Miller et al. 2011; Buckley et al. 2014; Tillery et al. 2014; Elliot et al. 2016; Sidman et al. 2016; Jones et al. 2017; Sankey et al. 2017). Much of this work has been motivated by payment for ecosystem service programs that seek to monetize the benefit of proactively mitigating risk by reducing fuels in source watersheds, and thus there has been a strong emphasis on modeling the easily valued impacts of reservoir sedimentation (Buckley et al. 2014; Elliot et al. 2016; Jones et al. 2017). Despite the considerable advancements in physical modeling, little is known about wildfire risk to whole source water collection systems, which may consist of multiple storage, conveyance, and diversion infrastructure that vary in their sensitivity to post-fire impacts and their contribution to system performance. Yet the details of how wildfire affects water supplies are critical to defining a community's level of risk, identifying potential mitigation measures, and evaluating mitigation effects on source water reliability.

Wildfire impacts to water supplies can include water quality impairment, reservoir sedimentation, sediment or debris blockage of conveyance or diversion structures, flooding,

restricted access to equipment, and lost power or communication for control systems (Sham et al. 2013; Martin 2016; Hallema et al. 2019). Previous wildfires in Colorado suggest the major impacts in this region are reservoir sedimentation (Moody and Martin 2001) and water quality degradation for brief periods following intense rainfall (Oropeza and Heath 2013; Murphy et al. 2015). Debris flow and channel erosion have also damaged diversion inlets and conveyance pipelines (Gibbens et al. 2013; Howell 2014). Hence, a major focus of pre- and post-fire hazard assessment is characterizing potential erosion magnitudes with models that incorporate environmental drivers like topography, soils, vegetation, and rainfall (Cannon et al. 2010; Miller et al. 2011, 2016; Tillery et al. 2014; Elliot et al. 2016; Sidman et al. 2016). Given the diversity of water supply assets and their varying level of susceptibility to post-fire watershed response, some assessments have focused only on characterizing hazards (Miller et al. 2011; Sankey et al. 2017), while others have used coarse measures of water supply importance or population served to infer water supply exposure and impacts (Thompson et al. 2013; Robinne et al. 2019). Efforts to relate post-fire hazards to water management costs have focused primarily on reservoir sedimentation (Buckley et al. 2014; Elliot et al. 2016; Jones et al. 2017). Reservoir storage is important for source water reliability in variable precipitation systems, but reduced storage capacity from post-fire sedimentation does not typically threaten short-term water supply. There is recognized need to improve modeling of post-fire contaminant mobilization, transport, and impacts on water quality to better characterize the risk of source water impairment that threatens to disrupt drinking water supplies in the immediate aftermath and period of recovery from wildfire (Sham et al. 2013; Nunes et al. 2018).

A variety of strategies have been proposed to mitigate wildfire risks to water supplies including reducing fuels in source watersheds, adding source redundancies, improving fire

containment, constructing sediment basins to protect sensitive infrastructure, improving the efficiency of post-fire rehabilitation, and optimizing operations with real-time water quality monitoring (Sham et al. 2013; Buckley et al. 2014; Martin 2016; Haas et al. 2017; Hallema et al. 2019). Proactively reducing fuels has received the most quantitative evaluation; several studies have linked wildfire and watershed models to show that reducing fuels should meaningfully lower erosion when treated areas burn (Buckley et al. 2014; Sidman et al. 2016; Jones et al. 2017). Source water redundancy has been advocated for as a means to mitigate the risk of water supply disruption (Sham et al. 2013; Martin 2016), but there has been limited exploration of how to assess risk to multi-source systems and value the benefits of redundancy. The recognition that most wildfire risk to water supplies is associated with rare but large wildfires implies that improved fire containment could reduce risks, but the effectiveness of this strategy has not been rigorously analyzed. Recent advances in Monte Carlo-based wildfire risk assessment (Thompson et al. 2016; Haas et al. 2017) provide a framework to characterize spatial and temporal variability in fire activity and watershed response that is needed to evaluate mitigation strategies that focus on fire extent and system redundancy. The remaining critical improvement in risk models to objectively evaluate green and grey infrastructure solutions is better characterization of infrastructure sensitivity to disturbance and importance for system function.

The focus of this dissertation is advancing quantitative frameworks for assessing wildfire-water supply risks and risk mitigation strategies. Chapter 2 develops a wildfire-water supply risk assessment model based on sediment impacts and applies it to three interconnected community water systems in Northern Colorado to assess baseline risk. A linear optimization model is then introduced to prioritize treatment location and type to maximize risk reduction accounting for treatment feasibility and cost constraints. Chapter 3 adapts the effects model

introduced in the second chapter to examine water quality impairment and system disruption risks using Monte Carlo simulation of annual wildfire and rainfall activity. A systems framework is used to examine the effects of redundancy and dependency on source water reliability in a multi-source water system. Chapter 4 evaluates the potential for improved fire containment to mitigate water quality impairment risk for a drinking water diversion from a large watershed in Colorado using a risk transmission framework. Risk is characterized with two effects measures – total sediment mass and whether water quality thresholds for treatment are exceeded – to illustrate how considering scale dependent effects changes mitigation value and priorities. Chapters 2, 3, and 4 were written for publishing elsewhere, so they are presented as independent papers with their own introductions, methods, results, and discussions. The risk assessment models introduced in chapters 2 through 4 have data, model, and model linkage uncertainties that are important to consider when interpreting the results. Chapter 5 reviews the model assumptions, uncertainties, and limitations and suggests research directions that could improve future models. The final chapter offers concluding remarks about wildfire-water supply risks and mitigation strategies.

REFERENCES FOR CHAPTER 1

Bladon KD, Emelko MB, Silins U, Stone M (2014) Wildfire and the future of water supply. *Environmental Science & Technology* **48**, 8936-8943. doi:10.1021/es500130g

Buckley M, Beck N, Bowden P, Miller ME, Hill B, Luce C, Elliot WJ, Enstice N, Podolak K, Winford E, Smith SL, Bokach M, Reichert M, Edelson D, Gaither J (2014) Mokelumne watershed avoided cost analysis: why Sierra fuel treatments make economic sense. A report prepared for the Sierra Nevada Conservancy, The Nature Conservancy, and USDA Forest Service. Sierra Nevada Conservancy. 294 p. (Auburn, CA, USA)

Cannon SH, Gartner JE, Rupert MG, Michael JA, Rea AH, Parrett C (2010) Predicting the probability and volume of post-wildfire debris flows in the intermountain western United States. *Geological Society of America Bulletin* **122**, 127-144. doi:10.1130/B26459.1

Elliot WJ, Miller ME, Enstice N (2016) Targeting forest management through fire and erosion modelling. *International Journal of Wildland Fire* **25**, 876-887. doi:10.1071/WF15007

Gibbens G, Johnson A, Piehl B (2013) Wildfires and forest health – Colorado-Big Thompson Project. Northern Water Conservancy White Paper. 18 p. (Berthoud, CO, USA)

Haas JR, Thompson M, Tillery A, Scott JH (2017) Capturing spatiotemporal variation in wildfires for improving post-wildfire debris-flow hazard assessments. In 'Natural hazard uncertainty assessment: modeling and decision support, geophysical monograph 223'. (Eds K Riley, P Webley, M Thompson) pp. 301-317. (John Wiley & Sons: Hoboken, NJ, USA)

Hallema DW, Kinoshita AM, Martin DA, Robinne F-N, Galleguillos M, McNulty SG, Sun G, Singh KK, Mordecai RS, Moore PF (2019) Fire, forests and city water supplies. *Unasylva 251* **70**, 58-66.

Howell E (2014) Lessons from the Waldo Canyon Fire. Presentation to the Watershed Wildfire Protection Group. Available from https://csfs.colostate.edu/media/sites/22/2014/12/wwpg-Howell-5-9-14.pdf

Jones KW, Cannon JB, Saavedra FA, Kampf SK, Addington RN, Cheng AS, MacDonald LH, Wilson C, Wolk B (2017) Return on investment from fuel treatments to reduce severe wildfire and erosion in a watershed investment program in Colorado. *Journal of Environmental Management* **198**, 66-77. doi:10.1016/j.jenvman.2017.05.023

Martin DA (2016) At the nexus of fire, water and society. Philosophical Transactions of the Royal Society of London. Series B, *Biological Sciences* **371**, 20150172. doi:10.1098/rstb.2015.0172

Miller ME, MacDonald LH, Robichaud PR, Elliot WJ (2011) Predicting post-fire hillslope erosion in forest lands of the western United States. *International Journal of Wildland Fire* **20**, 982-999. doi:10.1071/WF09142

Miller ME, Elliot WJ, Billmire M, Robichaud PR, Endsley KA (2016) Rapid-response tools and datasets for post-fire remediation: linking remote sensing and process-based hydrological models. *International Journal of Wildland Fire* **25**, 1061-1073. doi:10.1071/WF15162

Moody JA, Martin DA (2001) Initial hydrologic and geomorphic response following a wildfire in the Colorado Front Range. *Earth Surface Processes and Landforms* **26**, 1049-1070. doi:10.1002/esp.253

Murphy SF, Writer JH, McCleskey RB, Martin DA (2015) The role of precipitation type, intensity, and spatial distribution in source water quality after wildfire. *Environmental Research Letters* **10**, 084007. doi:10.1088/1748-9326/10/8/084007

Nunes JP, Doerr SH, Sheridan G, Neris J, Santín C, Emelko MB, Silins U, Robichaud PR, Elliot WJ, Keizer J (2018) Assessing water contamination risk from vegetation fires: challenges, opportunities and a framework for progress. *Hydrological Processes* **32**, 687-694. doi:10.1002/hyp.11434

Oropeza J, Heath J (2013) Effects of the 2012 Hewlett and High Park Wildfires on water quality of the Poudre River and Seaman Reservoir. City of Fort Collins Utilities Report. 33 p. (Fort Collins, CO, USA)

Robinne F-N, Bladon KD, Miller C, Parisien M-A, Mathieu J, Flannigan MD (2018) A spatial evaluation of global wildfire-water risks to human and natural systems. *Science of the Total Environment* **610-611**, 1193-1206. doi:10.1016/j.scitotenv.2017.08.112

Robinne F-N, Bladon KD, Silins U, Emelko MB, Flannigan MD, Parisien M-A, Wang X, Kienzle SW, Dupont DP (2019) A regional-scale index for assessing the exposure of drinking-water sources to wildfires. *Forests* **10**, 384. doi:10.3390/f10050384

Sankey JB, Kreitler J, Hawbaker TJ, McVay JL, Miller ME, Mueller ER, Vaillant NM, Lowe SE, Sankey TT (2017) Climate, wildfire, and erosion ensemble foretells more sediment in western USA watersheds. *Geophysical Research Letters* **44**, 8884-8892. doi:10.1002/2017GL073979

Sham CH, Tuccillo ME, Rooke J (2013) Effects of wildfire on drinking water utilities and best practices for wildfire risk reduction and mitigation. Water Research Foundation Report 4482. 119 p. Available from www.waterrf.org

Sidman G, Guertin DP, Goodrich DC, Thoma D, Falk D, Burns IS (2016) A coupled modelling approach to assess the effect of fuel treatments on post-wildfire runoff and erosion. *International Journal of Wildland Fire* **25**, 351-362. doi:10.1071/WF14058

Thompson MP, Scott J, Langowski PG, Gilbertson-Day JW, Haas JR, Bowne EM (2013) Assessing watershed -wildfire risks on national forest system lands in the Rocky Mountain region of the United States. *Water* **5**, 945-971. doi:10.3390/w5030945

Thompson MP, Gilbertson-Day JW, Scott JH (2016) Integrating pixel- and polygon-based approaches to wildfire risk assessment: applications to a high-value watershed on the Pike and San Isabel National Forests, Colorado, USA. *Environmental Modeling and Assessment* **21**, 1-15. doi:10.1007/s10666-015-9469-z

Tillery AC, Haas JR, Miller LW, Scott JH, Thompson MP (2014) Potential post-wildfire debris-flow hazards - a pre-wildfire evaluation for the Sandia and Manzano Mountains and surrounding areas, central New Mexico. US Geological Survey Scientific Investigations Report 2014-5161. 34 p. (Albuquerque, NM, USA)

CHAPTER 2 – PRIORITIZING FUELS REDUCTION FOR WATER SUPPLY PROTECTION

2.1 INTRODUCTION

Communities that rely on surface water from fire-prone watersheds are at risk of wildfire-related increases in sediment, debris, organic matter, other constituents, and peak flows that may damage water infrastructure, complicate water treatment, and reduce reservoir storage capacity (Moody and Martin 2001; Martin 2016; Nunes et al. 2018). In the western U.S., proactive fuels reduction has emerged as a popular strategy to mitigate wildfire risk to water supplies (Huber-Stearns 2015; Ozment et al. 2016). Fuels reduction, such as forest thinning and prescribed fire, is expected to reduce fire severity (Graham et al. 2004; Agee and Skinner 2005; Reinhardt et al. 2008; Martinson and Omi 2013) and therefore post-fire runoff, erosion, and debris flows (Benavides-Solorio and MacDonald 2001, 2005; Cannon et al. 2010). However, watershed investment programs have been challenged to quantify fuel treatment effects on water supply risk and to prioritize fuel treatment locations (Ozment et al. 2016). Understanding fuel treatment effects is fundamental to outcome-based investment strategies for land management that emphasize clearly articulated goals and spatial prioritization (USDA Forest Service 2018). Robust assessment and planning tools are needed to ensure large investments in watershed fuels reduction achieve desired risk mitigation to water supplies.

In the western U.S., wildfire affects water supplies primarily by increasing sediment supply which harms infrastructure and impairs water quality. Exposure to post-fire sediment can therefore serve as a useful metric of water supply impact (Buckley et al. 2014; Elliot et al. 2016; Jones et al. 2017). High severity wildfire reduces surface cover and alters soil properties leading to substantial increases in runoff and erosion (DeBano et al. 2005; Shakesby and Doerr 2006;

Moody and Martin 2009). Burn severity and correlated metrics, like percent bare soil, are strong predictors of erosion at plot to hillslope scales (Benavides-Solorio and MacDonald 2001, 2005; Schmeer et al. 2018), and climate, topography, soils, and vegetation also influence erosion potential at landscape to regional scales (Shakesby and Doerr 2006; Moody and Martin 2009). Water supply consequences further depend on water supply connectivity to fire-prone uplands and vulnerability to sediment and other mobilized contaminants.

Previous studies demonstrate that wildfire risk to water supplies varies across large landscapes due to the likelihood and intensity of fire, erosion potential, and connectivity to water supplies (Scott et al. 2012; Thompson et al. 2013a, 2013b, 2016). These studies quantify risk in relative terms by combining spatial predictions of fire likelihood and intensity with expert-defined functions of relative water supply loss by watershed exposure to broad classes of fire intensity (Scott et al. 2013). This approach emphasizes fire intensity as the primary driver of water supply impact, but multivariate response functions have been used to account for variable erosion potential due to soils and slope steepness (Thompson et al. 2013a, 2013b, 2016). Relative measures of water supply risk can be useful for prioritizing fuels reduction at broad scales, but they do not communicate the potential magnitude of economic damages from reservoir sedimentation or water quality impairment. Without concrete metrics of water supply risk, it is difficult for water managers to justify the need for risk mitigation, set objective mitigation goals, and evaluate the effectiveness of different mitigation strategies.

Spatially-explicit erosion and sediment transport models have been adapted to assess the potential consequences of future fires using modeled fire behavior metrics that approximate burn severity (Miller et al. 2011; Buckley et al. 2014; Tillery et al. 2014; Elliot et al. 2016; Sidman et al. 2016; Jones et al. 2017). Spatial watershed models improve upon multivariate response

functions (Thompson et al. 2013a, 2013b, 2016) by providing quantitative predictions of post-fire erosion and sediment delivery that account for the influence of cover, soils, topography, and rainfall. Sediment yield is a useful metric to water managers because it can be translated into water supply consequences such as dredging or replacement costs for reservoirs, conveyance infrastructure maintenance, and water treatability (Oropeza and Heath 2013; Buckley et al. 2014; Elliot et al. 2016; Jones et al. 2017). Using this framework, fuel treatment effects can be quantified by differencing predicted post-fire sediment delivery to water supplies for current and simulated post-treatment fuel conditions (Buckley et al. 2014; Elliot et al. 2016; Sidman et al. 2016; Jones et al. 2017). Fuel treatment targeting may be improved by considering not only baseline measures of risk but also variation in treatment effects due to starting fuel conditions, the intensity of treatment, topography, and fire weather (Graham 2004; Agee and Skinner 2005; Reinhardt et al. 2008; Martinson and Omi 2013).

Fuels reduction must be prioritized because treating entire watersheds would be cost prohibitive and often in conflict with other land management objectives. It is therefore important to integrate factors relating to costs, legal and administrative restrictions, operational constraints, and social acceptance (North et al. 2015). For example, Buckley et al. (2014) convened a group of multi-resource stakeholders to prioritize one landscape-scale fuel treatment scenario informed by wildfire risk analysis and stakeholder local knowledge. In contrast, Jones et al. (2017) evaluated a range of treatment scenarios that varied in extent and placement criteria. They found greater benefit of treatments prioritized using a multi-resource risk assessment that included erosion potential compared to those prioritized based on accessibility. The mismatch between where it is best to reduce fuels and where it is easiest to reduce fuels highlights the importance of jointly considering benefits, costs, and constraints when prioritizing fuels reduction.

Furthermore, managers often consider multiple fuel treatment types that vary in effects, feasibility, and cost. Optimization approaches that explicitly consider the benefits, costs, and constraints of fuel treatments (e.g., Ager et al. 2013 and Thompson et al. 2017) are useful for identifying efficient solutions to these multi-dimensional problems.

Our goal with this study is to leverage recent advances in watershed-wildfire risk modeling to prioritize fuels reduction for water supply protection. We introduce a linear program formulation to optimize decisions of fuel treatment type and location to maximize avoided sediment costs to water supplies subject to treatment feasibility and budget constraints. To demonstrate the utility of this approach, we parameterize and apply the model to allocate thinning, prescribed fire, and combined fuel treatments to planning units in two northern Colorado watersheds with highly valued water supplies. We also evaluate economic indicators of fuel treatment effectiveness across a wide range of budgets to show how the model can inform goals for a water supply protection program.

2.2 METHODS

2.2.1 General modeling framework

We developed an optimization framework to prioritize fuel treatment types and locations to maximize wildfire risk reduction to water supplies. We measured risk as the expected fire-related sediment impact costs to water supplies in US Dollars (USD) (Buckley et al. 2014; Elliot et al. 2016; Jones et al. 2017). A set of formal mathematical equations are presented to demonstrate the logic to prioritize fuel treatments to mitigate wildfire risk to water supplies in a large watershed. We focused on prioritizing treatment location and type because they are the primary decisions in near-term fuel treatment planning. Location is critical to water supply risk

because of spatial variability in fuel conditions, erosion potential, and connectivity to water supplies. We adopted the structure of the National Hydrography Dataset Plus (NHDPlus; USEPA and USGS 2012) to map the connectivity between sediment producing catchments and water supplies attached to the flowline network (see Figure 2.1 for spatial topology). NHDPlus catchments have sufficient resolution (mean size ~ 300 ha) to use as spatial units for large watershed (> 100 km^2) fuel treatment planning. Treatment type is also important because thinning, prescribed fire, and other treatments vary in effects, feasibility, and cost. We provide methods to parameterize the model for our test case in northern Colorado, but our focus is on the general optimization approach and application, as different data sources and process models may be more appropriate to use in other watersheds.

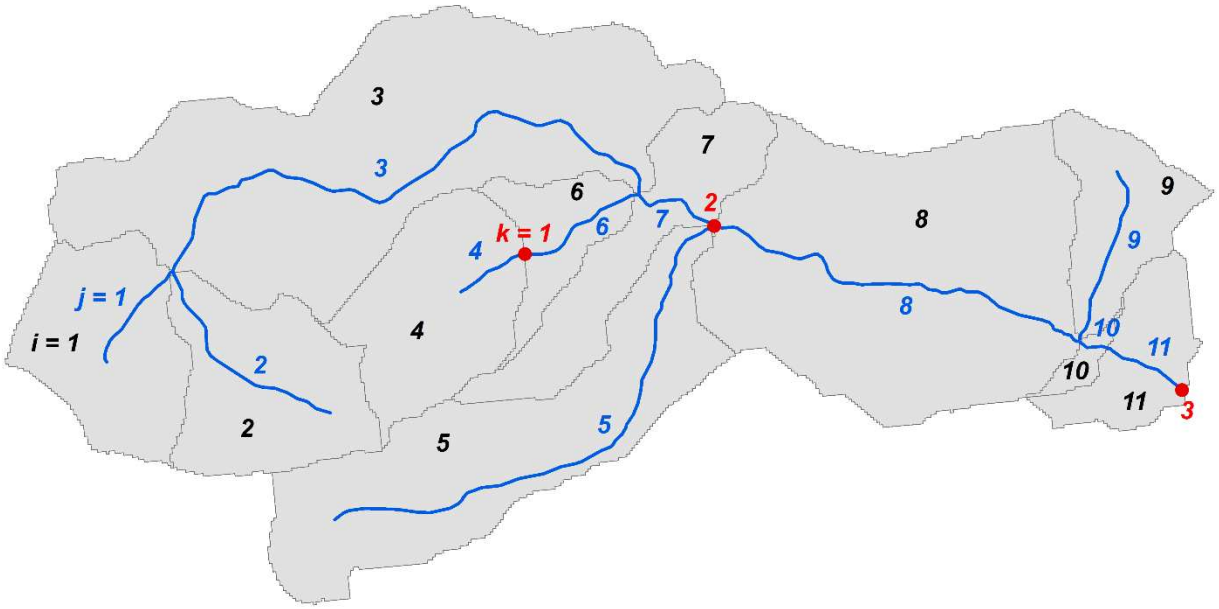

Figure 2.1. Watershed Topology

An example of the NHDPlus (USEPA and USGS 2012) watershed network consists of catchments (indexed by *i*) and flowlines (indexed by *j*). Catchment *i* and the flowline *j* within it share matching identifiers, i.e. *i*=1 and *j*=1. Each water supply of concern is indexed by *k* and is mapped to the end of the j^{th} flowline. Sediments produced in catchment *i* are routed to downstream water supply *k* (i.e. *k*=1, 2 or 3) accounting for the sediment transport efficiency of the flowlines connecting *i* and *k*.

2.2.2 General model formulations for fuel treatment prioritization

We formulated a linear programming optimization model to maximize risk reduction (USD) to water supplies for decisions of how many hectares to treat in each catchment by treatment type during a single fuel treatment planning period subject to a set of feasibility and cost constraints.

Objective function:

$$Maximize \sum_{i=1}^{N} \sum_{t=1}^{P} x_{i,t} * RR_{i,t} \qquad \textbf{Equation 2.1}$$

Subject to:

$$x_{i,t} \leq FE_{i,t} \qquad \forall i,t \qquad \textbf{Equation 2.2}$$

$$\sum_{t=1}^{\mathrm{P}} x_{i,t} \leq TotFE_i \qquad \forall i \qquad \textbf{Equation 2.3}$$

$$x_{i,t} \geq MinArea_{i,t} \qquad \forall i,t \qquad \textbf{Equation 2.4}$$

$$x_{i,t} \leq MaxArea_{i,t} \qquad \forall i,t \qquad \textbf{Equation 2.5}$$

$$\sum_{i=1}^{\mathrm{N}} \sum_{t=1}^{\mathrm{P}} x_{i,t} * TC_{i,t} \leq Budget \qquad \textbf{Equation 2.6}$$

$$x_{i,t} \geq 0 \qquad \forall i,t \qquad \textbf{Equation 2.7}$$

Subscripts:

i is used to index catchments from 1 to N

t is used to index fuel treatment types from 1 to P

Decision variables:

$x_{i,t}$ is the area (ha) of treatment type *t* scheduled in catchment *i*

Parameters:

N is the total number of catchments

P is the total number of treatment types

$RR_{i,t}$is the risk reduction (USD ha^{-1}) from treatment type *t* in catchment i

$FE_{i,t}$ is the feasible and effective area (ha) for treatment type *t* in catchment i

$TotFE_i$ is the total feasible and effective area (ha) in catchment *i* for all treatment types combined

$TC_{i,t}$ is the cost (USD ha^{-1}) for treatment type *t* in catchment i

$MinArea_{i,t}$ is the minimum project area (ha) for treatment type *t* in catchment i

$MaxArea_{i,t}$ is the maximum project area (ha) for treatment type *t* in catchment i

$Budget$ is the total investment upper bound for the fuel treatment program in USD

The objective function (Eqn 2.1) maximizes risk reduction to water supplies (measured in USD) from fuel treatment over the planning period. Eqn 2.2 constrains treatment to the feasible and effective area for each treatment type in each catchment. By "effective" we mean the treatment meaningfully lowers fire severity by producing a categorical change from high to moderate or moderate to low. The effectiveness criterion is meant to approximate fuels specialist judgement to restrict treatment within heterogeneous planning units from areas that do not need treatment and from areas where treatment is not expected to alter fire behavior and severity. Eqn 2.3 prevents overlapping treatments by restricting treatment to the total feasible and effective area in catchment *i*. In Eqn 2.4, the $MinArea_{i,t}$ constraint is used to specify the minimum project size at the catchment-level for implementing each treatment type. We expect watershed protection is one of several management objectives, so the $MaxArea_{i,t}$ constraint (Eqn 2.5) is used to specify the maximum project size (ha). The minimum and maximum area constraints are imposed before model formulation by modifying the $FE_{i,t}$ and $TotFE_i$ parameters. The expected risk reduction to water supplies, $RR_{i,t}$, is calculated as the mean risk reduction for the feasible and effective area for treatment type *t* in catchment *i*. Similarly, $TC_{i,t}$ in Eqn 2.6 is calculated as the mean treatment cost for the feasible and effective area for treatment type *t* in catchment *i*. Parameterizing $RR_{i,t}$,

$FE_{i,t}$, and $TC_{i,t}$ requires extensive data and modeling that we introduce through a test case. We emphasize that these methods are not universal and may require substantial modification for sites with different vegetation, fuel treatment methods, erosion processes, and water supply concerns.

2.2.3 Test case and analysis

We tested our fuel treatment planning approach on the mostly forested, 4809 km^2 upper portions of the Cache la Poudre (CLP) and Big Thompson (BT) Watersheds in northern Colorado, USA (Figure 2.2). CLP and BT provide drinking water to over 600000 residents in Fort Collins, Greeley, Loveland, and neighboring communities. The BT also includes the east slope distribution system of the Colorado-Big Thompson Project (C-BT), which conveys 200000 acre-feet of water annually to water users in the Northern Water Conservancy District. The BT and CLP watersheds range in elevation from 1500 to 4343 m above sea level (ASL). Mean annual temperature varies from 9.9° C in the plains to -4.6° C in the high alpine, and mean annual precipitation increases with elevation from 350 mm to 1300 mm (PRISM Climate Group 2016). Grass and shrub ecosystems occupy the lowest elevations and montane valleys; the mountains are primarily woodlands and forests; and the highest elevations are alpine tundra or bare rock. There is considerable variation in forest composition and density due to elevational and topographic controls on moisture (Peet 1981). Like much of the western U.S., these watersheds have experienced a recent increase in fire activity; since 2000, seven large fires (> 400 ha) burned nearly 49000 ha in the CLP and BT (MTBS 2015). Land ownership is 53.0% federal, 36.5% private, 7.5% state, 1.3% city, and 1.0% county. More than 20% of the study area has a protected status that limits active forest management including 50000 ha of wilderness in Rocky Mountain National Park and 48000 ha of wilderness and 10000 ha of upper tier roadless area on the Arapaho-Roosevelt National Forest.

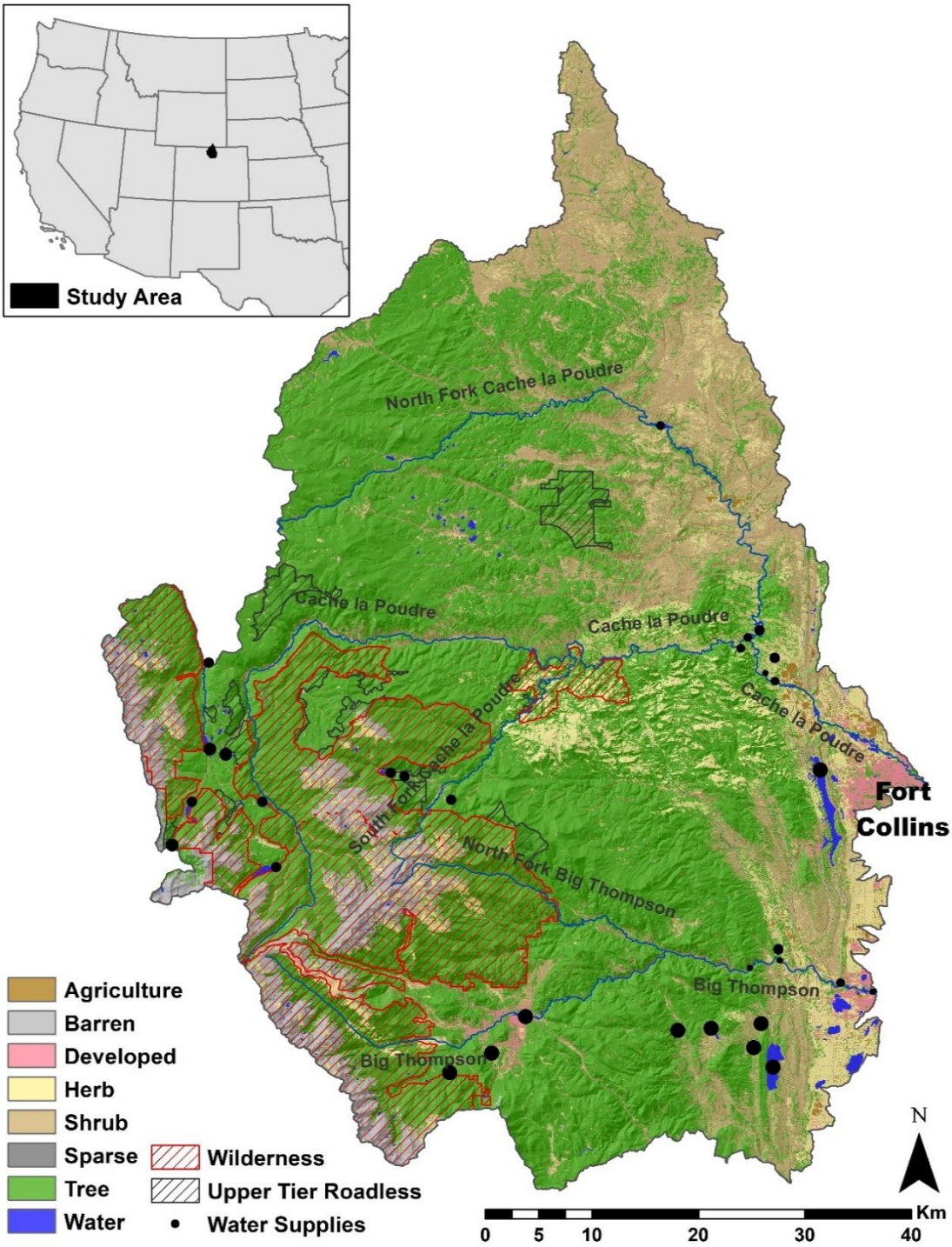

Figure 2.2. Test case watersheds

Test case location including the mainly forested upper portions of the Cache la Poudre and Big Thompson Watersheds in northern Colorado. Water supply points are sized based on sediment impact costs (described in the Sediment cost to water supplies section). Land cover from LANDFIRE (2016).

2.2.4 Water supply risk and fuel treatment effects

We linked fire, erosion, and sediment transport models with sediment impact costs to calculate wildfire risk to water supplies from each unit of the landscape (USD ha^{-1}) (Figure 2.3). We quantified risk reduction from fuel treatment (USD ha^{-1}) by modeling fire behavior and effects on water supplies for baseline and simulated post-treatment fuel conditions. We did not account for fuel treatment effects on burn probability because the primary objective of fuels reduction is to mitigate fire severity (Graham et al. 2004; Reinhardt et al. 2008), and fuel treatment has limited effect on landscape-scale burn probability (Thompson et al. 2013c).

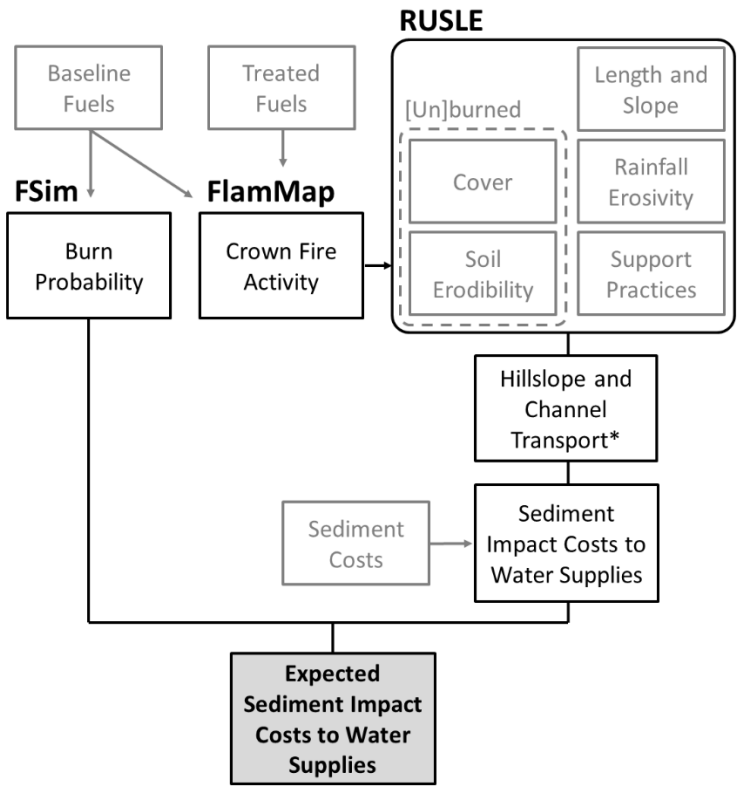

Figure 2.3. Risk assessment framework

Fuel treatment effects on wildfire risk to water supplies were quantified by linking models for burn probability (FSim; Short et al. 2016), fire behavior (FlamMap 5.0; Finney et al. 2015), erosion (Revised Universal Soil Loss Equation [RUSLE]; Renard et al. 1997), and sediment transport (*adaptations of Wagenbrenner and Robichaud 2014 and Frickel et al. 1975) with stakeholder-defined sediment impact costs to water supplies. The output quantifies the expected sediment impact costs to water supplies (i.e. risk) from each unit of the landscape.

2.2.5 Sediment cost to water supplies

We worked with water managers for Fort Collins, Greeley, Loveland, and Northern Water to map water supply infrastructure (hereafter "water supplies"), including 20 reservoirs and 11 diversions, to flowlines in the NHDPlus watershed network (Figure 2.1) and assigned them sediment impact costs (USD Mg^{-1}). Sediment impact costs are used in our analysis to approximate the economic consequence of sediment delivered to a water supply, e.g. the cost to dredge a reservoir, build replacement storage, repair infrastructure, or treat impaired water. For this analysis, we separated sediment impact costs into two components: 1) a base cost by water

supply type (in USD Mg^{-1} of sediment: 16 for reservoirs, 8 for municipal diversions, and 4 for primarily agricultural diversions), and 2) a relative importance weight (0 to 1 for low to high importance) assigned by water managers. We based the cost of reservoir sedimentation on the 25 USD m^{-3} (16 USD Mg^{-1} for a sediment bulk density of 1.6 Mg m^{-3}) reported for dredging costs by Buckley et al. (2014), which is also close to the local cost of buying or developing replacement storage. Relative importance weights were assigned by managers to express the significance of water supplies for system function based on infrastructure characteristics and the volume, priority, and timing of water rights. We assigned sediment impact costs as the product of the base values and the sum of relative importance weights for Fort Collins, Greeley, and Loveland (which together can sum to greater than 1). The mean sediment impact cost was 18.1 USD Mg^{-1} and the range was from 1.6 to 37.5 USD Mg^{-1}.

2.2.6 Burn probability

We used a 270-m resolution national dataset of burn probability (Short et al. 2016) modeled with the Large Fire Simulator (FSim; Finney et al. 2011) to quantify fire likelihood. FSim predicts wildland fire occurrence, growth, and suppression in response to climate-informed, stochastically generated weather streams for tens of thousands of fire seasons. We selected the national FSim burn probability over custom modeling because the FSim fire containment algorithm (Finney et al. 2009) produces more reasonable estimates of fire likelihood in the grass and shrub fuel types of our test watersheds. Burn probability was resampled to 30-m resolution using bilinear interpolation to match the fire and erosion modeling data used in the rest of the analysis. To simplify accounting of fuel treatment effects, we assume fuel treatments will be implemented immediately and remain at constant effectiveness for 25 years. The longevity of fuel treatments is not well-constrained, but a similar analysis assumed fuel

treatments remain effective for 20 years in the western U.S. (Rhodes and Baker 2008). We lengthened the effective longevity to 25 years for this study due to lower forest productivity in the study area (Peet 1981) and results of a stand dynamics modeling study, which suggest forest thinning should reduce torching for ~20 years and active crown fire for ~40 years (Tinkham et al. 2016) at the locally-observed regeneration density following forest thinning (Francis et al. 2018). Therefore, we converted mean annual burn probability from FSim to 25-year burn probability (Eqn 2.8) and focus on metrics of risk and risk reduction over a 25-year fuel treatment planning period.

$$BP_{25} = 1 - (1 - BP_1)^{25} \quad \textbf{Equation 2.8}$$

2.2.7 Fuel treatment simulation

We simulated fuel treatment effects by adjusting spatial fire modeling inputs, including the categorical fire behavior fuel model (FBFM; Scott and Burgan 2005), canopy base height, canopy height, canopy cover, and canopy bulk density. We acquired 30-m raster fuel data from LANDFIRE (2016). and modified them to represent current landscape fuel conditions. Based on our observations of recent fire behavior and effects in the study area (e.g., the 2012 High Park Fire), we shifted the FBFM for lodgepole pine (*Pinus contorta* subsp. *latifolia*) from moderate load conifer litter (TL3) to high load conifer litter (TL5) and we lowered the canopy base height 20% to increase crown fire potential. Fuels data were also updated with past fuel treatments (Caggiano 2017). We included three common fuel treatment types in the analysis – thinning only, thinning followed by prescribed fire, and prescribed fire only – that differ in their effects on surface and canopy fuels (Graham et al. 2004; Agee and Skinner 2005; Reinhardt et al. 2008). The average proportional change in canopy fuels from hazardous fuel and restoration treatments

in dry forests of the western U.S. (Stephens and Moghaddas 2005; Stephens et al. 2009; Fulé et al. 2012; Ziegler et al. 2017) were applied as multiplication factors to current canopy fuels to estimate post-treatment conditions (Table 2.1). We simulated treatment effects on surface fuels by changing the FBFM for the timber-understory and timber-litter fuel models (Scott and Burgan 2005) to reflect that thinning often increases surface fuel loads, while prescribed fire consistently removes fuel (Fulé et al. 2012, Stephens et al. 2009). We approximated these effects by changing the FBFM to increase surface fire intensity for the thinning only treatment, and to decrease surface fire intensity for the prescribed fire only treatment. We assumed that the combined thinning and prescribed fire treatment would not change the FBFM because the prescribed fire would consume thinning residues (e.g. branch and litter activity fuels). For grass, grass-shrub, and shrub fuel types, we conservatively assumed that treatments do not alter the FBFM.

Table 2.1. Fuel treatment effects on forest structure

Treatment effects adjustment factors used to simulate fuel treatments. Effects were applied as multipliers to the baseline fuel values to calculate the post-treatment conditions.

	Treatment Effects		
	Thinning Only	**Thinning & Prescribed Fire**	**Prescribed Fire Only**
Canopy Base Height	1.20	1.20	1.09
Canopy Height	1.20	1.20	1.13
Canopy Cover	0.70	0.75	0.95
Canopy Bulk Density	0.60	0.50	0.92

2.2.8 Fuel condition impacts on fire behavior

We used FlamMap 5.0 (Finney et al. 2015) to model crown fire activity (CFA; Scott and Reinhardt 2001) for baseline and post-treatment fuel conditions. CFA is a prediction of fire type in categories of unburned, surface fire, passive crown fire, and active crown fire, which has been used as a proxy for burn severity in previous watershed risk assessments (e.g., Tillery et al. 2014; Haas et al. 2017; Jones et al. 2017). Large fires driven by very dry and windy conditions are

responsible for most of the area burned in Colorado Front Range (Graham 2003; Sherriff et al. 2014; Haas et al. 2015), so we assessed risk using fire behavior modeled under extreme fire conditions. We used FireFamilyPlus 4.1 (Bradshaw and McCormick 2000) to summarize fuel moisture, wind speed, and wind direction for the fire season (1 April to 31 October) for three Remote Automated Weather Stations (RAWS) in the study area - Redfeather, Estes Park, and Redstone. The mean 3rd percentile fuel moistures for the three stations (1-hr 2, 10-hr 3, 100-hr 6, Herb. 30, Woody 63) were used in FlamMap without conditioning. Due to considerable variability in wind direction, we used the wind blowing uphill option in FlamMap. Wind speed was set to the 97th percentile 1 min mean wind speed (Crosby and Chandler 1966) averaged across stations (38.6 kph at 6 m).

2.2.9 Hillslope erosion

We modeled annual soil loss using a GIS-based implementation (Theobald et al. 2010) of the Revised Universal Soil Loss Equation (RUSLE; Renard et al. 1997). This approach was previously used to estimate wildfire-related erosion in the Southern Rockies for individual wildfire events (Miller et al. 2003; Yochum and Norman 2014, 2015) and for future wildfire and climate scenarios (Litschert et al. 2014). We recognize the potential uncertainties associated with applying RUSLE, which was developed primarily for gently sloping agricultural lands, to predict post-fire erosion from steep wildlands. We chose RUSLE for this initial application because of its computational efficiency at modeling erosion for multiple treatment scenarios over large landscapes. Research in the region has also compared RUSLE to the more physically based WEPP model and developed parameters for RUSLE that are suitable for burned landscapes (Larsen and MacDonald 2007). Spatial data and analyses were used to estimate each subfactor at 30-m resolution.

RUSLE estimates annual soil loss (A) in Mg ha^{-1} yr^{-1} as the product of five sub-factors: rainfall-runoff erosivity (R), soil erodibility (K), length and slope (LS), cover (C), and support practices (P) (Renard et al. 1997). Rainfall-runoff erosivity (R) is an annual metric of rainfall that combines total storm energy and maximum 30-minute intensity (MJ mm ha^{-1} hr^{-1}). NOAA 15-minute rainfall data (Perica et al. 2013) assembled for a separate study (Wilson et al. 2018) were processed with the Rainfall Intensity Summarization Tool (Dabney 2016) to calculate event-level rainfall erosivity. We summed the event values to calculate annual rainfall erosivity for the 11 rainfall stations that best represent our regional climate. This data set spans the years 1971 to 2010 and includes 403 station-years of annual erosivity observations. Annual rainfall erosivity is highly variable in space and time due to localized convective thunderstorms typical of the study area (Kampf et al. 2016). We therefore treat rainfall as a random variable described by the empirical distribution of the annual rainfall erosivity observations pooled across stations (Figure 2.4). To simplify the analysis, we focus on metrics of risk and risk reduction for median rainfall erosivity (615 MJ mm ha^{-1} hr^{-1}), but we also communicate uncertainty in these estimates by reporting risk reduction for 5^{th} through 95^{th} percentiles of rainfall erosivity.

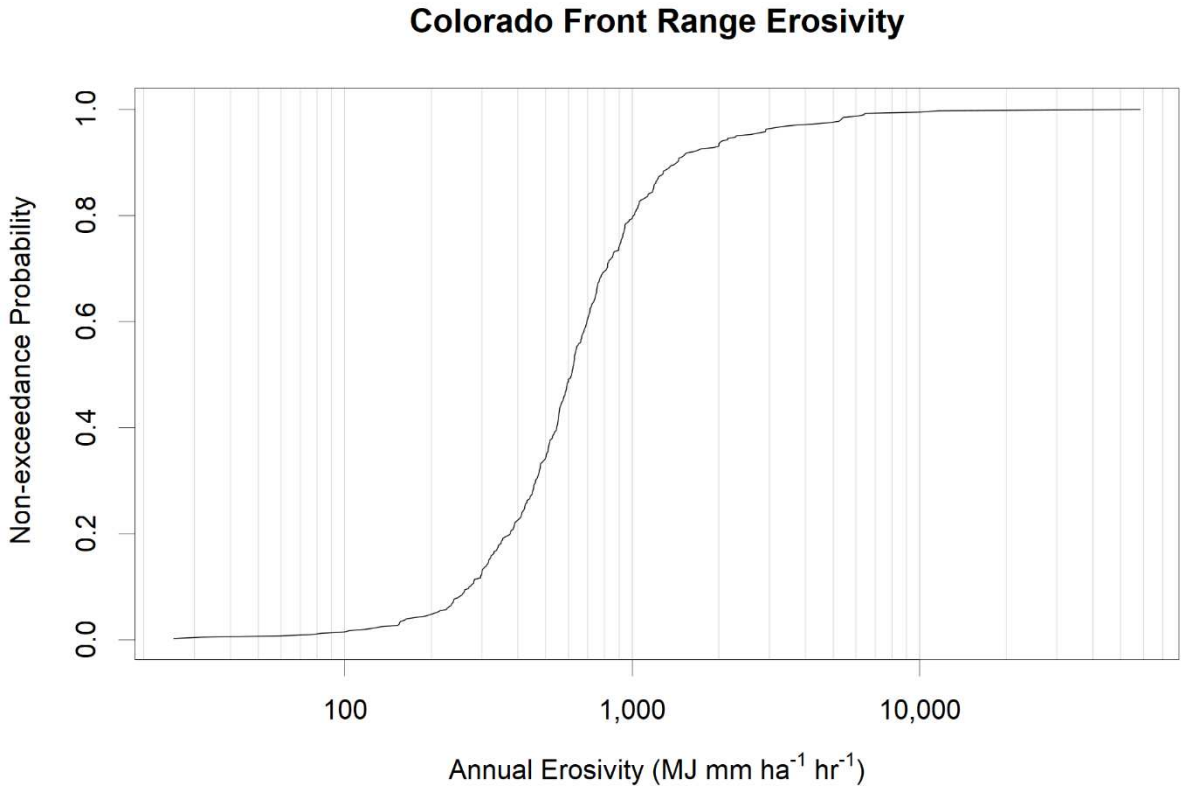

Figure 2.4. Rainfall erosivity distribution

Empirical cumulative distribution of Colorado Front Range annual erosivity from 403 station-years of annual erosivity observations from 11 NOAA 15-minute rainfall stations.

Soil erodibility (K) was extracted from the Soil Survey Geographic Database (SSURGO), and where necessary the State Soil Geographic Database (STATSGO) (NRCS Soil Survey Staff 2016). We followed the procedures of Yochum and Norman (2014) to calculate a weighted mean of whole soil K factor (Kwfact) for each map unit. First, we calculated the component depth-weighted mean K for the top 15 cm of soil. We then computed the map unit area-weighted mean K based on the proportional coverage of components. SSURGO map units that were missing K values for more than 50% of their area were gap-filled with equivalent metrics from STATSGO. All K values were converted to metric units (Renard et al. 1997).

The combined length and slope (LS) factors were calculated using terrain analysis of a 30-m DEM (USEPA and USGS 2012) following methods in Theobald et al. (2010). The slope portion (S) was calculated per Nearing (1997) where θ is slope steepness. We limited θ to 28.8 degrees when calculating S (Eqn 2.9) to not extrapolate beyond the range of Nearing's data (Theobald et al. 2010; Litschert et al. 2014).

$$S = -1.5 + \frac{17}{1 + e^{(2.3 - 6.1 * \sin\theta)}}$$ **Equation 2.9**

We then calculated LS using the methods of Winchell et al. (2008) (Eqns 2.10-2.13) where *A* is the contributing area to the cell inlet in m^2, *D* is the cell dimension in meters, *m* is slope-length exponent, and *x* is the shape factor calculated as a function of cell aspect (α) in radians. The slope-length exponent (*m*) is based on the ratio of rill to interrill erosion (β), which is estimated from slope steepness (θ) following McCool et al. (1989).

$$LS = S * \frac{(A + D^2)^{m+1} - A^{m+1}}{D^{m+2} * x^m * 22.13^m}$$ **Equation 2.10**

$$m = \frac{\beta}{1 + \beta}$$ **Equation 2.11**

$$\beta = \frac{\frac{\sin\theta}{0.0896}}{3 * \sin\theta^{0.8} + 0.56}$$ **Equation 2.12**

$$x = |\sin\alpha| + |\cos\alpha|$$ **Equation 2.13**

We calculated slope steepness (θ), slope aspect (α), and contributing area (*A*) from a 30-m resolution filled DEM using standard slope, aspect, and D8 flow direction methods in ArcGIS 10.3 (ESRI 2015). When calculating LS, we limited *A* to 0.9 ha to approximate the maximum hillslope length of 305 m suggested in Renard et al. (1997). We also limited LS values to the maximum of 72.15 from Renard et al. (1997).

We assigned each Existing Vegetation Type (EVT) from LANDFIRE (2016) an undisturbed cover factor (C) based on previous studies (McQuen 1998; Toy and Foster 1998;

Miller et al. 2003; Yang et al. 2003; Breiby 2006). Baseline C factor values ranged from 0.001-0.003 for forests, 0.025-0.029 for shrublands, 0.012-0.080 for grasslands, and up to 1.0 for barren areas associated with agriculture or mining. We assigned alpine barren areas (> 2,900 m ASL) a C of 0.002 due to high rock cover. Baseline estimates of C do not have to be precisely defined because they are small compared to post-wildfire C (Larsen and MacDonald 2007), especially for forests, which are the focus of our analysis.

2.2.10 Predicting post-fire erosion

We used crown fire activity (CFA; Scott and Reinhardt 2001) modeled with FlamMap 5.0 (Finney et al. 2015) as a proxy for burn severity by mapping surface, passive crown, and active crown fire to low, moderate, and high burn severity, respectively. Characterizing fire effects by burn severity category is consistent with how field-based erosion studies stratified their sampling (e.g. Benavides-Solorio and MacDonald 2005; Larsen and MacDonald 2007) and it is similar to using remotely sensed burn severity to predict post-fire erosion (Miller et al. 2016). Fire-related increases in erosion are primarily attributed to change in surface cover (Larsen et al. 2009) and altered soil properties (Shakesby and Doerr 2006). Therefore, we modeled fire effects on erosion by modifying the RUSLE C and K factors. For forests (≥ 10% canopy cover), we adopted the mean first year post-fire C from Larsen and MacDonald (2007) by fire severity (Table 2.2). Due to the diversity of non-forest vegetation types (< 10% canopy cover) and the more limited estimates of post-fire cover in these systems (Pierson and Williams 2016), we used proportional adjustment factors to model fire effects on C (Table 2.2). Fire effects on soils are diverse, but generally lead to decreased infiltration and cohesion from a range of processes including deposition of hydrophobic compounds, soil sealing, and consumption of organic material (DeBano et al. 2005; Shakesby and Doerr 2006). Direct measures of post-fire K

are lacking, but Larsen and MacDonald (2007) back-calculated a 2.5-fold increase in K for high burn severity. Since they did not directly measure K, we estimated fire effects on K with more conservative adjustment factors (Table 2.2) like Schmeer (2014).

Table 2.2. Fire effects on erosion

Mean post-fire C factor values by burn severity from Larsen and MacDonald (2007) were used to assign post-fire C for forests (≥ 10% LANDFIRE canopy cover). Fire effects on C factor for non-forest (< 10% LANDFIRE canopy cover) were applied as proportional adjustment factors. Fire effects on K factor for all vegetation were applied as proportional adjustment factors.

Crown Fire Activity	Burn Severity	Forest C	Fire Effects Non-forest C Adjustment Factor	K Adjustment Factor
Surface	Low	0.01	1.2	1.5
Passive	Moderate	0.05	1.5	1.75
Active	High	0.20	2.0	2.0

In the Colorado Front Range, post-fire hillslope erosion generally returns to pre-disturbance levels within 2-5 years (Benavides-Solorio and MacDonald 2005; Wagenbrenner et al. 2006; Robichaud et al. 2013a). Based on the rate of surface cover recovery and its influence on erosion, we estimate that the total sediment yield from erosion over the multiple years of recovery is approximately 2.1 times the first-year sediment yield (Benavides-Solorio and MacDonald 2005; Pietraszek 2006). We used this empirical correction factor to estimate the multi-year sediment yield from post-fire erosion.

2.2.11 Hillslope sediment transport

We used an empirical model of post-fire hillslope sediment delivery ratio (hSDR) for the western U.S. (Wagenbrenner and Robichaud 2014) to estimate the proportion of gross erosion delivered to streams. When hillslope erosion is the primary source of sediment, unit area sediment yields normally decline with increasing watershed size (hSDR < 1) because of increasing opportunities for sediment storage (Walling 1983). We estimated post-fire hSDR with

the annual length ratio (LR) model from Wagenbrenner and Robichaud (2014) (Eqns 2.14 and 2.15). We calculated the flow path length from each pixel to the nearest channel as the "catchment length" and the flow path length across the pixel as the "plot length" using a 30-m DEM (USEPA and USGS 2012) in ArcGIS 10.3 (ESRI 2015).

$$\log(hSDR) = -0.56 - 0.0094 * LR \quad \textbf{Equation 2.14}$$

$$LR = \frac{Flow\ path\ length\ to\ nearest\ channel}{Flow\ path\ length\ across\ pixel} \quad \textbf{Equation 2.15}$$

The moderate-resolution NHDPlus flowline network does not include all channels and it especially underestimates the extent of the channel network after wildfire (Wohl 2013). We therefore extended the channel network using a 10.8 ha contributing area threshold (Henkle et al. 2011) to define streams before calculating flow path length to nearest channel. The resulting hSDR values ranged between 0.05 and 0.27. The maximum hSDR for near stream environments is low compared to similar predictions of SDR based on travel time (Ferro and Porto 2000; Fernandez et al. 2003) and, as we show later in the results, the catchment and whole watershed sediment yields are much lower than field observations from the region. We therefore carried forward two scenarios through the subsequent analyses: a low SDR scenario using the base model predictions and a high SDR scenario with double the predicted SDR as an approximate calibration to the small catchment sediment yields from the Hayman Fire (Robichaud et al. 2008, 2013b). Channel pixels for both scenarios were assigned hSDR of 1.

2.2.12 Sediment delivery to infrastructure

Sediment transport in streams depends on characteristics of the sediment and flow. Streamflow has high spatial and temporal variability in the local semi-arid climate. Sediment rating curves or bedload transport functions based on critical sheer stress or stream power rely on accurate flow characterization, so there is a high degree of uncertainty when using these

approaches to predict sediment transport under unknown future hydrologic conditions. We instead adapted a simple model of channel SDR (cSDR) based on Frickel et al. (1975) to estimate the proportion of sediment transported through a stream segment as a function of Strahler stream order. Since nearly all burned tributaries were highly connected to water supplies after the High Park Fire (Miller et al. 2017), we assumed transport of fine-grained hillslope sediments would be very efficient for the steep, gravel-to-cobble bed streams typical of the study area. Post-fire monitoring of a similar montane watershed showed that clay and silt are efficiently transported even during low flow conditions, while transport of sand and larger particles may depend on higher flows associated with annual snowmelt or intense rainstorms (Ryan et al. 2011). We assigned cSDRs per 10 km of stream length of 0.75, 0.80, 0.85, and 0.95 to 1st, 2nd, 3rd, and 4th or higher order streams, respectively, to reflect that sediment transport may be less efficient in the lower order channels due to ephemeral or intermittent flow, and roughness from riparian vegetation and coarse woody debris. More sophisticated methods would be necessary for watersheds with low-gradient depositional reaches, routing large caliber sediments, or predicting storm-level sediment transport. We also assigned cSDR of 0.05 to all dammed flowlines to reflect that much of the sediment entering lakes or reservoirs should be trapped (Brune 1953). The proportion of sediment transported from a catchment to a downstream water supply was calculated as the product of the connecting flowline cSDRs.

2.2.13 Water supply risk

We combined estimates of burn probability and fire effects to calculate baseline wildfire risk in USD ha^{-1} to water supplies from pixels in catchment i as:

$$Risk = BP_{25} * \left(A_{b,nt} - A_{ub}\right) * 2.1 * hSDR * \sum_{k=1}^{N}(C_k \prod_{j=1}^{P} cSDR_j) \qquad \textbf{Equation 2.16}$$

where *b* and *ub* denote burned and unburned conditions; *t* and *nt* denote treatment and no treatment; *A* is annual soil loss (Mg ha^{-1}); coefficient 2.1 is the empirical correction factor to account for multiple years of elevated erosion; *hSDR* is the hillslope sediment delivery ratio; C_k is the sediment impact cost for the k^{th} connected downstream water supply (USD Mg^{-1}); and $cSDR_j$ is the channel sediment delivery ratio for the j^{th} flowline segment connecting the source catchment *i* to water supply *k*. The risk reduction (USD ha^{-1}) from applying treatment *t* in catchment *i* is estimated by instead differencing the burned not treated conditions ($A_{b,nt}$) and the burned treated conditions ($A_{b,t}$):

$$Risk\ Reduction = BP_{25} * \left(A_{b,nt} - A_{b,t}\right) * 2.1 * hSDR * \sum_{k=1}^{N}(C_k \prod_{j=1}^{P} cSDR_j)$$

Equation 2.17

We framed risk reduction here as the positive benefit of treatment to be maximized in Eqn 2.1. The risk reduction rate parameter ($RR_{i,t}$) in Eqn 2.1 is calculated as the mean risk reduction (USD ha^{-1}) for feasible and effective pixels to treat with *t* in catchment *i*.

2.2.14 Treatment constraints

We evaluated the feasibility and cost of each treatment type with spatial data on land designations, roads, and topography. Thinning is only feasible where there are forested fuels to modify (≥ 10% canopy cover) and mechanized equipment is permitted (not in wilderness or upper tier roadless). We assume that any area is feasible for prescribed fire after thinning, but before thinning, it must meet fire effects and safety criteria. We modeled fire behavior with an additional FlamMap run under 30th percentile fuel moistures and 16.1 kph winds at 6 m to approximate prescribed fire conditions. We assumed that any pixels with > 30% crown fraction burned (Scott and Reinhardt 2001) would exceed the desired overstory tree mortality. We further excluded prescribed fire from within 250 m of structures (mapped by Caggiano et al. 2016) and

from forest types associated with infrequent, stand-replacing fire (i.e. "wet forests"). Many factors influence the cost of thinning including site access, equipment operability, forest composition and structure, and the market value of timber or non-timber products. There is potential for merchantable timber extraction to offset some of the thinning cost, but we chose not to account for it here due to local emphasis on fuel reduction prescriptions that retain larger trees of fire-resistant species (Agee and Skinner 2005; Reinhard et al. 2008). Based on input from local forestry and logging professionals (B. Lebeda and M. Morgan, pers. comm.), we approximated thinning costs for mechanical harvesting equipment as functions of accessibility and operability using Eqn 2.18. We assumed that anywhere within 800 m of road and below 40% slope would cost 6200 USD ha^{-1} to thin. We assumed thinning costs would increase linearly from 6200 to 24700 USD ha^{-1} as distance from roads (D) increased from 800 to 6400 m and as slope (S) increased from 40 to 200 percent, up to a maximum of 24700 USD ha^{-1}.

$$Thin\ Cost = \begin{cases} 6200\ ;\ D \leq 800\ and\ S \leq 40 \\ 6200 + 3.3 * (D - 800) + 115.8 * (S - 40)\ ;\ D > 800\ and\ S > 40 \end{cases}$$

Equation 2.18

We estimated prescribed fire cost as 2500 USD ha^{-1} based on local manager experience (B. Karchut and J. White, pers. comm.). The thinning plus prescribed fire costs were calculated as the sum of thinning costs and prescribed fire costs.

2.2.15 Model parameterization and testing

For each catchment and treatment type we calculated the feasible and effective treatment area ($FE_{i,t}$), mean treatment risk reduction ($RR_{i,t}$), and mean treatment costs ($TC_{i,t}$). We formulated and solved the optimization model using the *lpSolve* package (Berkelaar et al. 2015) in R (R Core Team 2019), which uses the revised simplex method for continuous decision variables. We generated solutions for a large range of budget levels (10 to 500 million USD) to

illustrate how metrics of risk reduction respond to increasing investment. In addition to percent and absolute risk reduction (USD) over the planning period, we present the treatment benefit:cost ratio ($\frac{risk\ reduction}{treatment\ cost}$) and return on investment ($\frac{(risk\ reduction - treatment\ cost)}{treatment\ cost} * 100$).

2.3 RESULTS

2.3.1 Model parameterization

The study area-wide mean and maximum annual burn probabilities (Short et al. 2016) were 0.0028 and 0.0091, respectively. The 25-year planning period mean and maximum burn probabilities increase to 0.0659 and 0.2040, respectively, which corresponds to an expected area burned of 31702 ha over the planning period. Under extreme fuel and fire weather conditions, 37.1% of the study area is predicted to burn as surface fire, 16.6% as passive crown fire, and 36.5% as active crown fire, and the remaining 9.7% is non-burnable. Active crown fire was associated with dense forest conditions and steep slopes. For current conditions, the estimated increase in erosion during the first post-fire year was substantial (mean: 31 Mg ha^{-1}; median: 4.1 Mg ha^{-1}), but also highly variable across the watersheds (sd: 61 Mg ha^{-1}; range: 0-670 Mg ha^{-1}) due to the combination of fire effects on cover and soil erodibility and the large underlying gradient in length-slope. Predicted unit area sediment yields decline when accounting for hillslope sediment transport to stream channels and channel sediment transport to water supplies, as illustrated for a subset of the study area in Figure 2.5. The landscape-wide mean hSDR was 0.28 (range: 0.05-1) for the low scenario and 0.51 (range: 0.09-1) for the high scenario. The estimated mean increase in first-year post-fire sediment delivered to streams was 8.4 Mg ha^{-1} (sd: 19 Mg ha^{-1}) for the low SDR scenario and 15 Mg ha^{-1} (sd: 31 Mg ha^{-1}) for the high SDR scenario. We emphasize the results for the high SDR scenario in subsequent analyses since they

align better with the small catchment and whole watershed field observations (Figure 2.5). The decline in unit area sediment delivered to the water supplies varied with flow path length and the presence of dams. Including both hillslope and channel sediment transport, a metric ton of sediment generated from the average pixel will result in 6.2 USD of water supply impact (range: 0-37.5 USD) for the high SDR scenario.

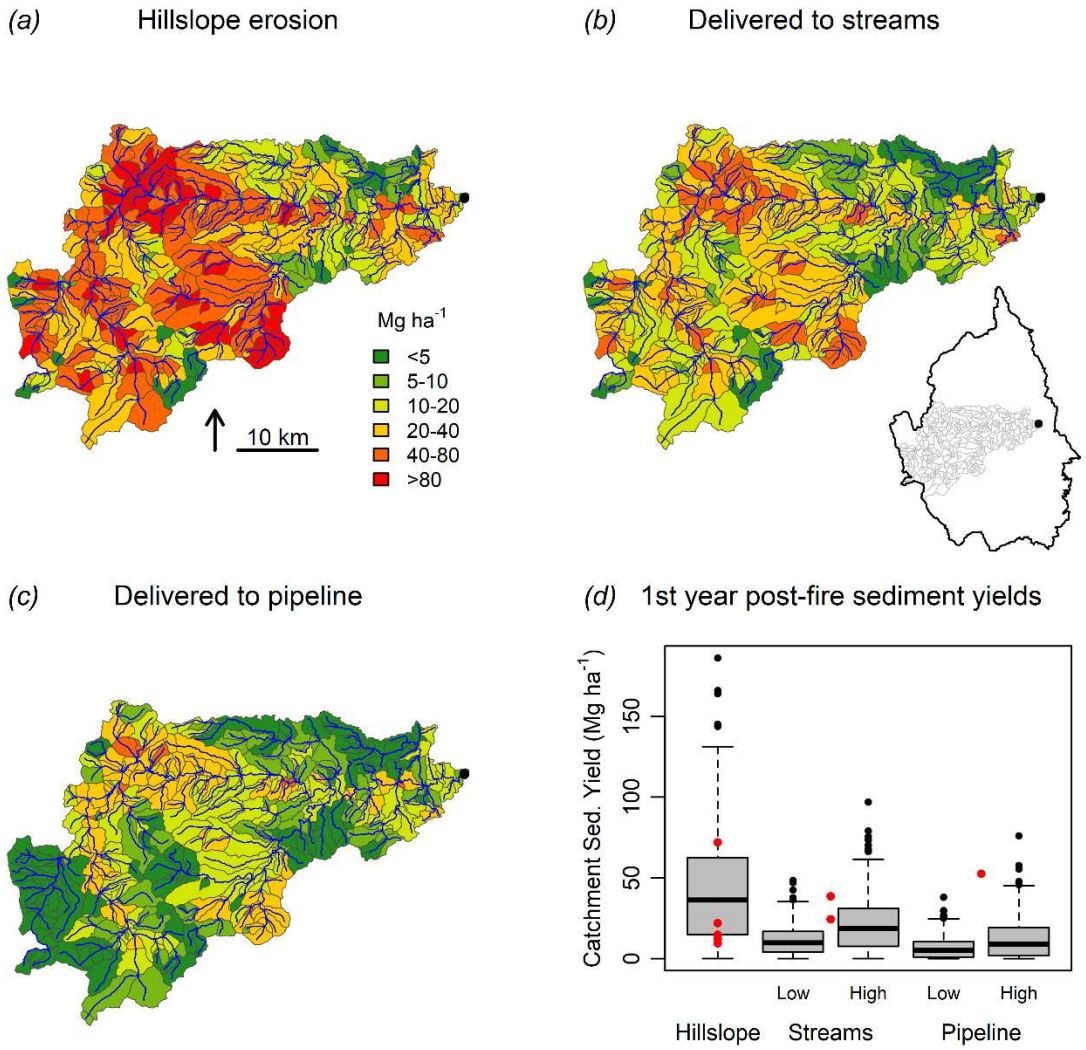

Figure 2.5. Watershed effects results and validation

Predicted 1st year post-fire sediment yields (Mg ha^{-1}) for the 435 catchments that contribute to a drinking water pipeline (a subset of the study area) are presented for hillslope erosion (A), sediment delivered to streams for the high SDR scenario (B), and sediment delivered to the pipeline for the high SDR scenario (C). Catchment mean sediment yields decline from hillslope to whole watershed scales (D). Low and high refer to the low and high SDR scenarios. Measured 1st year post-fire sediment yields from regional field studies (red dots) are presented for comparison: hillslope (Moody and Martin 2001; Wagenbrenner et al. 2006; Larsen et al. 2009; Robichaud et al. 2013a; Schmeer et al. 2018), small catchment for delivery to streams (Robichaud et al. 2008, 2013b), and whole watershed for delivery to pipeline (Martin and Moody 2001).

Risk is concentrated in the densely forested, steep canyons of the lower Big Thompson and Cache la Poudre rivers and portions of high elevation forests with strong connections to

water supplies. Pixel-level estimates of wildfire risk to water supplies for the high SDR scenario (Figure 2.6) range from 0 to 3500 USD ha^{-1} over the 25-year planning period (mean: 24 USD ha^{-1}; median: 1.1 USD ha^{-1}). Note that despite high connectivity to water supplies, the lower portion of the Cache la Poudre watershed is currently mapped as low risk due to recent fuels reduction from the 2012 High Park and Hewlett Gulch fires (Figure 2.6). The total risk to water supplies is estimated at 11.5 USD million over the 25-year planning period for median rainfall erosivity and the high SDR scenario.

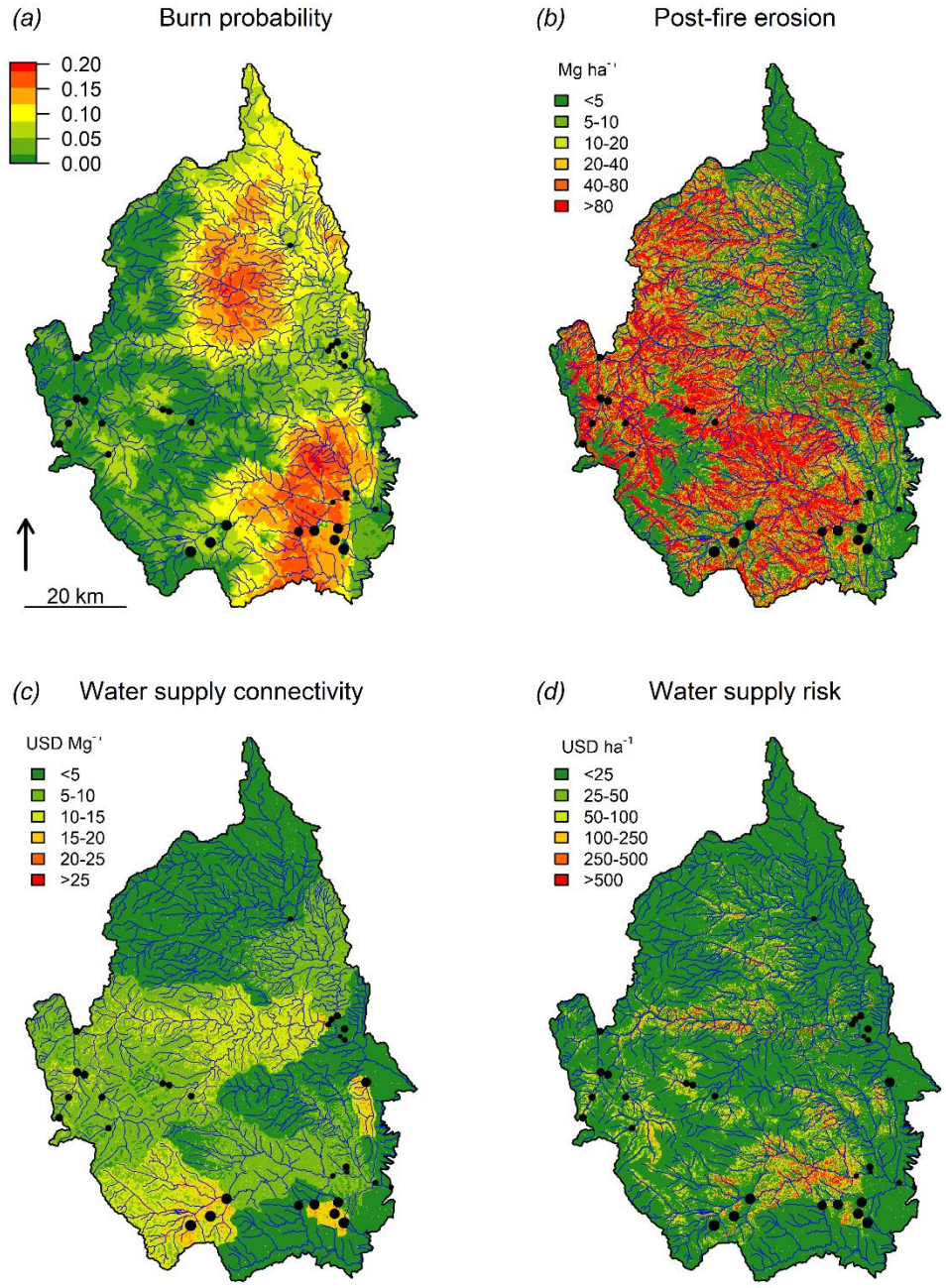

Figure 2.6. Wildfire-water supply risk components

Our integrated measure of water supply risk (D) describes the expected cost of wildfire impacts to water supplies over the planning period (USD ha^{-1}) by combining planning period burn probability (A), post-fire increase in hillslope erosion over multiple years (B), and connectivity to downstream water supply impact costs for the high SDR scenario (combination of hillslope and channel transport and water supply impact costs) (C).

Fuels reduction is constrained in our model to locations that are feasible to treat, and treatment is effective at modifying crown fire activity. The presence of non-forest vegetation and land management designations limit the area feasible for thinning or combined thinning and prescribed fire treatments to 226000 ha of the study area (47%). Just over 68000 ha is feasible for prescribed fire as the first-entry treatment (14%) based on criteria for proximity to homes, crown fire behavior, and ecological setting. Fuel treatments must alter fire behavior as a precondition to reduce post-fire erosion. Under extreme fuel and fire weather conditions, the thinning only treatment is expected to reduce crown fire activity on 115000 ha of the feasible treatment area (51%) (Table 2.3). The thinning only treatment effectively lowered active crown fire to passive crown fire on 114000 ha of the feasible treatment area. Thinning alone was not effective at reducing active or passive crown fire to surface fire (< 1% of the feasible treatment area) due to a combination of low initial canopy base heights and the increase in surface fire intensity from fuels added by thinning. The thinning only treatment is expected to intensify surface fire to crown fire on approximately 6800 ha (3% of the feasible treatment area), due primarily to increased surface fuels and secondarily to reduced canopy wind sheltering. Thinning plus prescribed fire was slightly more effective than thinning alone; the combined treatment reduced crown fire activity on 119000 ha of the feasible treatment area (53%) (Table 2.3). Most change was from modifying active crown fire to passive crown fire (118000 ha), but a larger area was reduced to surface fire behavior (610 ha), and fire behavior was only intensified on a small area (230 ha). Prescribed fire was the least effective treatment for moderating crown fire activity (8300 ha or 12% of the feasible treatment area) (Table 2.3), but it was the most effective treatment at reducing active and passive crown fire to surface fire (2500 ha) because of the reduced surface fire intensity.

Table 2.3. Fuel treatment effects on fire behavior

Effectiveness of fuel treatments at modifying crown fire activity (Scott and Reinhardt 2001) under extreme fuel and fire behavior for the feasible treatment areas. Passive and active refer to crown fire. Treatment is considered effective if it reduces crown fire activity.

Area (ha)	Thinning Only			Thinning and Prescribed Fire			Prescribed Fire Only		
Pre-treatment	**Surface**	**Passive**	**Active**	**Surface**	**Passive**	**Active**	**Surface**	**Passive**	**Active**
Surface	28539	6763	72	35142	232	1	20215	0	0
Passive	46	66846	0	321	66571	0	2137	31471	0
Active	44	114433	9352	291	118348	5190	322	5841	8548
Total Feasible			226096			226096			68534
Total Feasible and Effective			114523			118960			8300

Catchment-level mean risk reduction is highly variable across treatment type and location (Table 2.4; Figure 2.7) due to differences in treatment effects (Table 2.3), erosion potential, and connectivity to water supplies (Figure 2.6). More than 70% of the 1827 catchments in the study area have some feasible and effective area to thin. Over half of the catchments have area that prescribed fire can be used safely and effectively, but many catchments do not have enough area to plan a prescribed fire project (mean: 8.5 ha) (Table 2.4). For the high SDR scenario, the mean risk reduction for catchments with feasible and effective area to treat was similar for the thinning only and combined thinning and prescribed fire treatments (44.2-44.6 USD ha^{-1}), but lower for the prescribed fire treatment (29.6 USD ha^{-1}). Given that thinning is far more expensive than prescribed fire, prescribed fire is the most cost-effective treatment for these watersheds (Table 2.4). Because the combined treatment option is more expensive, it is also less cost-effective than thinning only (Table 2.4).

Table 2.4. Optimization model parameters

Mean and range (in parentheses) of model parameters for catchments with feasible and effective area to treat under the high SDR scenario.

Treatment Type	Catchments with Feasible and Effective Area	Feasible and Effective Area (ha)	Risk Reduction (USD ha^{-1})	Treatment Cost (USD ha^{-1})	Benefit:Cost Ratio
Thinning Only	1334	86.3 (0.1 - 1070.9)	44.2 (0 – 500.5)	6851.6 (6177.6 - 16865.8)	0.0062 (0.0000 - 0.0566)
Thinning and Prescribed Fire	1342	89.2 (0.1 - 1165.1)	44.6 (0 – 582.6)	9352.1 (8648.7 - 19347.5)	0.0046 (0.0000 - 0.0435)
Prescribed Fire	978	8.5 (0.1 - 182.4)	29.6 (0 – 448.1)	2471.1 (2471.1 - 2471.1)	0.0120 (0.0000 - 0.1813)

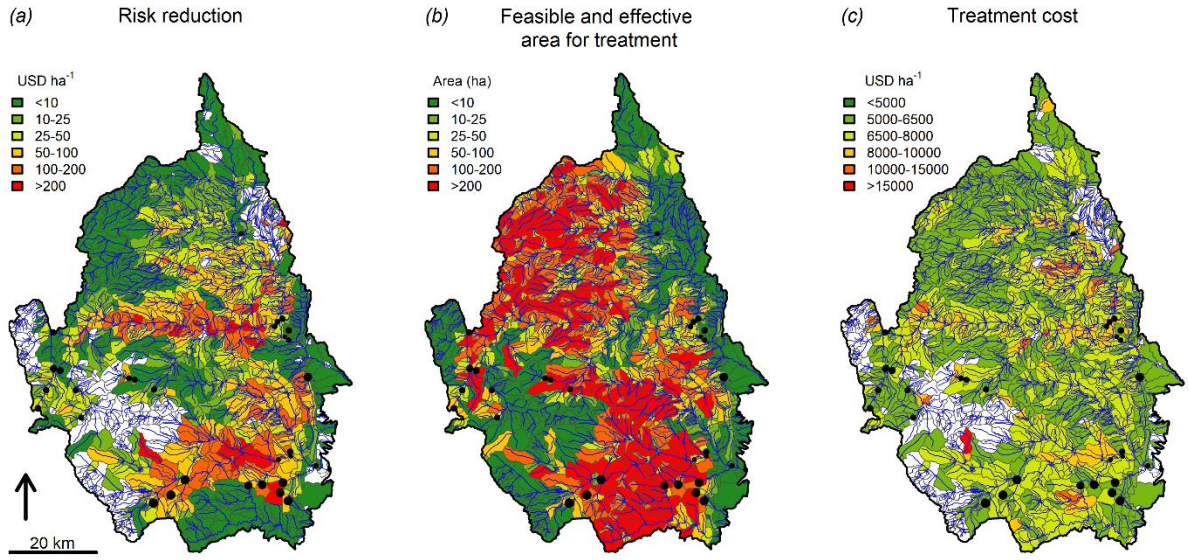

Figure 2.7. Spatial distribution of optimization model parameters

Catchment-level statistics for the thinning only treatment used to parameterize the optimization model. Catchment mean risk reduction for the high SDR scenario (A) and treatment cost (C) are calculated for the feasible and effective area to treat in each catchment (B).

2.3.2 Optimization model test case

Our model suggests that water supply risk can be reduced in these watersheds by a maximum of 54% with fuels reduction without project size and budget limitations. However, in practice, there is often a minimum project size because of the significant cost to mobilize

equipment and staff to a project site. It is also rare that fuels are reduced uniformly over large areas due to other management objectives. Assuming minimum treatment areas of 10 ha for thinning and 20 ha for prescribed fire, and a maximum of 30% area treated in each catchment, we estimate that fuels reduction can reduce total water supply risk by approximately one third (Table 2.5). More than half of this risk reduction can be achieved by investing 100 million USD to treat 14400 ha, and 90% of this risk reduction can be addressed by spending 250 million USD to reduce fuels on 36000 ha. There is very low marginal benefit to investing more than 300 million USD (Table 2.5). At lower budget levels, fuel treatments should be concentrated along the main stems of the Cache la Poudre and Big Thompson rivers and near C-BT reservoirs (Figure 2.8). As budget increases, fuels reduction could be allocated to areas that are less connected to water supplies (Figure 2.8). Despite the higher cost-effectiveness of prescribed fire (Table 2.4), it is not selected often because few catchments have > 20 ha of feasible and effective area to treat with prescribed fire (Table 2.5). The thinning only treatment is favored at lower budget levels (Table 2.5). The model prioritizes thinning on steep slopes despite the increased cost; the mean cost of thinning treatments selected for the 10 million USD budget was 8060 USD ha^{-1} (30% higher than the base cost). As budget increases beyond 250 million USD, much of the marginal gain in risk reduction is made by converting thinning or prescribed fire only treatments to the combined treatment type (Table 2.5). The estimated risk reduction from treatment is small compared to the cost of fuels reduction across all budget levels and percentiles of rainfall erosivity (Table 2.5).

Table 2.5. Optimization model performance metrics

Performance metrics for optimal fuel treatment plans across a range of investment levels assuming 10 ha minimum area for thinning, 20 ha minimum area for prescribed fire, a maximum of 30% area treated in each catchment, and the high SDR scenario.

		Budget (USD millions)									
Performance metric		**50**	**100**	**150**	**200**	**250**	**300**	**350**	**400**	**450**	**500**
Risk Reduction (%)		12.3	19.6	24.9	28.7	31.2	32.7	33.6	34.2	34.5	34.6
Risk Reduction (USD millions) for percentiles of post-fire rainfall erosivity	5th	0.48	0.77	0.98	1.13	1.23	1.29	1.32	1.34	1.36	1.36
	25th	0.98	1.55	1.97	2.27	2.47	2.59	2.66	2.70	2.73	2.74
	50th	1.42	2.26	2.86	3.30	3.58	3.76	3.87	3.93	3.96	3.98
	75th	0.98	1.55	1.97	2.27	2.47	2.59	2.66	2.70	2.73	2.74
	95th	5.30	8.44	10.70	12.32	13.40	14.06	14.47	14.69	14.82	14.88
Benefit:Cost Ratio		0.03	0.02	0.02	0.02	0.01	0.01	0.01	0.01	0.01	0.01
Return on Investment (%)		-97.16	-97.74	-98.09	-98.35	-98.57	-98.75	-98.89	-99.02	-99.12	-99.20
Catchments (#)		89	162	254	336	434	513	580	639	696	747
Catchments x treatment type (#)		104	199	329	454	615	739	817	886	954	994
Total Treatment (ha)		7,165	14,432	21,872	29,037	35,980	42,652	48,384	53,339	58,469	61,823
Thinning only (ha)		6,649	13,256	20,090	26,657	32,492	37,372	39,131	38,320	37,230	30,427
Thinning and prescribed fire (ha)		71	188	352	837	1,785	3,564	7,791	13,970	20,406	30,947
Prescribed fire only (ha)		445	989	1,430	1,542	1,703	1,717	1,461	1,049	832	448

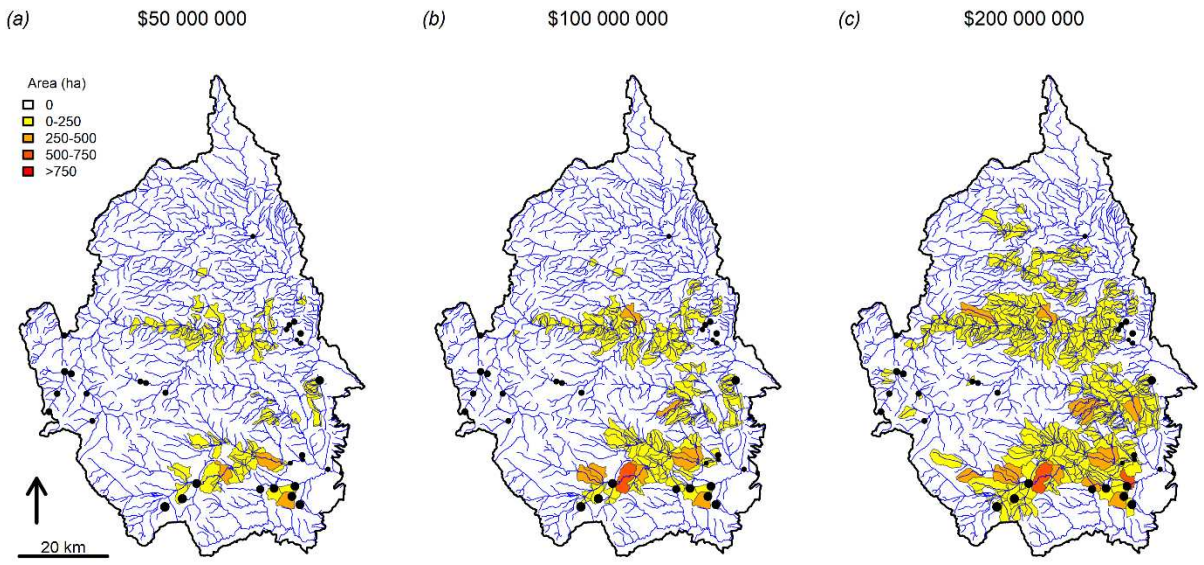

Figure 2.8. Fuel treatment optimization results

Example optimal landscape fuel treatment plans for 50 (A), 100 (B), and 200 (C) USD million budgets using 10 ha minimum area for thinning, 20 ha minimum area for prescribed fire, a maximum of 30% area treated in each catchment, and the high SDR scenario. Areas reported are for all treatment types combined.

2.4 DISCUSSION

Combining quantitative measures of risk reduction with fuel treatment constraints facilitates fuel treatment targeting and realistic assessment of fuel treatment benefits. Our analysis extends common risk assessment methods (Scott et al. 2013) with a spatial topology and effects modeling framework (Figure 2.1 and Figure 2.3) that provides quantitative measures of risk for whole water systems (Figure 2.6). This risk assessment framework should be useful for communities with large source watersheds and multiple water supplies. Our fuel treatment assessment and optimization approach provides more information than a spatial risk assessment. By modeling fuel treatment effects on fire behavior and water supply consequences, accomplishments can be reported in terms of risk reduction (USD), rather than area treated (USDA Forest Service 2018). Our fuel treatment optimization model demonstrates the potential to meaningfully reduce wildfire risk to water supplies by treating a small portion of the forested area (Table 2.5; Figure 2.8). For example, in this study area, it was previously estimated that 191145 ha of the CLP and BT require fuels reduction based on vegetation condition (Talberth et al. 2013), but we estimate that 90% of the achievable risk reduction (31% of total risk) with project size constraints can be accomplished with only 36000 ha of treatment. Greater risk reduction is possible if we assume that there are no minimum project area requirements and that entire catchments can be thinned for water supply protection (54%). Our analysis also demonstrates that it is more efficient to reduce fuels on erosion-prone steep slopes despite the higher cost of treatment. Fuel treatment targeting may be improved in similar landscapes by integrating fuel treatment feasibility and cost constraints into the prioritization process. The availability of tools to assess baseline risk and fuel treatment benefits (Figure 2.6; Table 2.5)

should help groups engaged in fuels reduction for water supply protection define clear risk reduction goals and treatment priorities (Ozment et al. 2016).

We estimate wildfire risk to water supplies in the CLP and BT at 11.5 USD million over the next 25 years based on median rainfall erosivity and our high SDR scenario, which is about half the costs Denver Water incurred from the Buffalo Creek and Hayman fires (~ 26 USD million; Jones et al. 2017). This difference can be attributed to the much higher than median rainfall at Buffalo Creek that initiated massive hillslope and channel erosion (Moody and Martin 2001) and the lower values assigned to sediment impacts in the CLP and BT. The mean value assigned to sediment impacts in this study was 18.1 USD Mg^{-1}, which is much lower than the 62.5 USD Mg^{-1} Denver Water paid to dredge Strontia Springs after the Buffalo Creek and Hayman Fires (Jones et al. 2017). The three municipal water providers we studied all have multi-source systems, which provides flexibility to cope with wildfire impacts (Oropeza and Heath 2013). Communities with single-source water systems would likely value wildfire-related sediment impacts higher than we do in our analysis.

Our results suggest the avoided costs to water supplies from fuels reduction is less than the cost to treat fuels, which corroborates findings from a similar study of the Mokelumne Watershed in California (Buckley et al. 2014; Elliot et al. 2016). Our estimated rates of return for fuel treatment (Table 2.5) are similar in magnitude to the 1 million USD avoided sediment impacts to water supplies for 68 million USD of fuels reduction reported by Buckley et al. (2014). Fuel treatments are only predicted to avoid more impacts to water supplies than they cost given fuel treatments are exposed to both extreme wildfire and extreme rainfall (Jones et al. 2017). Our measure of water supply risk incorporates the likelihood of fuel treatment encountering wildfire over 25 years using modeled burn probability (Short et al. 2016) calibrated

to historical rates of burning (Finney et al. 2011). Increasing fire frequency, however, has the potential to magnify wildfire risk to water supplies (Sankey et al. 2017) and therefore increase the value of proactive fuels reduction. Additionally, our narrow focus on sediment impacts likely underestimates risk to water supplies and undervalues the full suite of fuel treatment benefits. For example, we did not account for potential reductions in post-fire watershed rehabilitation spending, nor avoided home loss within the wildland-urban interface. We also did not account for fuel treatment effects on burn probability. A similar study in Oregon suggests a large fuel treatment program may reduce annual area burned by up to 36% within treated areas, but only 11% across the full landscape. We chose not to quantify this additional benefit of fuel treatment due to the computational demands of burn probability modeling and uncertainty in how burn probability will change with potentially greater grass and shrub production in thinned forests (Reinhardt et al. 2008).

In this study, we did not account for the sediment generated from the direct effects of the fuel treatments and any associated road building. The priority locations we identified for fuel treatments are erosion prone slopes close to main channels, so it is important that the fuel treatments themselves not accelerate erosion. A small increase in erosion over the no treatment scenario (~3%) was predicted from similar fuel treatments in California (Elliot et al. 2016). In Colorado, fuel treatments retain close to 80% surface cover (Libohova 2004), which should avoid large increases in erosion (Larsen et al. 2009). Prescribed fire has the potential to increase erosion but limiting the extent and patch size of high burn severity should minimize impacts (Benavides-Solorio and MacDonald 2005). Much larger increases in sediment production would be expected from expanding the unpaved road network (Libohova 2004). We did not account for new road construction here because we assumed thinning operations would use the existing road

network and costs would increase with skidding distance (Eqn 2.18). Treatment-related sediment may be important to consider if it has the potential to exacerbate chronic sediment issues, but it may not matter if acute sediment impacts following wildfire are the primary concern.

The high cost of forest thinning is a substantial barrier to wildfire risk reduction and forest restoration in the western U.S. (North et al. 2015). This is especially true in our study watersheds due to challenging terrain and the limited market for small diameter materials. It may be possible to offset some cost of treatment by harvesting more large trees, but large (or old) tree harvesting is often controversial (e.g., Sánchez Meador et al. 2015) and sometimes counter to fuel treatment objectives (Agee and Skinner 2005; Reinhardt et al. 2008). Despite higher treatment costs, we found it is more efficient to thin forests on erosion-prone steep slopes. Our analysis also shows that prescribed fire is the most-cost effective and least-feasible treatment in these watersheds (Table 2.4). Due to a lack of local data, we based our prescribed fire effects (Table 2.1) on research from more productive forests with larger trees (Stephens and Moghaddas 2005). This may underestimate prescribed fire effects on canopy fuels in the shorter-statured forests of the Colorado Front Range. Prescribed fire feasibility would increase if managers accept the potential for more extreme fire behavior in remote areas, or where there are barriers to fire spread protecting highly valued resources or assets. More accurate definition of prescribed fire constraints would help to identify where limited investments in thinning could expand the feasibility of prescribed fire. These same analyses could be useful for identifying appropriate conditions to manage wildfire for resource benefit.

2.4.1 Modeling caveats

Linked fire-erosion and sediment transport models can provide quantitative effects measures, but it is important to recognize the uncertainties from linking models (Elliot et al. 2016; Jones et al. 2017), the meager predictive performance of erosion models (Larsen and MacDonald 2007), and the high variability in sediment transport (Wagenbrenner and Robichaud 2014). Our use of crown fire activity as a proxy for fire severity limited the resolution at which we could detect fuel treatment effects. More precise methods for simulating fuel treatments and measuring fire behavior could better differentiate treatment effects (e.g. the value of following thinning with prescribed fire; Martinson and Omi 2013). Previous studies accomplished the link between fire and erosion using predicted fire behavior (Elliot et al. 2016; Jones et al. 2017) or more-detailed ecological models (Miller et al. 2011; Sidman et al. 2016). Confidence in these methods would improve with more understanding of the first-order fire effects on soils in relation to fire intensity, heat per unit area, or residence time (Moody et al. 2013; Shakesby et al. 2016).

Our sediment yield estimates are close to regional field observations, except for possible overprediction of hillslope erosion on very steep slopes (Figure 2.5). This issue may be addressed by process-based erosion models, including WEPP and KINEROS, which are commonly used for post-fire erosion prediction (e.g., Miller et al. 2016; Elliot et al. 2016; Sidman et al. 2016; Jones et al. 2017). RUSLE may also be improved for erosion prediction in steep mountain topography with higher resolution elevation data and alternative flow routing algorithms to avoid the long flow paths mapped by D8 on near planar slopes. Current methods to calculate the LS factor (Winchell et al. 2008) also assign high erosion rates to areas of convergent flow, which aligns with local observations of high erosion in low-order drainages

(Moody and Martin 2001; Pietraszek 2006; Rengers et al. 2016) but also diverges from the original intent of RULSE for predicting erosion from near-planar hillslopes. It is also possible that RUSLE correctly predicts high erosion potential on steep slopes, but sediment yields should be adjusted to reflect sediment supply limitations due to the often poorly developed soils.

Data to validate erosion and sediment transport models beyond the hillslope scale are needed to test the accuracy of these approaches and inform model improvements. Our estimates of sediment transport are coarse approximations of highly dynamic physical processes that we roughly calibrated to sparse regional observations of sediment yields at small catchment and whole watershed scales (Figure 2.5). We emphasized the high SDR scenario in the results, which doubled the predicted hSDR, because it better aligned our net sediment delivery to streams predictions with the small catchment sediment yields from the Hayman Fire (Robichaud et al. 2008, 2013b). However, it is questionable if these limited observations apply to other watersheds and hydrologic conditions. It is also possible that the lack of declining per unit area sediment yield with increasing catchment area at the Hayman Fire (Wagenbrenner and Robichaud 2014) is the result of concentrated erosion in drainage bottoms adding to hillslope sources instead of hillslope sources being transported with high efficiency. The channel transport component of our model relies on coarse approximations of transport efficiency by channel order, which aligns with local observations of efficient sediment transport in high order channels (Moody and Martin 2001; Miller et al. 2017), but ignore other important controls like channel slope, flow conditions, and floodplain connectivity.

We provided only a cursory analysis of post-fire rainfall because of its high spatial and temporal variability and therefore low utility for spatially characterizing risk. Ideally, a full accounting of risk would consider joint probabilities of fire occurrence, severity, and post-fire

rainfall conditions over several years of recovery (e.g. Jones et al. 2014). We also did not discount avoided sediment impacts to net present value. Assuming equal probability of fire over the 25-year planning period and a 3% interest rate, our risk reduction estimates should be reduced approximately 30%. We used burn probability to represent the spatial and temporal variability in wildfire occurrence (Scott et al. 2013), which limits our ability to quantify wildfire consequences that are tied to fire and storm magnitudes, such as exceeding thresholds for water treatment (Oropeza and Heath 2013; Hohner et al. 2016). Simulation-based risk analysis methods (Thompson et al. 2016; Haas et al. 2017) could be used to better quantify the fuels reduction effects on fire event consequences and probabilities for exceeding thresholds of impact.

2.4.2 Management implications and future directions

Spatial fuel treatment optimization can improve the efficiency of fuels reduction for water supply protection. However, fuel treatment is not expected to produce a positive return on investment when only considering avoided sediment impacts to water supplies (this study; Buckley et al. 2014; Elliot et al. 2016). Wildfire risk assessment is an important first step to appraise risk and develop risk reduction goals. Evaluating fuel treatment effects can inform whether fuels reduction should be part of a risk mitigation strategy and where in the watershed it will be most effective. Previous assessments show that most of the economic benefit of fuel treatment is from reduced suppression costs and avoided damage to homes and infrastructure (Buckley et al. 2014; Talberth et al. 2013; Thompson et al. 2013c). Water providers are often interested in these and other co-benefits of fuels reduction (Jones et al. 2017). In many cases, public agencies support these benefits by matching water provider investments (Ozment et al. 2016). Identifying where water supply protection goals align with other ecosystem restoration, risk reduction, and fire management objectives may provide opportunities to further leverage

funding. Ideally, fuel treatment contributes to landscape conditions that allow more natural or prescribed fires to maintain and expand the footprint of low fuel conditions. Efforts to identify where limited investments in forest thinning will support the use of prescribed or managed fire may be more cost-effective than using it alone as an area-wide treatment. Coordination among forest and fire managers is needed to understand how and where fuels reduction can facilitate more beneficial fire on the landscape.

2.5 CONCLUSION

Our study suggests that combining fuel treatment effectiveness measures and constraints in an optimization framework has potential to improve fuel treatment targeting for water supply protection. Moreover, the framework facilitates program-level assessment of potential risk reduction and fuel treatment costs, which can help interested stakeholders frame risk reduction goals and evaluate the efficacy of fuels reduction compared to alternative risk reduction strategies. There are many uncertainties in the data used to parameterize the models and to evaluate the risk reduction to water supplies from fuel treatments, but our estimate that risk reduction is much smaller than the cost of treatment closely matches results from a similar study in California (Buckley et al. 2014; Elliot et al. 2016). This raises questions about the economic efficiency of mitigating wildfire risk to water supplies with area-wide fuel treatment. It also highlights the needs to expand more cost-effective fuel treatment methods and identify where water supply protection priorities overlap with other wildfire risk reduction and ecological restoration objectives.

REFERENCES FOR CHAPTER 2

Agee JK, Skinner CN (2005) Basic principles of forest fuel reduction treatments. *Forest Ecology and Management* **211**, 83-96. doi:10.1016/j.foreco.2005.01.034

Ager AA, Vaillant NM, McMahan A (2013) Restoration of fire in managed forests: a model to prioritize landscapes and analyze trade-offs. *Ecosphere* **4**, 1-19. doi:10.1890/ES13-00007.1

Benavides-Solorio JD, MacDonald LH (2001) Post-fire runoff and erosion from simulated rainfall on small plots, Colorado Front Range. *Hydrological Processes* **15**, 2931-2952. doi:10.1002/hyp.383

Benavides-Solorio JD, MacDonald LH (2005) Measurement and prediction of post-fire erosion at the hillslope scale, Colorado Front Range. *International Journal of Wildland Fire* **14**, 457-474. doi:10.1071/WF05042

Michel Berkelaar and others (2015) lpSolve: Interface to 'Lp_solve' v. 5.5 to Solve Linear/Integer Programs, R package version 5.6.12 [Software]. Available from https://CRAN.R-project.org/package=lpSolve

Bradshaw L, McCormick E (2000) FireFamily Plus user's guide, version 2.0. USDA Forest Service, Rocky Mountain Research Station, General Technical Report RMRS-GTR-67WWW. (Ogden, UT, USA)

Breiby T (2006) Assessment of soil erosion risk within a subwatershed using GIS and RUSLE with a comparative analysis of the use of STATSGO and SSURGO soil databases. Papers in Resource Analysis, Volume 8. Saint Mary's University of Minnesota Central Services Press. pp. 1-22. (Saint Mary's University of Minnesota Central Services Press: Winona, MN, USA)

Brune GM (1953) Trap efficiency of reservoirs. *Transactions - American Geophysical Union* **34**, 407-418. doi:10.1029/TR034i003p00407

Buckley M, Beck N, Bowden P, Miller ME, Hill B, Luce C, Elliot WJ, Enstice N, Podolak K, Winford E, Smith SL, Bokach M, Reichert M, Edelson D, Gaither J (2014) Mokelumne watershed avoided cost analysis: why Sierra fuel treatments make economic sense. A report prepared for the Sierra Nevada Conservancy, The Nature Conservancy, and USDA Forest Service. Sierra Nevada Conservancy. (Auburn, CA, USA)

Caggiano MD (2017) Front Range round table 2016 interagency fuel treatment database. Colorado Forest Restoration Institute Technical Report CFRI-1701. (Fort Collins, CO, USA)

Caggiano MD, Tinkham WT, Hoffman C, Cheng AS, Hawbaker TJ (2016) High- resolution mapping of development in the wildland–-urban interface using object- based image extraction. *Heliyon* **2**, e00174. doi:10.1016/j.heliyon.2016.e00174

Cannon SH, Gartner JE, Rupert MG, Michael JA, Rea AH, Parrett C (2010) Predicting the probability and volume of post-wildfire debris flows in the intermountain western United States. *Geological Society of America Bulletin* **122**, 127-144. doi:10.1130/B26459.1

Crosby JS, Chandler CC (1966) Get the most from your windspeed observation. *Fire Control Notes* **27**, 12-13.

Dabney S (2016) Rainfall intensity summarization tool (RIST), version 3.96. USDA Agricultural Research Service, National Sedimentation Laboratory. (Oxford, MS, USA)

DeBano LF, Neary DG, Ffolliott PF (2005) Soil physical processes. In 'Wildland fire in ecosystems: effects of fire on soils and water'. (Eds DG Neary, KC Ryan, LF DeBano)

USDA Forest Service, Rocky Mountain Research Station, General Technical Report RMRS-GTR-42-Vol. 4. (Eds DG Neary, KC Ryan, LF DeBano) pp. 29-51. (Ogden, UT, USA)
Elliot WJ, Miller ME, Enstice N (2016) Targeting forest management through fire and erosion modelling. *International Journal of Wildland Fire* **25**, 876-887. doi:10.1071/WF15007
ESRI (2015) ArcGIS software, version 10.3 [Software]. Available from https://www.esri.com/en-us/home (Redlands, CA, USA)
Fernandez C, Wu JQ, McCool DK, Stöckle CO (2003) Estimating water erosion and sediment yield with GIS, RUSLE, and SEDD. *Journal of Soil and Water Conservation* **58(3)**, 128-136.
Ferro V, Porto P (2000) Sediment Delivery Distributed (SEDD) Model. *Journal of Hydrologic Engineering* **5(4)**, 411-422.
Finney M, Grenfell IC, McHugh CW (2009) Modeling containment of large wildfires using generalized linear mixed-model analysis. *Forest Science* **55**, 249-255.
Finney MA, McHugh CW, Grenfell IC, Riley KL, Short KC (2011) A simulation of probabilistic wildfire risk components for the continental United States. *Stochastic Environmental Research and Risk Assessment* **25**, 973-1000. doi:10.1007/s00477-011-0462-z
Finney MA, Brittain S, Seli RC, McHugh CW, Gangi L (2015) FlamMap: fire mapping and analysis system (version 5.0) [Software]. Available from http://www.firelab.org/document/flammap-software
Francis D, Ex S, Hoffman C (2018) Stand composition and aspect are related to conifer regeneration densities following hazardous fuels treatments in Colorado, USA. *Forest Ecology and Management* **409(1)**, 417-424. doi:10.1016/j.foreco.2017.11.053
Frickel DG, Shown LM, Patton PC (1975) An evaluation of hillslope and channel erosion related to oil-shale development in the Piceance basin, north-western Colorado. Colorado Department of Natural Resources, Colorado Water Resources Circular 30. (Denver, CO, USA)
Fulé PZ, Crouse JE, Roccaforte JP, Kalies EL (2012) Do thinning and/or burning treatments in the western USA ponderosa or Jeffrey pine-dominated forests help restore natural fire behavior? *Forest Ecology and Management* **269**, 68-81. doi:10.1016/j.foreco.2011.12.025
Graham RT (2003) Hayman Fire case study. USDA Forest Service, Rocky Mountain Research Station, General Technical Report RMRS-GTR-114. (Ogden, UT, USA)
Graham RT, McCaffrey S, Jain TB (2004) Science basis for changing forest structure to modify wildfire behavior and severity. USDA Forest Service, Rocky Mountain Research Station, General Technical Report RMRS-GTR-120. (Fort Collins, CO, USA)
Haas JR, Calkin DE, Thompson MP (2015) Wildfire risk transmission in the Colorado Front Range, USA. *Risk Analysis* **35(2)**, 226-240. doi:10.1111/risa.12270
Haas JR, Thompson M, Tillery A, Scott JH (2017) Capturing spatiotemporal variation in wildfires for improving post-wildfire debris-flow hazard assessments. In 'Natural hazard uncertainty assessment: modeling and decision support, geophysical monograph 223'. (Eds K Riley, P Webley, M Thompson) p. 301-317. (John Wiley & Sons: Hoboken, NJ, USA)
Henkle JE, Wohl E, Beckman N (2011) Locations of channel heads in the semiarid Colorado Front Range, USA. *Geomorphology* **129**, 309-319. doi:10.1016/j.geomorph.2011.02.026
Hohner AK, Terry LG, Townsend EB, Summers RS, Rosario-Ortiz FL (2017) Water treatment process evaluation of wildfire-affected sediment leachates. *Environmental Science: Water Research & Technology* **3**, 352-365. doi:10.1039/C6EW00247A

Huber-Stearns HR (2015) Investments in watershed services: understanding a new arena of environmental governance in the western United States. PhD dissertation. Colorado State University. (Fort Collins, CO, USA)

Jones OD, Nyman P, Sheridan GJ (2014) Modelling the effects of fire and rainfall regimes on extreme erosion events in forested landscapes. *Stochastic Environmental Research and Risk Assessment* **28**, 2015-2025. doi:10.1007/s00477-014-0891-6

Jones KW, Cannon JB, Saavedra FA, Kampf SK, Addington RN, Cheng AS, MacDonald LH, Wilson C, Wolk B (2017) Return on investment from fuel treatments to reduce severe wildfire and erosion in a watershed investment program in Colorado. *Journal of Environmental Management* **198**, 66-77. doi:10.1016/j.jenvman.2017.05.023

Kampf SK, Brogan DJ, Schmeer S, MacDonald LH, Nelson PA (2016) How do geomorphic effects of rainfall vary with storm type and spatial scale in a post-fire landscape? *Geomorphology* **273**, 39-51. doi:10.1016/j.geomorph.2016.08.001

LANDFIRE (2016) Fuel, topography, existing vegetation type, and fuel disturbance layers, LANDFIRE 1.4.0., U.S. Geological Survey. Available from http://landfire.cr.usgs.gov/viewer/

Larsen IJ, MacDonald LH (2007) Predicting post-fire sediment yields at the hillslope scale: testing RUSLE and disturbed WEPP. *Water Resources Research* **43**, W11412. doi:10.1029/2006WR005560

Larsen IJ, MacDonald LH, Brown E, Rough D, Welsh MJ, Pietraszek JH, Libohova Z, Benavides-Solorio JD, Schaffrath K (2009) Causes of post-fire runoff and erosion: water repellency, cover, or soil sealing? *Soil Science Society of America Journal* **73**, 1393-1407. doi:10.2136/sssaj2007.0432

Libohova Z (2004) Effects of thinning and a wildfire on sediment production rates, channel morphology, and water quality in the Upper South Platte River Watershed. Thesis. Colorado State University. (Fort Collins, CO, USA.)

Litschert SE, Theobald DM, Brown TC (2014) Effects of climate change and wildfire on soil loss in the Southern Rockies ecoregion. *Catena* **118**, 206-219. doi:10.1016/j.catena.2014.01.007

Martin DA (2016) At the nexus of fire, water and society. Philosophical Transactions of the Royal Society of London. Series B, *Biological Sciences* **371**, 20150172. doi:10.1098/rstb.2015.0172

Martinson EJ, Omi PN (2013) Fuel treatments and fire severity: a meta-analysis. USDA Forest Service, Rocky Mountain Research Station, Research Paper RMRS-RP-103WWW. (Fort Collins, CO, USA)

McCool DK, Foster GR, Mutchler CK, Meyer LD (1989) Revised slope length factor for the Universal Soil Loss Equation. *Transactions of the American Society of Agricultural Engineers* **32**, 1571-1576. doi:10.13031/2013.31192

McCuen RH (1998) 'Hydrologic analysis and design, – second 2nd edition.' (Prentice-Hall: New Jersey, NJ, USA)

Miller JD, Nyhan JW, Yool SR (2003) Modeling potential erosion due to the Cerro Grande Fire with a GIS-based implementation of the Revised Universal Soil Loss Equation. *International Journal of Wildland Fire* **12**, 85-100. doi:10.1071/WF02017

Miller ME, MacDonald LH, Robichaud PR, Elliot WJ (2011) Predicting post-fire hillslope erosion in forest lands of the western United States. *International Journal of Wildland Fire* **20**, 982-999. doi:10.1071/WF09142

Miller ME, Elliot WJ, Billmire M, Robichaud PR, Endsley KA (2016) Rapid-response tools and datasets for post-fire remediation: linking remote sensing and process-based hydrological models. *International Journal of Wildland Fire* **25**, 1061-1073. doi:10.1071/WF15162

Miller S, Rhodes C, Robichaud P, Ryan S, Kovecses J, Chambers C, Rathburn S, Heath J, Kampf S, Wilson C, Brogan D, Piehl B, Miller ME, Giordanengo J, Berryman E, Rocca M (2017) Learn from the burn: the High Park Fire 5 years later. USDA Forest Service, Rocky Mountain Research Station, Science You Can Use Bulletin, Issue 25. (Fort Collins, CO, USA)

Monitoring Trends in Burn Severity (MTBS) (2015) Large fire perimeter dataset – 1984-2015. USDA Forest Service and U.S. Geological Survey. Available from http://mtbs.gov/direct-download

Moody JA, Martin DA (2001) Initial hydrologic and geomorphic response following a wildfire in the Colorado Front Range. *Earth Surface Processes and Landforms* **26**, 1049-1070. doi:10.1002/esp.253

Moody JA, Martin DA (2009) Synthesis of sediment yields after wildland fire in different rainfall regimes in the western United States. *International Journal of Wildland Fire* **18**, 96-115. doi:10.1071/WF07162

Moody JA, Shakesby RA, Robichaud PR, Cannon SH, Martin DA (2013) Current research issues related to post-wildfire runoff and erosion processes. *Earth-Science Reviews* **122**, 10-37. doi:10.1016/j.earscirev.2013.03.004

Nearing MA (1997) A single, continuous function for slope steepness influence on soil loss. *Soil Science Society of America Journal* **61**, 917-919. doi:10.2136/sssaj1997.03615995006100030029x

North M, Brough A, Long J, Collins B, Bowden P, Yasuda D, Miller J, Sugihara N (2015) Constraints on mechanized treatment significantly limit mechanical fuels reduction extent in the Sierra Nevada. *Journal of Forestry* **113**, 40-48. doi:10.5849/jof.14-058

NRCS Soil Survey Staff (2016) Web soil survey. USDA Natural Resources Conservation Service. Available online at: https://websoilsurvey.nrcs.usda.gov/

Nunes JP, Doerr SH, Sheridan G, Neris J, Santín C, Emelko MB, Silins U, Robichaud PR, Elliot WJ, Keizer J (2018) Assessing water contamination risk from vegetation fires: challenges, opportunities and a framework for progress. *Hydrological Processes* **32**, 687-694. doi:10.1002/hyp.11434

Oropeza J, Heath J (2013) Effects of the 2012 Hewlett and High Park Wildfires on water quality of the Poudre River and Seaman Reservoir. City of Fort Collins Utilities Report. (Fort Collins, CO, USA)

Ozment S, Gartner T, Huber-Stearns H, Difrancesco K, Lichten N, Tognetti S (2016) Protecting drinking water at the source: lessons learned from watershed investment programs in the United States. World Resources Institute Report. (Washington, DC, USA)

Peet RK (1981) Forest vegetation of the Colorado Front Range. *Vegetatio* **45**, 3-75. doi:10.1007/BF00240202

Perica S, Martin D, Pavlovic S, Roy I, St. Laurent M, Trypaluk C, Unruh D, Yekta M, Bonnin G (2013) 'NOAA Atlas 14, Volume 8 Version 2, precipitation-frequency atlas of the United States, Midwestern States.' (Silver Spring, MD, USA).

Pierson FB, Williams CJ (2016) Ecohydrologic impacts of rangeland fire on runoff and erosion: a literature synthesis. USDA Forest Service, Rocky Mountain Research Station, General Technical Report RMRS-GTR-351. (Fort Collins, CO, USA)

Pietraszek JH (2006) Controls on post-fire erosion at the hillslope scale, Colorado Front Range. Thesis. Colorado State University. (Fort Collins, CO, USA)

PRISM Climate Group (2016) 30-year monthly precipitation normals. Oregon State University. Available online at: http://prism.oregonstate.edu

R Core Team (2019) R: A language and environment for statistical computing [Software]. R Foundation for Statistical Computing, Vienna, Austria. Available from https://www.R-project.org/

Reinhardt ED, Keane RE, Calkin DE, Cohen JD (2008) Objectives and considerations for wildland fuel treatment in forested ecosystems of the interior western United States. *Forest Ecology and Management* **256**, 1997-2006. doi:10.1016/j.foreco.2008.09.016

Renard KG, Foster GR, Weesies GA, McCool DK, Yoder DC (1997) Predicting soil erosion by water: a guide to conservation planning with the Revised Universal Soil Loss Equation (RUSLE). USDA Agricultural Research Service Agricultural Handbook no. 703. (Washington, DC, USA)

Rengers FK, Tucker GE, Moody JA, Ebel BA (2016) Illuminating wildfire erosion and deposition patterns with repeat terrestrial lidar. *Journal of Geophysical Research: Earth Surface* **121**, 588-608. doi:10.1002/2015JF003600

Rhodes JJ, Baker WL (2008) Fire probability, fuel treatment effectiveness and ecological tradeoffs in western U.S. public forests. *The Open Forest Science Journal* **1**, 1-7. doi:10.2174/1874398600801010001

Robichaud PR, Wagenbrenner JW, Brown RE, Wohlgemuth PM, Beyers JL (2008) Evaluating the effectiveness of contour-felled log erosion barriers as a post-fire runoff and erosion mitigation treatment in the western United States. *International Journal of Wildland Fire* **17**, 255-273. doi:10.1071/WF07032

Robichaud PR, Lewis SA, Wagenbrenner JW, Ashmun LE, Brown RE (2013a) Post-fire mulching for runoff and erosion mitigation. Part I: effectiveness at reducing hillslope erosion rates. *Catena* **105**, 75-92. doi:10.1016/j.catena.2012.11.015

Robichaud PR, Wagenbrenner JW, Lewis SA, Ashmun LE, Brown RE, Wohlgemuth PM (2013b) Post-fire mulching for runoff and erosion mitigation. Part II: effectiveness in reducing runoff and sediment yields from small catchments. *Catena* **105**, 93-111. doi:10.1016/j.catena.2012.11.016

Ryan SE, Dwire KA, Dixon MK (2011) Impacts of wildfire on runoff and sediment loads at Little Granite Creek, western Wyoming. *Geomorphology* **129**, 113-130. doi:10.1016/j.geomorph.2011.01.017

Sánchez Meador AJ, Waring KM, Kalies EL (2015) Implications of diameter caps on multiple forest resource responses in the context of the Four Forests Restoration Initiative: results from the Forest Vegetation Simulator. *Journal of Forestry* **113**, 219-230. doi:10.5849/jof.14-021

Sankey JB, Kreitler J, Hawbaker TJ, McVay JL, Miller ME, Mueller ER, Vaillant NM, Lowe SE, Sankey TT (2017) Climate, wildfire, and erosion ensemble foretells more sediment in western USA watersheds. *Geophysical Research Letters* **44**, 8884-8892. doi:10.1002/2017GL073979

Schmeer SR (2014) Post-fire erosion response and recovery, High Park Fire, Colorado. MS Thesis. Colorado State University. (Fort Collins, CO, USA)

Schmeer SR, Kampf SK, MacDonald LH, Hewitt J, Wilson C (2018) Empirical models of annual post-fire erosion on mulched and unmulched hillslopes. *Catena* **163**, 276-287. doi:10.1016/j.catena.2017.12.029

Scott JH, Burgan RE (2005) Standard fire behavior fuel models: a comprehensive set for use with Rothermel's surface fire spread model. USDA Forest Service, Rocky Mountain Research Station, General Technical Report RMRS-GTR-153. (Fort Collins, CO, USA)

Scott J, Helmbrecht D, Thompson MP, Calkin DE, Marcille K (2012) Probabilistic assessment of wildfire hazard and municipal watershed exposure. *Natural Hazards* **64**, 707-728. doi:10.1007/s11069-012-0265-7

Scott JH, Reinhardt ED (2001) Assessing crown fire potential by linking models of surface and crown fire behavior. USDA Forest Service, Rocky Mountain Research Station, General Technical Research Paper RMRS-RP-29. (Fort Collins, CO, USA)

Scott JH, Thompson MP, Calkin DE (2013) A wildfire risk assessment framework for land and resource management. USDA Forest Service, Rocky Mountain Research Station, General Technical Report RMRS-GTR-315. (Fort Collins, CO, USA)

Shakesby RA, Doerr SH (2006) Wildfire as a hydrological and geomorphological agent. *Earth-Science Reviews* **74**, 269-307. doi:10.1016/j.earscirev.2005.10.006

Shakesby RA, Moody JA, Martin DA, Robichaud PR (2016) Synthesising empirical results to improve predictions of post-wildfire runoff and erosion response. *International Journal of Wildland Fire* **25**, 257-261. doi:10.1071/WF16021

Sherriff RL, Platt RV, Veblen TT, Schoennagel TL, Gartner MH (2014) Historical, observed, and modeled wildfire severity in montane forests of the Colorado Front Range. *PLoS One* **9**, e106971. doi:10.1371/journal.pone.0106971

Short KC, Finney MA, Scott JH, Gilbertson-Day JW, Grenfell IC (2016) Spatial dataset of probabilistic wildfire risk components for the conterminous United States. USDA Forest Service Research Data Archive. (Fort Collins, CO, USA) doi:10.2737/RDS-2016-0034. (Fort Collins, CO)

Sidman G, Guertin DP, Goodrich DC, Thoma D, Falk D, Burns IS (2016) A coupled modelling approach to assess the effect of fuel treatments on post-wildfire runoff and erosion. *International Journal of Wildland Fire* **25**, 351-362. doi:10.1071/WF14058

Stephens SL, Moghaddas JJ (2005) Experimental fuel treatment impacts on forest structure, potential fire behavior, and predicted tree mortality in a California mixed- conifer forest. *Forest Ecology and Management* **215**, 21-36. doi:10.1016/j.foreco.2005.03.070

Stephens SL, Moghaddas JJ, Edminster C, Fielder CE, Haase S, Harrington M, Keeley JE, Knapp EE, McIver JD, Metlen K, Skinner CN, Youngblood A (2009) Fire treatment effects on vegetation structure, fuels, and potential fire severity in western U.S. forests. *Ecological Applications* **19**, 305-320. doi:10.1890/07-1755.1

Talberth J, Mulligan J, Bird B, Gartner T (2013) A preliminary green–-gray analysis for the Cache la Poudre and Big Thompson watersheds of Colorado's Front Range. Center for Sustainable Economy and World Resource Institute Report. 21 p.

Theobald DM, Merritt DM, Norman JB (2010) Assessment of threats to riparian ecosystems in the western U.S. Report to the Western Environmental Threats Assessment Center, Prineville, OR by the USDA Stream Systems Technology Center and Colorado State University. (Fort Collins, CO, USA)

Thompson MP, Scott J, Helmbrecht D, Calkin DE (2013a) Integrated wildfire risk assessment: framework development and application on the Lewis and Clark National Forest in Montana,

USA. *Integrated Environmental Assessment and Management* **9**, 329-342. doi:10.1002/ieam.1365

Thompson MP, Scott J, Langowski PG, Gilbertson-Day JW, Haas JR, Bowne EM (2013b) Assessing watershed -wildfire risks on national forest system lands in the Rocky Mountain region of the United States. *Water* **5**, 945-971. doi:10.3390/w5030945

Thompson MP, Vaillant NM, Haas JR, Gebert KM, Stockmann KD (2013c) Quantifying the potential impacts of fuel treatments on wildfire suppression costs. *Journal of Forestry* **111**, 49-58. doi:10.5849/jof.12-027

Thompson MP, Gilbertson-Day JW, Scott JH (2016) Integrating pixel- and polygon-based approaches to wildfire risk assessment: applications to a high-value watershed on the Pike and San Isabel National Forests, Colorado, USA. *Environmental Modeling and Assessment* **21**, 1-15. doi:10.1007/s10666-015-9469-z

Thompson MP, Riley K, Loeffler D, Haas JR (2017) Modeling fuel treatment leverage: encounter rates, risk reduction, and suppression cost impacts. *Forests* **8**, 469. doi:10.3390/f8120469

Tillery AC, Haas JR, Miller LW, Scott JH, Thompson MP (2014) Potential post-wildfire debris-flow hazards - a pre-wildfire evaluation for the Sandia and Manzano Mountains and surrounding areas, central New Mexico. US Geological Survey Scientific Investigations Report 2014-5161. (Albuquerque, NM, USA)

Tinkham WT, Hoffman CM, Ex SA, Battaglia MA, Saralecos JD (2016) Ponderosa pine forest restoration treatment longevity: implications of regeneration on fire hazard. *Forests* **7**, 137. doi:10.3390/f7070137

Toy TJ, Foster GR (1998) Guidelines for the use of the Revised Universal Soil Loss Equation (RUSLE) version 1.06 on mined lands, construction sites, and reclaimed lands. Office of Surface Mining and Reclamation (OSM), Western Regional Coordinating Center. (Denver, CO, USA)

US Environmental Protection Agency (USEPA) and the US Geological Survey (USGS) (2012) National Hydrography Dataset Plus - NHDPlus. Version 2.1. Available online at: http://www.horizon-systems.com/NHDPlus/index.php

USDA Forest Service (2018) Toward shared stewardship across landscapes: an outcome-based investment strategy. USDA Forest Service Report FS-118. (Washington, DC, USA)

Wagenbrenner JW, MacDonald LH, Rough D (2006) Effectiveness of three post-fire rehabilitation treatments in the Colorado Front Range. *Hydrological Processes* **20**, 2989-3006. doi:10.1002/hyp.6146

Wagenbrenner JW, Robichaud PR (2014) Post-fire bedload sediment delivery across spatial scales in the interior western United States. *Earth Surface Processes and Landforms* **39**, 865-876. doi:10.1002/esp.3488

Walling DE (1983) The sediment delivery problem. *Journal of Hydrology* **65**, 209-237. doi:10.1016/0022-1694(83)90217-2

Wilson C, Kampf SK, Wagenbrenner JW, MacDonald LH (2018) Rainfall thresholds for post-fire runoff and sediment delivery from plot to watershed scales. *Forest Ecology and Management* **430**, 346-356. doi:10.1016/j.foreco.2018.08.025

Winchell MF, Jackson SH, Wadley AM, Srinivasan R (2008) Extension and validation of a geographic information system-based method for calculating the Revised Universal Soil Loss Equation length-slope factor for erosion risk assessments in large watersheds. *Journal of Soil and Water Conservation* **63**, 105-111. doi:10.2489/jswc.63.3.105

Wohl E (2013) Migration of channel heads following wildfire in the Colorado Front Range, USA. *Earth Surface Processes and Landforms* **38**, 1049-1053. doi:10.1002/esp.3429

Yang D, Kanae S, Oki T, Koike T, Musiake K (2003) Global potential soil erosion with reference to land use and climate changes. *Hydrological Processes* **17**, 2913-2928. doi:10.1002/hyp.1441

Yochum SE, Norman J (2014) West Fork Complex Fire: potential increase in flooding and erosion. USDA Natural Resources Conservation Service Report. (Denver, CO, USA)

Yochum SE, Norman JB (2015) Wildfire-induced flooding and erosion-potential modeling: examples from Colorado, 2012 and 2013. In 'Proceedings of the 3rd joint federal interagency conference on sedimentation and hydrologic modeling'. pp. 953-964. (Reno, NV, USA)

Ziegler JP, Hoffman C, Battaglia M, Mell W (2017) Spatially explicit measurements of forest structure and fire behavior following restoration treatments in dry forests. *Forest Ecology and Management* **386**, 1-12. doi:10.1016/j.foreco.2016.12.002

CHAPTER 3 – SYSTEM ANALYSIS OF WILDFIRE-WATER SUPPLY RISK WITH MONTE CARLO WILDFIRE AND RAINFALL SIMULATION

3.1 INTRODUCTION

Wildfire is a growing concern in source water management due to high profile incidents of infrastructure and water quality impairment (Smith et al. 2011; Martin 2016) and the potential for increasing wildfire activity to exacerbate the problem (Sankey et al. 2017). To improve awareness and inform broad mitigation strategies, factors controlling wildfire occurrence and intensity, watershed response, and water utilization have been combined to map relative measures of wildfire-water supply risk across large regions (Thompson et al. 2013b; Robinne et al. 2019). Wildfire-watershed simulation models have also been used to quantify the economic risk of reservoir sedimentation and the mitigation effectiveness of reducing fuels in source watersheds (Buckley et al. 2014; Elliot et al. 2016; Jones et al. 2017). In contrast, the risk of water quality impairment (hereafter "impairment risk") remains poorly quantified despite recognition that water quality impairment is usually the most significant short-term water management challenge after wildfire (Sham et al. 2013). Most worrisome is the potential for wildfire to disrupt municipal water supply (hereafter "disruption risk") by severely impairing one or more critical sources. Analyzing disruption risk requires improvements to physical modeling of contaminant mobilization, transport, and dilution to assess water supply impairment (Nunes et al. 2018) and a systems perspective to evaluate impairment consequences for communities with multiple sources.

Impairment risk is a function of spatially and temporally variable wildfire and rainfall activity, which must overlap in space and time with sufficient magnitude to mobilize problematic

quantities of contaminants into source waterbodies. Jones et al. (2014) explored the frequency of this interaction for rainstorms above a typical threshold for debris flow occurrence in Australia using a germ-grain model. This is a convenient method to account for spatial and temporal variability in wildfire and rainfall, but their simplifying assumptions of uniform erosion potential and water supply exposure ignore the considerable spatial variability in erosion and sediment transport potential present in real watersheds (e.g., Elliot et al. 2016, Chapter 2). Water quality impacts also depend on the size of the receiving water body and its ability to dilute contaminants below thresholds of concern for water treatment (Smith et al. 2011; Nunes et al. 2018; Robinne et al. 2019); thus, the magnitude of problematic wildfire and rainfall activity should vary based on reservoir volume or stream flow. Furthermore, source water redundancy has been identified as a promising strategy to mitigate risk of water supply disruption (Smith et al. 2011; Sham et al. 2013; Writer et al. 2014; Murphy et al. 2015; Martin 2016), highlighting the need for a systems perspective when assessing wildfire-water supply risks. Risk assessment should therefore account for the spatial and temporal occurrence of wildfire and rainfall and their joint effects on erosion and sediment transport, water supply exposure and susceptibility to water quality degradation, and the resulting consequences for system performance.

Wildfire risk assessment methods developed for land and resource management (Finney 2005, Scott et al. 2013) are ill-suited for quantifying impairment risk because fire exposure and consequences are evaluated independently for small units of the landscape. Fire likelihood is represented in this framework by flattening the stochastically simulated spatial and temporal occurrence of wildfire into an ensemble burn probability raster, thus precluding consideration of fire size, which is known to influence the magnitude of watershed response (Cannon et al. 2010). Despite these limitations, conventional wildfire risk assessment methods are still a viable option

to inform mitigation planning at broad spatial and temporal scales (e.g., Thompson et al. 2013b) and to assess risks, such as reservoir sedimentation, that are relatively insensitive to individual event magnitudes (Elliot et al. 2016; Jones et al. 2017). Monte Carlo simulation methods that focus instead on characterizing the frequency distribution of fire consequences for many discrete wildfire events are better suited for assessing risks that depend on fire size, and more generally, for characterizing the likelihood of rare but high consequence fires (Thompson et al. 2017)**.** Stochastic simulation has been used to characterize the potential variability in area burned and watershed response magnitude due to biophysical drivers of fire occurrence and post-fire erosion (Thompson et al. 2013b, 2016; Tillery et al. 2014; Haas et al. 2017). Event-based Monte Carlo methods are particularly attractive for their ability to simulate frequency distributions of disturbance magnitudes that can be used for traditional engineering risk and reliability analyses (Singh et al. 2007).

The primary stochastic drivers of impairment risk are wildfire and rainfall activity, but previous assessments have either ignored rainfall characteristics entirely (Thompson et al. 2013b) or accounted for their influence by reporting variation in watershed response for several rainfall return intervals (Haas et al. 2017; Jones et al. 2017; Gannon et al. 2019). Empirical studies have found that rainfall metrics are often the second most important predictor of post-fire erosion after percent bare soil (Benavides-Solorio and MacDonald 2005; Schmeer et al. 2018) and rainfall frequency, depth, intensity, seasonality, and consistency are known to influence erosion mechanisms and magnitudes across broad regions (Moody and Martin 2009). In our study region – the U.S. Southern Rockies – most erosion is associated with summer convective thunderstorms (Benavides-Solorio and MacDonald 2005) that have high spatial and temporal variability in occurrence and magnitude (Wagenbrenner et al. 2006; Murphy et al. 2015; Kampf

et al. 2016). Incorporating rainfall uncertainty into impairment risk analyses is critical for accurate assessment of the potential variability in watershed response to wildfire.

Wildfire impacts to water quality include increased sediment, carbon, nitrogen, heavy metals, and other contaminants of concern, which can render water expensive to treat or unusable when contaminant concentrations exceed thresholds for effective treatment (Smith et al. 2011; Abraham et al. 2017; Nunes et al. 2018). Water erosion is the dominant process mobilizing post-fire contaminants, especially in montane watersheds (Smith et al. 2011; Abraham et al. 2017; Nunes et al. 2018); hence, spatially-explicit erosion models are commonly employed in pre- and post-fire contexts to characterize the potential contaminant sources and magnitudes across heterogenous watersheds (e.g. Elliot et al. 2016; Miller et al. 2016). In our study region, surface water treatment systems are poorly adapted to high concentrations of suspended sediment, which can interfere with conveyance, filtration, and treatment (Smith et al. 2011; Sham et al. 2013). Suspended sediment is also a reasonable proxy in our study region for other contaminants of concern because carbon and nitrogen concentrations tend to co-vary with suspended sediment in response to intense rainfall (Murphy et al. 2015).

Quantifying impairment risk in terms of contaminant concentration exceedances provides a clear means to account for varying water supply susceptibility to post-fire impacts, because receiving water body size controls concentration. By including water yield in their source exposure index, Robinne et al. (2019) were able to represent the effect of waterbody size on contaminant dilution to show that small communities, which primarily source their water from small watersheds, are most exposed to wildfire hazards. Quantitative predictions of contaminant yield from post-fire erosion could be used for direct evaluation of water quality impairment by calculating contaminant concentration in the receiving waterbody and comparing it to common

water quality standards (Smith et al. 2011). This is similar to methods used to analyze the potential water treatment impacts of the Fourmile Canyon Fire based on post-fire water quality observations (Murphy et al. 2015). It is also consistent with the use of instream turbidity monitors to avoid the intake of impaired water after the High Park Fire (Oropeza and Heath 2013). This evaluation framework could also incorporate different water quality thresholds owing to variation in other infrastructure characteristics or use (e.g., municipal, agricultural, or hydropower).

Wildfire-water supply risk assessment has so far lacked a systems perspective for evaluating the consequences of water quality impairment despite the demonstrated utility of alternative sources for moderating wildfire impacts (Writer et al. 2014) and recommendations for this as an approach to engineer water system reliability (Sham et al. 2013; Murphy et al. 2015; Martin 2016). Due to the limitations with ensemble burn probability-based wildfire risk assessment discussed previously, it is difficult to incorporate water system characteristics into effects analyses beyond measures of infrastructure importance and sensitivity to post-fire contaminants (Chapter 2). Event-based simulation is better suited for systems risk analysis because wildfire exposure and post-fire water quality can be tracked across component water supplies to determine their impairment states, and the resulting consequence for system performance can be evaluated in light of the component states and functions (Haimes 2012). The critical contribution of event-based simulation is to define the joint probabilities of impairment across system components, which would take centuries to accurately define from observational data. This systems assessment framework can represent both redundancies, such as alternative water sources, and dependencies, such as conveyance paths with multiple impact points. Beyond

improved risk assessment for complex water systems, a systems assessment framework could be used to test the effects of operational or infrastructure changes on water supply reliability.

Here we demonstrate an event-based Monte Carlo simulation risk analysis method to estimate the probability of water impairment and system supply disruption. We focus on a multi-source water system in Colorado as a test case. To account for key uncertainties, we combine 10000 years of stochastically simulated wildfire and rainfall activity to model post-storm turbidity for water supply streams and reservoirs with coupled burn severity, erosion and sediment transport models. We then assess impairment risk for individual water supplies as the annual probability of exceeding suspended sediment thresholds for water treatment. System supply disruption is assessed by evaluating whether water demands can be met based on water supply impairment states and contributions to system performance. We apply this framework to assess disruption risk for systems representing two common forms of connectivity – redundancy from alternative sources and conveyance paths and dependency along conveyance paths – to illustrate how wildfire risk may either be mitigated or magnified by the functional relationships between water system components.

3.2 METHODS

3.2.1. Water System

The study water system is in the Front Range Mountains of Colorado, USA. The names of the communities, infrastructure, and other geographic features within the analysis area are withheld for security reasons. The water system consists of the primary diversion for a community and the conveyance system and terminal reservoirs for a regional water project that supplements the community's primary source (Figure 3.1; Table 3.1). The total upland

contributing area to the system is 2127 km^2. Elevation ranges from 1616 to 4343 m above sea level. The watersheds are steep; 68.5% of the area is greater than 20% slope and 29.2% is greater than 40% slope. The climate is continental with warm dry summers and cold winters. Thunderstorms between June and October provide the majority of erosive power (Benavides-Solorio and MacDonald 2005). Forest is the dominant land cover (73.1%) followed by barren alpine (9.6%), grassland (7.8%), and shrubland (7.0%) (LANDFIRE 2016). The Colorado Front Range has a history of wind-driven fires that have burned large areas at moderate and high severity resulting in problematic erosion, reservoir sedimentation, and degraded water quality (Moody and Martin 2001; Graham 2003; Wagenbrenner et al. 2006; Oropeza and Heath 2013; Murphy et al. 2015).

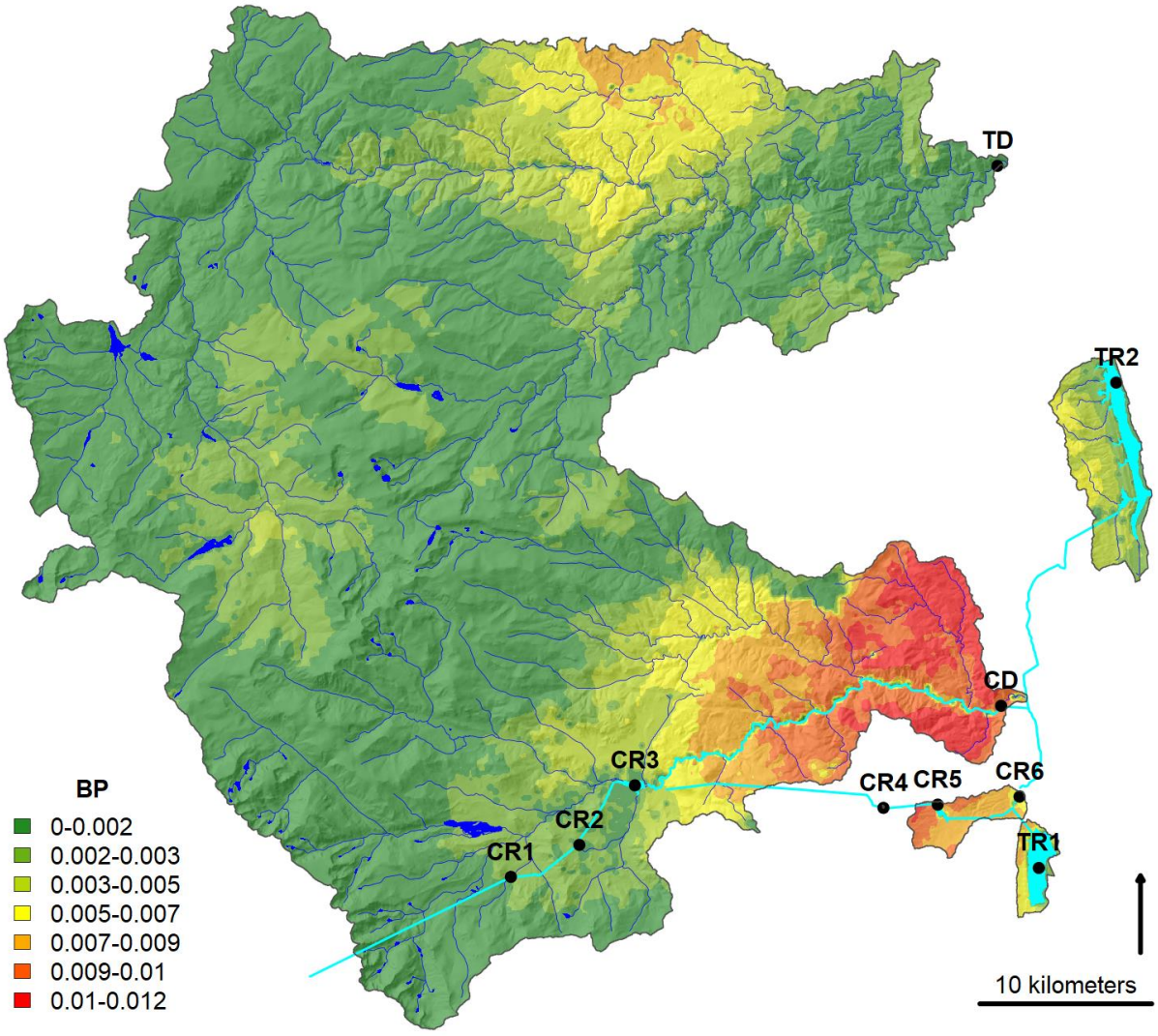

Figure 3.1. Study water system

The study water system consists of six conveyance reservoirs (CR), two terminal reservoirs (TR), one conveyance diversion (CD), and one terminal diversion (TD). The major conveyance paths and reservoirs are cyan. Burn probability (BP) depicts the predicted annual likelihood of wildfire activity across the water system.

Table 3.1. Water system characteristics

Water system infrastructure characteristics including volume for reservoirs and discharge for diversions. Discharge is the mean annual discharge from May through October from NHDPlus (USEPA and USGS 2012). Burnable contributing area is defined based on fuel model mapping from LANDFIRE (2016).

Code	Name	Network placement	Volume	Discharge	Total contributing area	Burnable contributing area
			(ha-m)	(cms)	(ha)	(ha)
CR1	Conveyance reservoir 1	Off	6	NA	1,148	1,126
CR2	Conveyance reservoir 2	Off	114	NA	101	81
CR3	Conveyance reservoir 3	On	378	NA	39,031	29,088
CR4	Conveyance reservoir 4	Off	12	NA	1	1
CR5	Conveyance reservoir 5	Off	269	NA	795	757
CR6	Conveyance reservoir 6	Off	94	NA	615	596
CD	Conveyance diversion	On	NA	5.5	77,810	66,100
TD	Terminal diversion	On	NA	17.1	126,739	108,606
TR1	Terminal reservoir 1	Off	13,843	NA	979	510
TR2	Terminal reservoir 2	Off	19,333	NA	4,443	3,567

3.2.2 Monte Carlo Simulation

Probability of exceeding water quality thresholds for treatment and conveyance was assessed with Monte Carlo simulation of post-storm suspended sediment concentrations over 10000 years of stochastic wildfire and rainfall (Figure 3.2). Wildfire activity was modeled using a combination of stochastic wildfire perimeters from the Large Fire Simulator (FSim; Finney et al. 2011) to describe wildfire occurrence in space and time, and static predictions of crown fire activity from FlamMap 5 (Finney et al. 2015) to characterize the spatial variability in burn severity within fire perimeters. Interannual variability in rainfall erosivity and the number of sediment-generating storms was represented by randomly resampling historical rainfall records (Perica et al. 2013). Post-fire hillslope erosion was modeled at an annual time step with the Revised Universal Soil Loss Equation (RUSLE; Renard et al. 1997). Sediment transport to infrastructure was approximated with hillslope and channel sediment delivery ratio models (Wagenbrenner and Robichaud 2014; Frickel et al. 1975) adapted for the study watersheds

(Chapter 2). Average annual post-storm suspended sediment was calculated by dividing the annual sediment load by the number of sediment-generating storms and assuming this average storm sediment load is evenly mixed in the receiving water body volume.

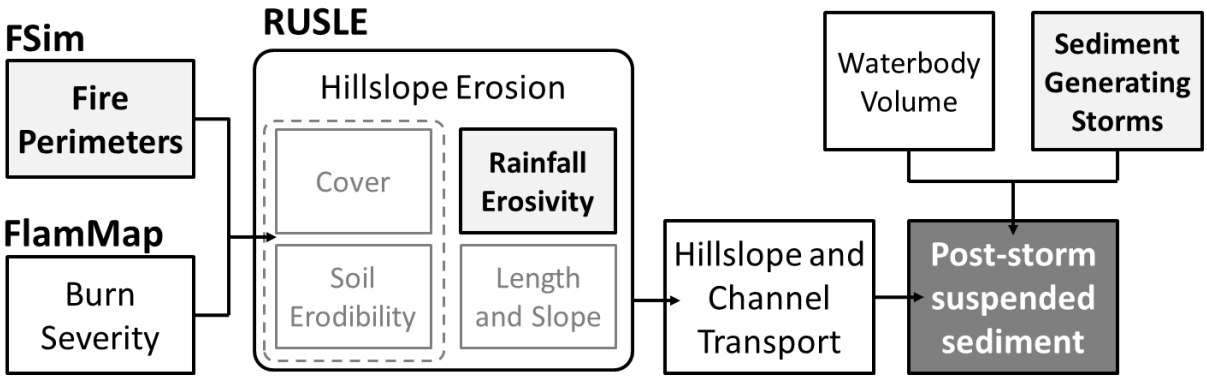

Figure 3.2. Monte Carlo simulation framework

Stochastic components are bold with light grey fill. Annual average post-storm suspended sediment was simulated based on spatially and temporally varying wildfire activity with FSim, static estimates of crown fire activity to approximate burn severity with FlamMap 5, and temporally varying rainfall based on resampling historical records. Post-fire hillslope erosion was modeled with RUSLE and sediment transport to infrastructure was estimated with hillslope and channel sediment delivery ratio models. Average annual post-storm suspended sediment was calculated by dividing the annual sediment load by the number of sediment-generating storms and assuming this average storm sediment load is evenly mixed in the receiving water body volume.

3.2.2.1 Fire Perimeters

Fire occurrence was simulated with FSim (Finney et al. 2011), which models large fire occurrence, growth, and containment over many hypothetical fire seasons. Daily large fire occurrence is determined in the model as a function of an artificial time series of the National Fire Danger Rating System Energy Release Component (ERC) for fuel model G calibrated with time series analysis of historical weather data. FSim models fire growth using the minimum travel time algorithm (Finney 2002) based on current fuels and topography (LANDFIRE 2016), and daily fuel moisture, wind speed, and wind direction. Daily wind speed and direction are drawn randomly from their historical joint probability distribution by month. Fire containment is

modeled based on primary fuel type and daily fire growth metrics (Finney et al. 2009). We used fire perimeters simulated with FSim over 10000 hypothetical fire seasons from a separate effort to update the U.S. national probabilistic wildfire risk components (Short et al. 2016). For this application, FSim was calibrated to approximate the historical fire size distribution and rate of burning within biophysical regions, called "pyromes", which have similar controls on wildfire activity. Wildfires from three pyromes intersected the study water system. FSim treats fuels as stationary, so modeled wildfire activity should be interpreted as representing 10000 possible realizations of the next fire season. The simulation year was used here only as a reference for tracking post-fire erosion over multiple years of watershed recovery.

3.2.2.2 Rainfall

Two annual rainfall metrics were employed to model average post-storm turbidities: 1) rainfall erosivity was used to predict annual sediment yield from hillslope erosion (Renard et al. 1997), and 2) the number of storms exceeding intensity thresholds for erosion was used to distribute the annual sediment yield among storm events. Both metrics were represented in the analysis by randomly sampling historical rainfall records to generate 10000 years of representative rainfall activity. Stations were sampled randomly with replacement and their time-ordered records were sequentially appended until reaching 10000 years. This approach is similar in principle to stochastic rainfall generation in the Watershed Erosion Prediction Project model that is commonly used for to estimate uncertainty in post-fire erosion (e.g., Miller et al. 2016, Elliot et al. 2016). The historical data came from eleven rainfall gages with 15 min resolution located in the Colorado Front Range (Perica et al. 2013) that were assembled for a separate study of storm-level thresholds for erosion (Wilson et al. 2018). Hillslope erosion has a strong positive relationship with rainfall erosivity (Renard et al. 1997; Benavides-Solorio and MacDonald 2005;

Schmeer et al. 2018). Rainfall erosivity, also called "rainfall-runoff erosivity", is calculated as the product of storm maximum rainfall intensity and kinetic energy per unit area (Renard et al. 1997), which represent the dual triggers of hillslope erosion: sediment detachment and transport via surface runoff. Rainfall erosivity is known to be highly variable in the Colorado Front Range due to the prevalence of locally powerful convective thunderstorms that are responsible for the majority of erosion (Wagenbrenner et al. 2006; Robichaud et al. 2013a; Murphy et al. 2015; Kampf et al. 2016). We focused on total annual rainfall erosivity for the period May through October because the majority of hillslope erosion in the region is associated with intense summer rainfall (Benavides-Solorio and MacDonald 2005) and much of the precipitation during the remaining months falls as snow. Annual rainfall erosivity time series for the stations used in our analysis are shown in Figure 3.3. The individual station records come from the period 1971 to 2010. The mean and maximum of the pooled 403 station-years of observations are 684 and 58468 MJ mm ha^{-1} h^{-1}, respectively. The associated number of sediment-generating storms was estimated using the 7 mm h^{-1} rainfall intensity (60 min duration) threshold identified by Wilson et al. (2018) for erosion occurrence during the first two post-fire years. The mean and maximum of the pooled 403 station-years of observations were 4 and 18 sediment-generating storms per year respectively in the May through October period.

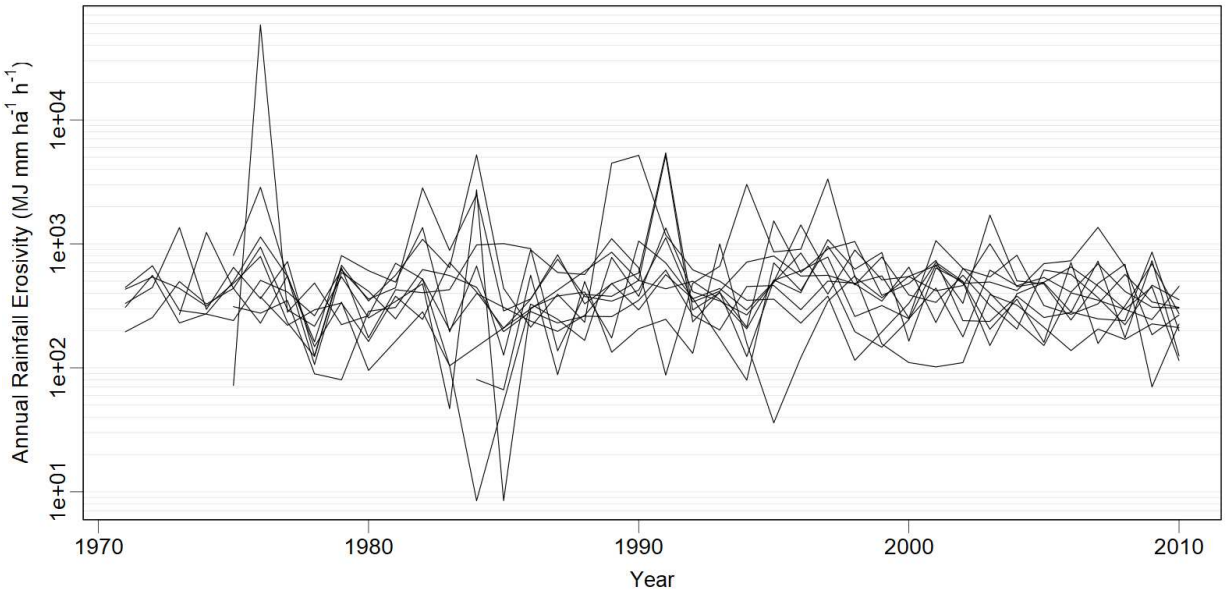

Figure 3.3. Rainfall erosivity variability

Annual rainfall erosivity for the May through October period from eleven stations representative of the Colorado Front Range climate (Perica et al. 2013).

3.2.2.3 Burn Severity

Crown fire activity (CFA) (Scott and Reinhardt 2001) was modelled using FlamMap 5.0 (Finney et al. 2015) as a proxy for soil burn severity similar to previous risk assessments (Tillery et al. 2014; Haas et al. 2017; Chapter 2) by mapping surface fire, passive crown fire, and active crown fire behavior to low, moderate, and high burn severity, respectively. Most area burns in the Colorado Front Range during dry and windy conditions (Graham 2003; Haas et al. 2015), so CFA was modeled for 3rd percentile (low) fuel moisture (1-h 2%, 10-h 3%, 100-h 6%, herbaceous 30%, woody 63%) and 97th percentile (high) mean 1-minute wind speed (39 km h^{-1} at 6 m) for the core fire season (1 April to 31 October) from three Remote Automated Weather Stations located in the study area. Fuel moisture and wind speed percentiles were calculated with FireFamilyPlus 4.1 (Bradshaw and McCormick 2000) and wind speed was converted from a 10-minute to 1-minute average based on Crosby and Chandler (1966). The wind blowing uphill option was used in FlamMap to represent a consistent worst-case scenario across aspects.

3.2.2.4 Watershed Modeling

The mass of post-fire sediment delivered to water supplies was estimated with coupled hillslope erosion, hillslope sediment transport, and channel sediment transport models as described in Chapter 2 with minor modifications (Figure 3.2; Figure 3.4). Only a brief review of the methods is provided here. Model evaluation is reserved for the results section. Chapter 5 also reviews the limitations of the system of models and highlights potential future improvements. The NHDPlus watershed network was used to represent the spatial topology between sediment-producing uplands and water supplies (USEPA and USGS 2012). NHDPlus consists of medium resolution flowlines and their associated upland contributing areas, or catchments, delineated from a 30-m resolution Digital Elevation Model (DEM). Gross hillslope erosion was modeled for each burned pixel with RUSLE (Renard et al. 1997). The proportion of sediment delivered from each pixel to the stream network was estimated with an empirical model of post-fire hillslope sediment delivery from the western U.S. (Wagenbrenner and Robichaud 2014). Sediment was then summed for each catchment and routed down the flowline network to water supply nodes based on a simple channel sediment delivery ratio model (Frickel et al. 1975) adapted to the channel types in the study area.

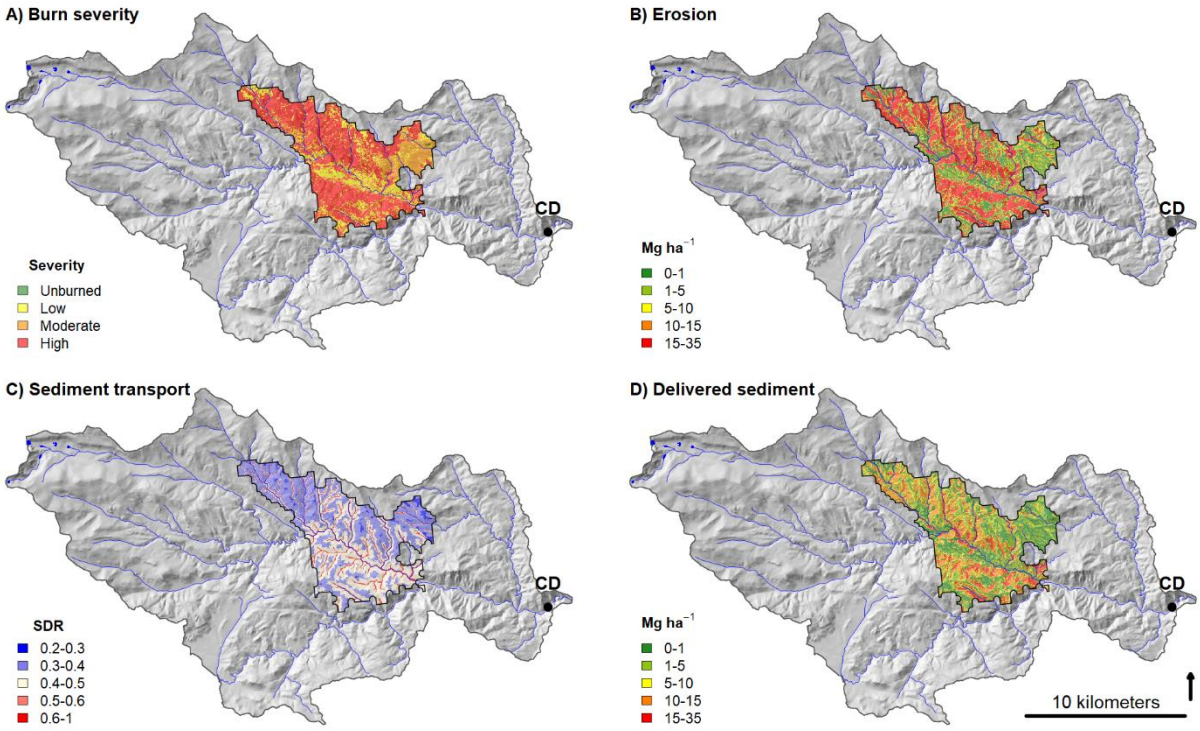

Figure 3.4. Watershed modeling example

The watershed modeling workflow is demonstrated for a 5234 ha fire from year 1610 of the Monte Carlo simulation. Panel A shows the modeled burn severity. Panel B maps the first-year post-fire erosion of fine sediments for a rainfall erosivity of 735 MJ mm ha^{-1} h^{-1} from the resampled annual rainfall time series. Panel C shows the combined hillslope and channel sediment delivery ratio (SDR) for our high SDR scenario. Panel D depicts the annual sediment contributed from each pixel to the conveyance diversion. The total post-fire sediment delivered to the diversion in the first-year post-fire is 34689 Mg, which is distributed over six sediment producing storms in the season for an average storm yield of 5781 Mg. For a mean daily flow volume of 4.73 x 10^8 lpd, the average post-storm suspended sediment concentration is estimated at 12218 Mg l^{-1} with an associated turbidity of 10476 NTU.

3.2.2.4.1 Hillslope Erosion

Post-fire increase in hillslope erosion was modeled with a Geographic Information System implementation (Theobald et al. 2010) of RUSLE (Renard et al. 2019). RUSLE predicts gross erosion (Mg ha^{-1} yr^{-1}) as the product of factors for rainfall erosivity (R), soil erodibility (K), length and slope (LS), cover (C), and support practices (P). Undisturbed erosion rates are generally not problematic in the study water system, so our assessment focused on the fire-related increase in erosion. R came from the stochastic series of rainfall erosivity described previously. LS for both conditions was calculated using terrain analysis of a 30-m resolution

digital elevation model (USEPA and USGS 2012) per Winchell et al. (2008) with a maximum flow accumulation of 0.9 ha imposed to approximate the original hillslope length guidance of Renard et al. (1997). Pre-fire K was mapped using the Soil Survey Geographic Database (SSURGO) where available and the State Soil Geographic Database (STATSGO) to fill missing data (NRCS Soil Survey Staff 2016). K and C factors were varied based on wildfire extent and burn severity (Larsen and MacDonald 2007; Chapter 2) to represent the primary effects of fire on soils and surface cover (Shakesby and Doerr 2006; Larsen et al. 2009). No support practices were considered.

For each fire, the increase in erosion was tracked over the first three post-fire years. Characterizing recovery directly from erosion observations is complicated by rainfall variability across years. We estimated that with constant rainfall, erosion in year two should be 15% lower than in year one and erosion in year three should be 75% less than year one, based on the rate of surface cover recovery and its influence on erosion (Pietraszek 2006; Benavides-Solorio and MacDonald 2005; Larsen et al. 2009). Therefore, annual fire-related erosion (A_y) was calculated with a recovery adjustment factor, *RAF*, of 1, 0.85, and 0.25 for post-fire years one through three respectively (Eqn 3.1).

$$A_y = R_y \times LS \times [(K_b \times C_b) - (K \times C)] \times RAF_{pfy} \quad \textbf{Equation 3.1}$$

The subscript *y* is the index for the common fire and rainfall simulation year, the subscript *b* indicates the burned condition for K and C factors, and *pfy* is the index for time since fire starting at one for the fire year. RUSLE can predict unrealistically high erosion rates on very steep slopes, so we limited pixel-scale erosion predictions to the maximum rate of 100 Mg ha^{-1} yr^{-1} observed from hillslope plots in the study region (Moody and Martin 2009).

3.2.2.4.2 Hillslope Sediment Transport

The proportion of eroded hillslope sediment delivered to streams was estimated with an empirical model of post-wildfire hillslope sediment delivery ratio (*hSDR*) from the western U.S. (Wagenbrenner and Robichaud 2014). First, the NHDPlus stream channel network was extended to include all pixels with a contributing area greater than 10.8 ha (Henkle et al. 2011) because the flowline network does not include many of the lowest order channels. The annual length ratio model from Wagenbrenner and Robichaud (2014) (Eqn 3.2) was then used to estimate post-fire *hSDR* based on the flow path length from each pixel to the nearest stream channel as the "catchment length" and the flow path length across the pixel as the "plot length" from terrain analysis of the NHDPlus 30-m resolution DEM in ArcGIS 10.3 (ESRI 2015). The maximum *hSDR* of 0.27 predicted by the model for near stream areas seemed unrealistically low for our study area based on observed catchment sediment yields in Colorado (Hayman Fire in Wagenbrenner and Robichaud 2014). We therefore explored an alternative high *hSDR* scenario in which we doubled the predicted *hSDR*. This increased the maximum *hSDR* from 0.27 to 0.54 for areas near streams and it increased the minimum *hSDR* from 0.05 to 0.10 for locations furthest from streams. Channels pixels were assigned *hSDR* of 1.

$$log(hSDR) = -0.56 - 0.0094 \times \left(\frac{Flow\ path\ length\ to\ nearest\ channel}{Flow\ path\ length\ across\ pixel}\right) \quad \textbf{Equation 3.2}$$

The annual mass of fire-related sediment (Mg) delivered from a catchment to the stream network (TS_y) was calculated as the sumproduct of the annual hillslope erosion rate (A_y), the pixel area, and hSDR for all burned pixels (*N*) in the catchment (Eqn 3.3).

$$TS_y = \sum_{i=1}^{N} A_{y,i} \times 0.09 \frac{ha}{pixel} \times hSDR_i \quad \textbf{Equation 3.3}$$

3.2.2.4.3 Channel Sediment Transport

A channel sediment delivery ratio (*cSDR*) model adapted from Frickel et al. (1975) was used to predict the proportional throughput of sediment for flowlines (channels) based on stream order (Chapter 2). Transport of sand and smaller sediments should be efficient based on post-fire observations in the study area (Miller et al. 2017) and a similar watershed in Wyoming (Ryan et al. 2011). Low order channels in the study area are characterized by ephemeral or intermittent flow and high roughness from coarse bed material and streamside vegetation. The highest order channels are still steep mountain streams with considerably greater transport capacity due to higher magnitude perennial flows. To approximate these trends, *cSDRs* of 0.75, 0.80, 0.85 and 0.95 per 10 km of stream length were assigned to 1st, 2nd, 3rd, and 4th or higher-order streams, respectively. Flowlines intercepting lakes and reservoirs were assigned a *cSDR* of 0.05 to reflect that most sediment will be trapped. The annual mass of fire-related sediment (Mg) delivered to a water supply (TWS_y) was calculated as the sum of sediment delivered to streams for all upstream catchments multiplied by the product of *cSDRs* for the intervening flowlines (Eqn 3.4).

$$TWS_y = \sum_{j=1}^{O}(TS_{y,j} \times \prod_{k=1}^{P} cSDR_k) \qquad \textbf{Equation 3.4}$$

The subscript *j* is the index for the *O* upstream catchments and the subscript *k* is the index for the *P* intervening flowlines between catchment *j* and the water supply.

3.2.2.4.4 Suspended Sediment

In our study region, post-fire suspended sediment concentrations rise to concerning levels for short periods (hours to days) following rainstorms (Oropeza and Heath 2013; Sham et al. 2013), so we estimated suspended sediment concentrations using standard daily load calculations for either the reservoir or stream daily flow volume (Table 3.1). Previous research in a similar watershed in Wyoming suggests the suspended sediment after summer thunderstorms is

primarily clay and silt (70-85%) and the remainder is mostly fine-grained organics (Ryan et al. 2011). Monitoring of hillslope erosion after a large wildfire in the study region shows that clay and silt account for ~25% of eroded sediment mass (Schmeer 2014). Hence, we made the gross assumption that up to 35% of the hillslope erosion predicted by RUSLE is part of the fine-grained inorganic and organic components that contribute to suspended sediment. Average post-storm suspended sediment concentration (SSC) was estimated by first dividing 35% of TWS_y equally among the annual number of sediment-generating storms from the stochastic rainfall series to calculate the average storm load of fine sediment. Then, SSC was approximated by assuming the average storm load of fine sediment is perfectly mixed in the reservoir or stream daily flow volume. SSC is often monitored optically with a turbidity sensor, so treatment limits are commonly expressed in Nephelometric Turbidity Units (NTUs). Various turbidity limits for effective water treatment ranging from 20-100 NTU have been reported in the literature (Writer et al. 2014; Murphy et al. 2015). For this analysis, we use the 100 NTU limit for all water supplies to be conservative in our assessment of risk. Turbidity and suspended sediment concentration (SSC) are closely related, but the nature of the relationship can vary across sensors and watersheds due to varying sediment composition. A conversion equation developed from monitoring of the Fourmile Canyon Fire was used to estimate turbidity (NTU) from SSC (mg l^{-1}) (Murphy et al. 2015; Eqn 3.5).

$$Turbidity = \frac{SSC - 2.84}{1.166} \qquad \textbf{Equation 3.5}$$

3.2.3. Risk Analysis

For individual infrastructure components, probability of impairment was calculated as the frequency of annual turbidity exceedances over the total number of simulation years. Water quality was considered impaired when turbidity exceeded 100 NTU. The wildfire and watershed

components of the Monte Carlo simulation (**Error! Reference source not found.**) have been s hown to make reasonable predictions of post-fire sediment yields in this region (Chapter 2), but the assumptions required to estimate suspended sediment concentrations add additional levels of uncertainty. To assess risk metric sensitivity to data and model uncertainties, we also calculated impairment probabilities for 10 NTU and 1000 NTU impact thresholds assuming the suspended sediment predictions are unlikely to be more than an order of magnitude off in either direction.

To examine system level risks from water quality impairment, we focused on four subsystems that represent examples of redundancy and dependency. For each subsystem, the number of impaired components was tracked on an annual basis and the consequences of impairment were interpreted in light of the subsystem function as follows:

1. **Redundant sources (TD and TR2)** can meet the dependent community's water demand if at least one source is operating at full capacity. Therefore, water shortage will only occur if both sources are impaired in the same year.
2. **Conveyance path 1 (CR1 -> CR2 -> CR3 -> CR4 -> CR5 -> CR6)** is the primary conveyance path for a regional water project that distributes water to several terminal reservoirs including TR1 and TR2. The conveyance reservoirs are considered nodes at which impaired water may disrupt conveyance.
3. **Conveyance path 2 (CR1 -> CR2 -> CR3 -> CD)** is an alternative conveyance path that bypasses CR4, CR5, and CR6.
4. **Redundant conveyance (paths 1 and 2)** provides operational flexibility to deliver water to TR2. System performance was assessed on an annual basis using the least impaired path.

All data analysis and figure generation was completed with R version 3.5.3 (R Core Team 2019) using the following packages: *raster* version 2.8-19 (Hijmans 2019), *rgdal* version 1.4-3 (Bivand et al. 2019), *rgeos* version 0.4-2 (Bivand and Rundel 2018), and *plyr* version 1.8.4 (Wickham 2011).

3.3 RESULTS

3.3.1 Wildfire Occurrence

A total of 5741 fire perimeters from FSim intersected the study area. Including area burned outside the study area, their sizes ranged from 2 to 131922 ha with a median of 59 ha and mean of 1758 ha. Simulated wildfire activity is strongly related to vegetation and fuel type; the dry forests and woodlands in the low mountains and foothills are expected to burn more frequently than the alpine tundra and high elevation forests (Figure 3.1). The area just upstream of TD has low predicted burn probability because fuels were recently reduced by wildfire. Wildfire is expected to occur most frequently and to impact the greatest area in watersheds associated with the on-network diversions – CD and TD (Figure 3.1; Table 3.2). Wildfires occurred in 19.4% of years in the CD watershed and 27.1% of years in the TD watershed. CD and TD have the greatest exposure to wildfire because they have the largest watersheds (Table 3.1) and these watersheds extend into the lower elevation vegetation types predicted to have the greatest wildfire activity (Figure 3.1). The other on-network water supply, CR3, is expected to receive considerably less wildfire activity because of its smaller watershed and the lower frequency of burning at higher elevations (Figure 3.1; Table 3.2). Wildfire activity is predicted to be low in the local contributing areas to the off-network reservoirs (Table 3.2). TR2 is the most-

frequently impacted off-network water supply (2.4% of years), because of its relatively large contributing area and lower elevation.

The scale at which wildfire activity becomes problematic should vary by erosion potential, post-fire rainfall, proximity to water supplies, and receiving waterbody size, but area burned is often a reasonable indicator of impact magnitude. The most notable historical impacts from wildfires in this region are associated with a 4690 ha wildfire combined with exceptional post-fire rainfall (Moody and Martin 2001) and two fires larger than 35000 ha (Writer et al. 2014; Martin 2016). More than 50% of years with fire activity did not exceed 100 ha watershed area burned, suggesting much of the simulated fire activity will not meaningfully impact water supplies (Table 3.2). More than 1000 and 10000 ha of a watershed burning in a single year is even more rare (Table 3.2). Only four water supplies – CR3, CD, TD, and TR2 – were exposed to more than 1000 ha of fire activity in a year. Greater than 10000 ha of annual fire activity was only observed for the three on-network water supplies – CR3, CD, and TD – and this level of fire activity was very rare (Table 3.2). Only CD and TD experienced greater than 30000 ha in a year. Although off network water supplies were rarely exposed to wildfire, it was common for more than 20% of their watersheds to burn in a single year (Table 3.2).

Table 3.2. Watershed exposure to wildfire

Frequency of fire by watershed area burned and conditional statistics on annual area burned. * Of the burnable contributing area conditional on fire occurrence.

Code	Frequency by watershed area burned (% of years)						Conditional watershed area burned (ha)				
	> 0 ha	> 100 ha	> 1,000 ha	> 10,000 ha	> 20%*	> 50%*	Median	Mean	Max	St. Dev.	Skew
CR1	0.82	0.24	0.00	0.00	13.41	7.32	27	120	918	202	2.4
CR2	0.33	0.06	0.00	0.00	60.61	54.55	57	48	101	39	0.1
CR3	8.38	2.85	0.89	0.01	1.07	0.00	31	397	12,100	1,124	5.4
CR4	0.94	0.00	0.00	0.00	100.00	100.00	1	1	1	0	NA
CR5	1.92	1.22	0.00	0.00	58.85	39.06	214	327	795	303	0.5
CR6	1.62	1.01	0.00	0.00	59.26	40.74	218	255	615	229	0.4
CD	19.36	8.99	3.96	0.49	1.70	0.05	78	1,147	33,445	3,130	4.9
TD	27.14	10.75	3.89	0.37	0.22	0.00	46	730	31,177	2,313	6.4
TR1	1.21	0.67	0.00	0.00	55.37	30.58	154	227	979	262	1.8
TR2	2.41	1.20	0.48	0.00	24.90	9.54	95	502	3,447	778	1.9

3.3.2 Burn Severity and Suspended Sediment

Potential post-fire contribution of suspended sediment to water supplies differs considerably across the study area due to variability in fuel conditions and topography that influence burn severity, soil conditions and topography that effect hillslope erosion, and proximity to water supplies that controls sediment transport efficiency (Figure 3.5). Low, moderate, and high severity burning is predicted to occur on 24.4%, 16.5%, and 44.4% of the study area, respectively. The remaining 14.7% of the study area is non-burnable cover (barren alpine, water, urban, etc.). Watershed area burned at moderate and high severity ranged between 38.6% to 78.6% by water supply. Under median post-fire rainfall (403 MJ mm ha^{-1} h^{-1}), erosion is predicted to increase after fire between 0 and 100 Mg ha^{-1} with a mean of 23.0 Mg ha^{-1} and a standard deviation of 32.0 Mg ha^{-1}. The associated mean production of fine sediments is 8.1 Mg ha^{-1}. A substantial portion of the eroded sediment is retained in the uplands, so the mean fine sediment delivery to streams is only 2.2 Mg ha^{-1} for the low SDR scenario and 4.0 Mg ha^{-1} for the high SDR scenario. Retention in the channel network further reduces the average

contribution to water supplies to a mean of 1.4 Mg ha^{-1} for the low SDR scenario and a mean of 2.6 Mg ha^{-1} for the high SDR scenario. Much of the channel transport losses are from reservoirs and lakes that reduce downstream connectivity (Figure 3.5).

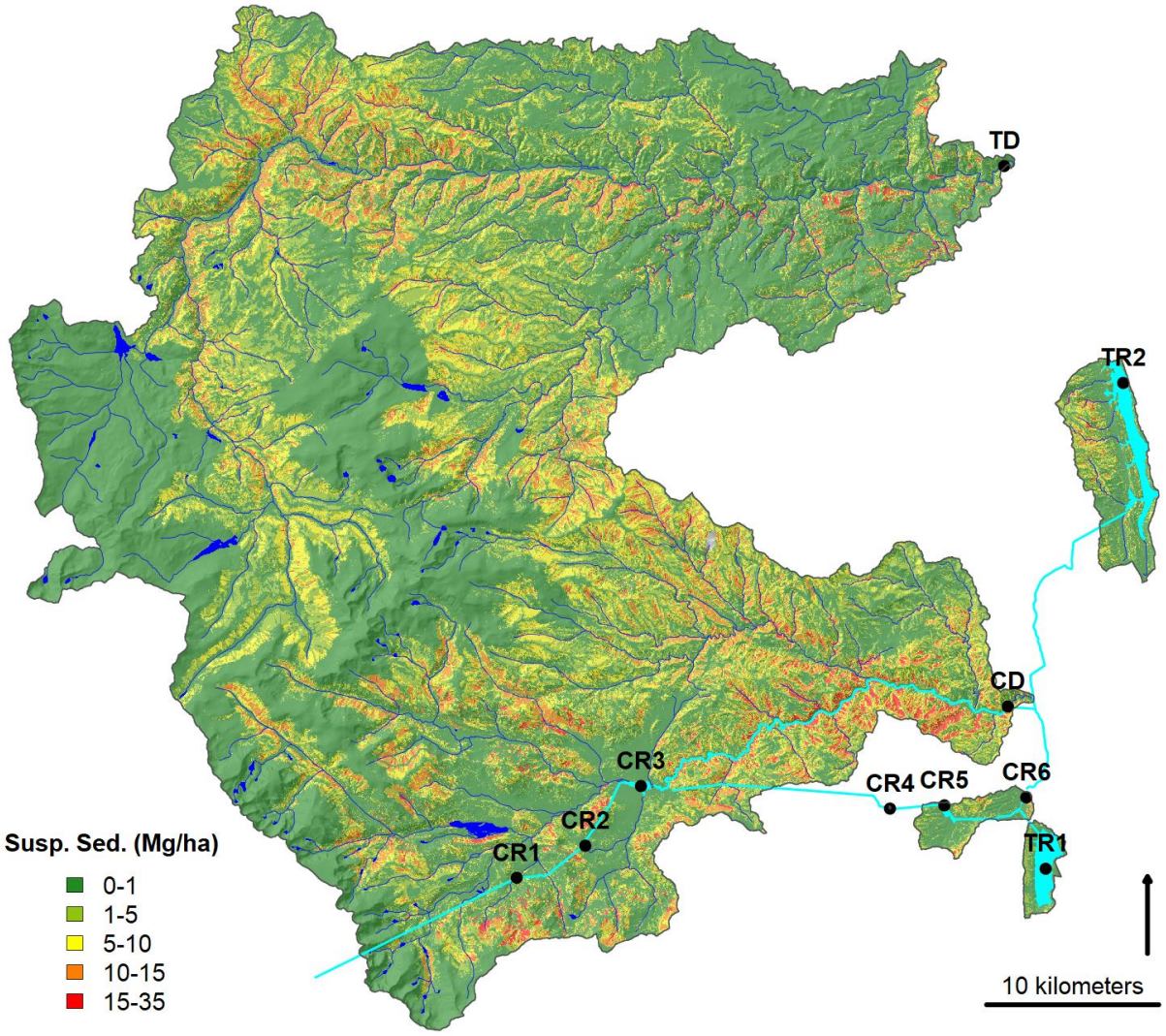

Figure 3.5. Conditional water supply exposure to sediment

Predicted contribution to water supply suspended sediment during the first-year post fire under median annual rainfall erosivity (403 MJ mm ha^{-1} h^{-1}) and the high SDR scenario. The major conveyance paths and reservoirs are cyan.

The sediment yields from individual wildfires vary widely owing to differences in the erosion potential within their extents and the post-fire rainfall they are exposed to. For ease of comparison with field observations, Table 3.3 describes the distribution of first-year post-fire total sediment yields (including coarse and fine fractions) grouped into broad categories of rainfall erosivity. Gross erosion for the average fire is 18.1, 32.6, and 49.5 Mg ha^{-1} for the low, medium, and high rainfall erosivity categories, respectively. Net sediment delivery to streams is approximately one quarter of the gross erosion for the low SDR scenario and one half of the gross erosion for the high SDR scenario. Our fire-level predictions of first-year post-fire erosion and net sediment delivery to streams are close to the ranges reported for previous fires in the Colorado Front Range. At low rainfall erosivity, our simulated erosion rates (Table 3.3) are near the study-wide means of 9.5-22.2 Mg ha^{-1} and the range of individual hillslope observations of 0.1-38.2 Mg ha^{-1} reported for most fires in the region (Wagenbrenner et al. 2006; Larsen et al. 2009; Robichaud et al. 2013a; Schmeer et al. 2018). Approximately 25% of fires exposed to high rainfall erosivity (Table 3.3) meet or exceed the 72 Mg ha^{-1} of rill and interrill erosion observed in response to extreme rainfall after the Buffalo Creek Fire (Martin and Moody [2001]; volume estimates converted with bulk density of 1.6 Mg m^{-3}). For the low SDR scenario, only the top decile of fires exposed to high rainfall erosivity are predicted to deliver sediment to streams at the rates approaching the low end of the 22.0-38.6 Mg ha^{-1} range observed from small catchments in the first two years after the Hayman Fire (Robichaud et al. 2008, 2013b) (Table 3.3). For the high SDR scenario, approximately a quarter of the fires with moderate rainfall erosivity and the top half of fires with high rainfall erosivity meet or exceed the low end of the observed range. The channel transport losses with further lower sediment yields, so none of the

simulated fires at any rainfall level are expected to reach the normalized reservoir input of 52.5 Mg ha^{-1} from the Buffalo Creek Fire (Moody and Martin 2001).

Table 3.3. Fire-level erosion and net sediment to streams

Summary statistics of first-year post fire erosion and sediment delivery to streams (Mg ha^{-1}) for the portion of wildfires that burned the study watersheds in three categories rainfall erosivity. These are total sediment yields including the coarse and fine fractions. Low and high refer to the low and high hillslope SDR scenarios.

	<500 MJ mm ha^{-1} h^{-1} n = 3,738 fires			**500-1,000 MJ mm ha^{-1} h^{-1} n = 1,496 fires**			**> 1,000 MJ mm ha^{-1} h^{-1} n= 507 fires**		
		To streams			**To streams**			**To streams**	
Statistic	**Erosion**	**Low**	**High**	**Erosion**	**Low**	**High**	**Erosion**	**Low**	**High**
Lower decile	1.9	0.5	0.9	5.2	1.4	2.5	12.7	3.2	6.1
Lower quartile	5.7	1.5	2.8	14.6	3.9	7.2	27.5	7.8	14.3
Median	13.6	3.6	6.7	30.4	8.1	15.1	50.7	13.5	25.0
Mean	18.1	4.9	9.0	32.6	8.9	16.3	49.5	13.3	24.5
Upper quartile	26.3	7.0	13.1	48.0	13.0	24.0	70.1	18.6	34.3
Upper decile	40.5	10.7	19.8	64.2	17.0	31.3	85.8	22.4	41.3

3.3.2 Water Supply Exposure to Suspended Sediment

The Monte Carlo simulation links time and location varying wildfire occurrence and time varying rainfall to predict the annual average post-storm suspended sediment from all wildfire activity accounting for recovery for the first three post-fire years (Figure 3.2). Figure 3.6 illustrates a 500-year subset of the simulation for TD. Wildfire is frequent in the watershed due to its large size, but not all wildfire results in problematic suspended sediment concentrations, either because it does not affect enough area or because it does not combine with high rainfall erosivity. Within this subset of the simulation, 50 years had greater than 100 ha of wildfire activity resulting in 79 years that turbidity exceeded the 100 NTU impairment threshold. Impairment is more frequent than large fire occurrence because burned areas are susceptible to erosion for multiple years. Wildfire activity occasionally exceeds 100 NTU for a single year, but it is more common for two or more years of problematic water quality after fire because the first two years have similar erosion potential.

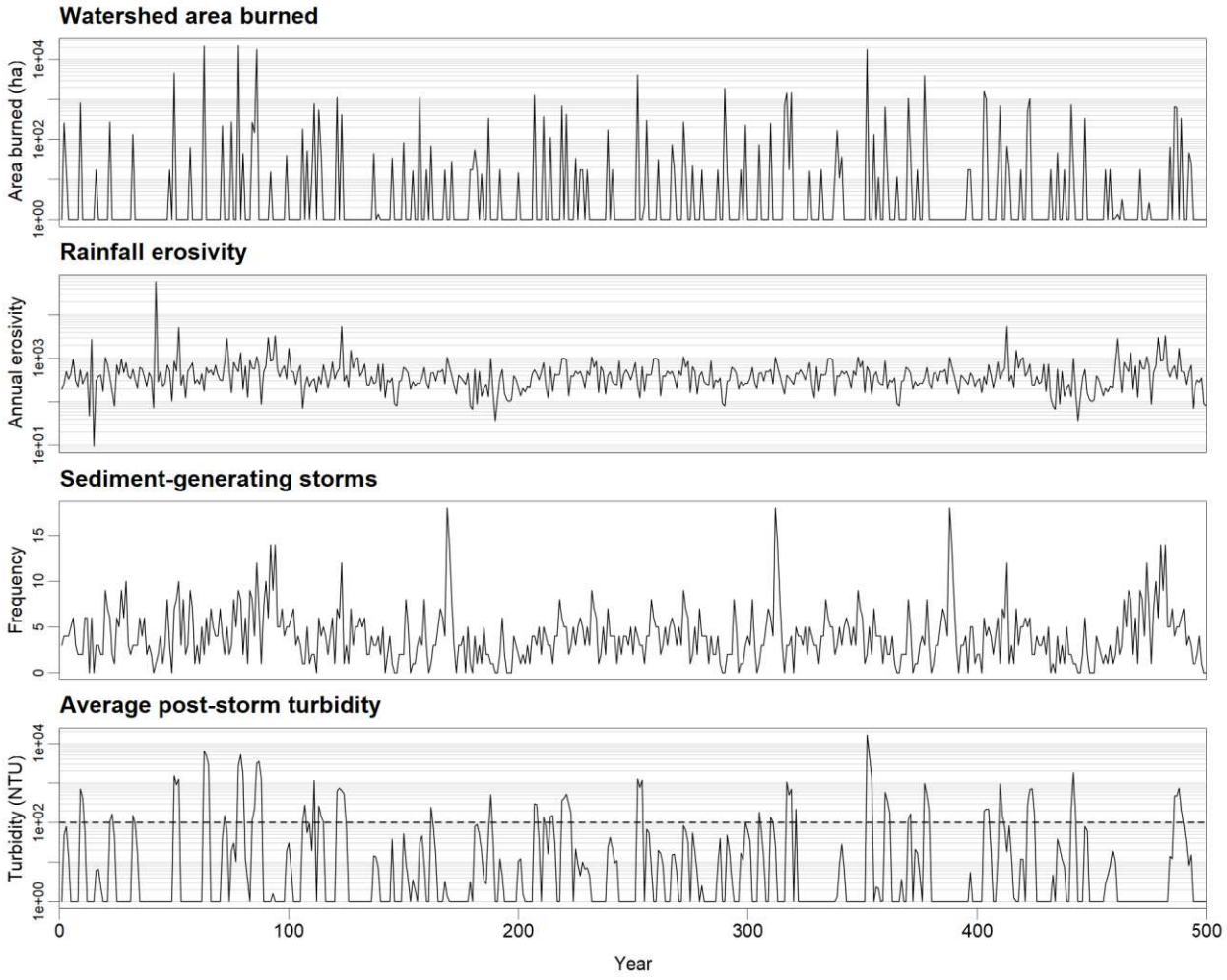

Figure 3.6. Monte Carlo simulation example

An example 500-year subset of the Monte Carlo simulation results for the terminal diversion (TD) showing annual watershed area burned, rainfall erosivity, number of sediment-generating storms, and average post storm turbidity for the high SDR scenario. The dashed horizontal line marks the 100 NTU impairment threshold. The 100 NTU exceedance probability for this subset of the simulation is 0.158.

Extending this analysis to the full 10000-year simulation period and all water supplies results in impairment probabilities of 0 to 0.1689 for the low SDR scenario and 0 to 0.1935 for the high SDR scenario (Table 3.4). Given the minor differences between the low and high SDR scenarios, we focus on the high SDR scenario for the remainder of our analyses. Cumulative frequency distributions of annual average post-storm turbidity for the full 10000-year simulation

period are shown for each of the water supplies in Figure 3.7. Mean post-storm turbidity, conditional on fire occurrence, varied from 2 to 2129 NTU for reservoirs and from 381 to 2943 NTU for diversions. Turbidity only exceeded 1000 NTU in 5% or more of the fire-affected years at CR1, CD, and TD. The on-network water supplies – CR3, CD, and TD – were most likely to experience wildfire-related water quality impacts owing to their greater exposure to wildfire activity. CD is most vulnerable to impairment; its source water is predicted to exceed 100 NTU in 19.35% of years. Off-network reservoirs were rarely exposed to fire-related water quality impacts due to their limited exposure to wildfire and the small size of their local contributing areas compared to the receiving waterbody size (Figure 3.7). Off-network reservoirs exceeded 100 NTU in at most 1.67% of simulation years. Two reservoirs – CR4 and TR1 – never exceeded 100 NTU during the 10000 simulation years. CR4 is at low risk because it has less than 2 ha of burnable contributing area. TR1 has only 510 ha of burnable contributing area, which is unlikely to generate enough sediment to impair a 13843 ha-m reservoir. The other terminal reservoir – TR2 – exceeded 100 NTU only once in 10000 years.

Table 3.4. Turbidity exceedance probabilities

Turbidity exceedance probabilities by water system component for thresholds of 10, 100, and 1000 NTU and low and high SDR scenarios.

Scenario	NTU	CR1	CR2	CR3	CR4	CR5	CR6	CD	TD	TR1	TR2
Low SDR	10	0.0202	0.0041	0.0610	0.0001	0.0206	0.0278	0.2685	0.2607	0.0000	0.0002
	100	0.0137	0.0001	0.0177	0.0000	0.0007	0.0063	0.1689	0.1218	0.0000	0.0000
	1000	0.0057	0.0000	0.0008	0.0000	0.0000	0.0000	0.0809	0.0231	0.0000	0.0000
High SDR	10	0.0209	0.0048	0.0769	0.0014	0.0292	0.0313	0.2977	0.3147	0.0000	0.0009
	100	0.0167	0.0008	0.0276	0.0000	0.0031	0.0142	0.1935	0.1574	0.0000	0.0001
	1000	0.0083	0.0000	0.0022	0.0000	0.0000	0.0001	0.1018	0.0423	0.0000	0.0000

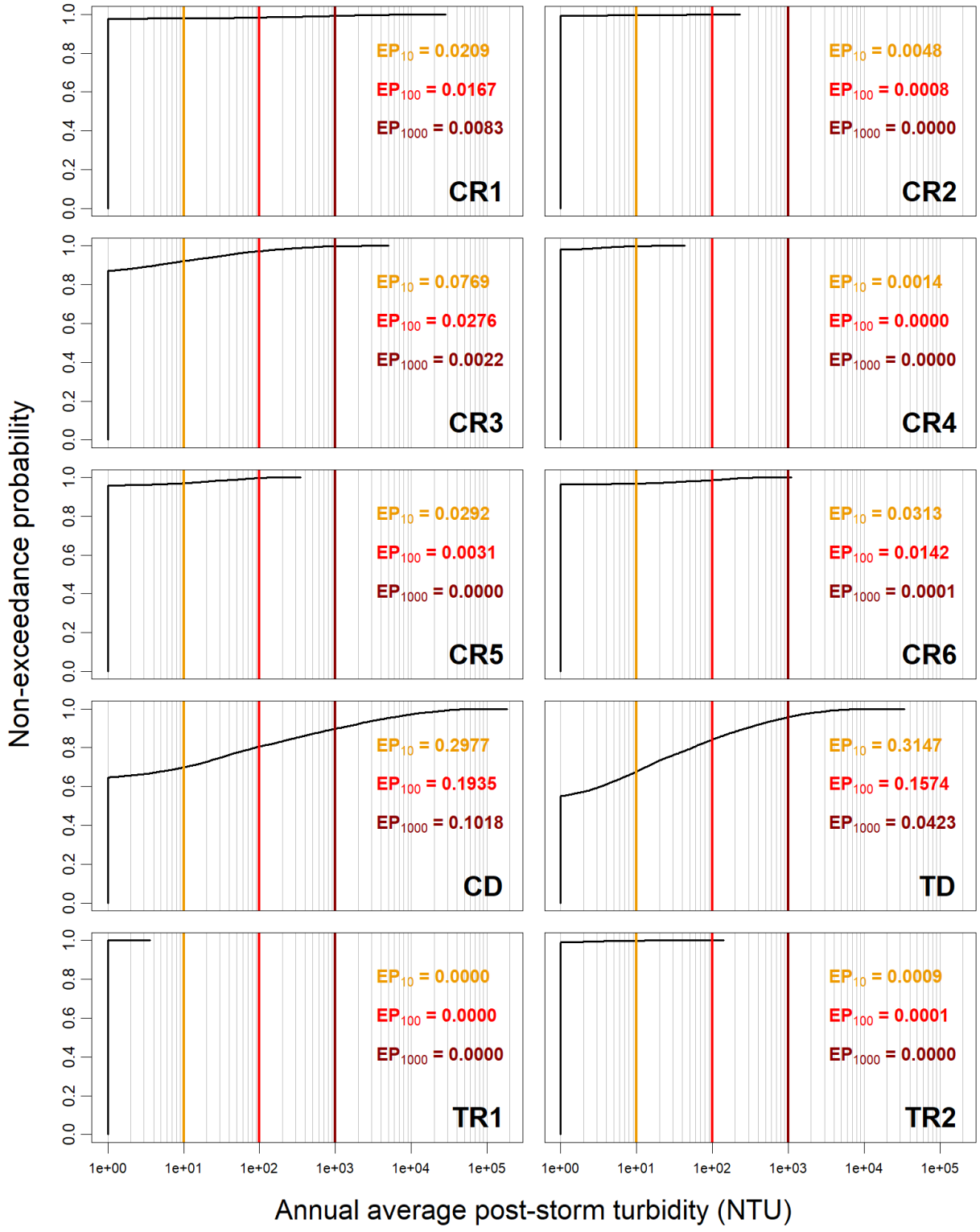

Figure 3.7. Annual average post-storm turbidity distributions

Cumulative frequency distributions of annual average post-storm turbidity by water supply with 10, 100, and 1000 NTU exceedance probabilities (EP) for the high SDR scenario.

3.3.3 System-level Consequences

The frequency of component impairment is presented by subsystem and turbidity impairment threshold in Table 3.5. The redundant sources subsystem experienced at least one component impairment in 15.74% of years, but co-impairment of the dual sources only occurred once in 10000 years. Accounting for this redundancy decreases the risk of water supply disruption by 99.9% compared to the naïve assumption of disruption whenever a single component is impaired. In contrast, dependency magnifies risk. CR3 is the most frequently impaired component on conveyance path 1 at 2.76% of years, but at least one component is impaired along the full path in 5.17% of years because the multiple nodes of impact increase exposure to wildfire. If two or more impaired components are required to substantially reduce annual water conveyance, conveyance route 1 is only expected to experience a shortage in 0.96% of years. Conveyance path 2 is much risker due to the frequent impairment of CD (Figure 3.7). One or more components of conveyance path 2 are expected to be impaired in 20.97% of years and two or more components should be impaired in 2.41% of years. Despite the low reliability of conveyance path 2, it provides some level of redundancy for path 1. The redundant conveyance scenario reduces the frequency of at least one impairment from 5.17% to 4.95% of years (a 4.3% reduction) and it reduces the frequency of at least two impairments from 0.96% to 0.72% of years (a 25.0% reduction).

Table 3.5. System-level accounting of impaired components

Frequency of impaired components by subsystem and NTU impact threshold for the high SDR scenario.

Scenario	NTU	Impaired components (% of years)								
		0	1	2	3	4	5	6	≥ 1	≥ 2
Redundant sources	10	68.50	31.44	0.06	NA	NA	NA	NA	31.50	0.06
	100	84.26	15.73	0.01	NA	NA	NA	NA	15.74	0.01
	1000	95.77	4.23	0.00	NA	NA	NA	NA	4.23	0.00
Conveyance path 1	10	88.15	8.38	2.57	0.71	0.15	0.04	0.00	11.85	3.47
	100	94.83	4.21	0.86	0.09	0.01	0.00	0.00	5.17	0.96
	1000	99.05	0.84	0.11	0.00	0.00	0.00	0.00	0.95	0.11
Conveyance path 2	10	67.86	25.67	5.27	0.98	0.22	NA	NA	32.14	6.47
	100	79.03	18.56	1.96	0.42	0.03	NA	NA	20.97	2.41
	1000	89.17	10.52	0.22	0.09	0.00	NA	NA	10.83	0.31
Redundant conveyance	10	88.84	9.23	1.52	0.37	0.04	0.00	0.00	11.16	1.93
	100	95.05	4.23	0.65	0.07	0.00	0.00	0.00	4.95	0.72
	1000	99.05	0.84	0.11	0.00	0.00	0.00	0.00	0.95	0.11

3.4 DISCUSSION

This work demonstrates that wildfire risk to water supplies is considerably more nuanced than indicated by coarse-scale analyses that consider few water system characteristics (Thompson et al. 2013b; Robinne et al. 2018). The Monte Carlo simulation included realistic representations of wildfire and rainfall activity, post-fire watershed response, and water supply sensitivity to sediment to estimate the probability of water impairment. Our results suggest that water supply infrastructure with large contributing areas are most at risk of impairment due to their frequent exposure to wildfires large enough to mobilize problematic sediment quantities. Off-network water supplies are at lower risk because wildfire is less likely to encounter small watersheds. Larger waterbodies are also more resistant to water quality impairment due their greater capacity to dilute contaminants. Hence, large off-network reservoirs are at very low risk of impairment. The results also demonstrate that risk of system disruption is reduced by

redundancy and magnified by dependency. Our test scenarios show how disruption risk can be lowered with both reliable off-network reservoirs and alternative conveyance routes. In contrast, conveyance systems with multiple nodes of impact may magnify risk because it is more likely that fire will encounter their collective watershed areas.

This study built upon previous applications of Monte Carlo simulation to assess wildfire-water supply risks. Thompson et al. (2013a) characterized water supply exposure to wildfire by intersecting wildfire perimeters from FSim with municipal watersheds. Similar to their results, we found wide variation in fire occurrence across watersheds and high conditional area burned in the smallest watersheds. Water managers should expect their largest watersheds to encounter large wildfires most frequently, all else being equal, but it is likely that a significant portion of their smallest watersheds will burn when they do encounter large wildfires. When the scale of problematic wildfire activity is known and landscape conditions are fairly uniform, an exposure analysis to characterize the frequency distribution of area burned may be all that is necessary to assess risks, similar to the germ-grain analysis from Jones et al. (2014). However, water managers are often seeking information on how wildfire effects may vary across large watersheds. Stochastically simulated wildfire events have also been linked to spatially explicit wildfire effects analysis in two previous studies, but the relative measures of conditional net value change used by Thompson et al. (2016) are difficult to translate into meaningful consequences for water management and the debris flow modeling in Haas et al. (2017) was not linked to water supply exposure.

A novel contribution of this study is linking stochastic wildfire and rainfall activity with approximations of watershed response and water supply sensitivity to assess risk of water quality impairment. Beyond wildfire size and rainfall magnitude, the location and pattern of wildfire

activity relative to spatial variation in biophysical drivers of fire behavior, post-fire erosion, and sediment transport substantially modify watershed response and water supply impacts (Figure 3.5). The rates of annual suspended sediment generation predicted by our watershed model with the high SDR scenario (0-35 Mg ha^{-1} yr^{-1}) are reasonable compared to the range of 0.017 to 50 Mg ha^{-1} yr^{-1} reported by previous studies (Smith et al. 2011) and most of the post-storm turbidities are in the common range of 100-1000 NTU observed after wildfires in the study region (Figure 3.7; Rhoades et al. 2011; Oropeza and Heath 2013; Murphy et al. 2015). The peak turbidities modeled for the on-network diversions – 34000 to 180000 NTU – are above the limits for most turbidity sensors but the corresponding suspended sediment concentrations of 39000 to 210000 mg L^{-1} fall below the maximum of 500000 mg L^{-1} observed after fires worldwide (Smith et al. 2011). A key result of our analysis is that much of the wildfire and rainfall activity in the larger watersheds is not predicted to cause water impairment (Figure 3.7); for example, the 100 NTU threshold was only exceeded at TD in 35.0% of the years that TD was exposed to wildfire-related sediment. This result seems reasonable given that not every large fire in the region has significantly impaired water sources. It also highlights the benefit of pairing exposure and effects analysis to identify the subset of wildfire and rainfall conditions that lead to impairment.

The annual impairment probabilities modeled in this study for individual water supplies span the range of 0 to 0.1935 for the 100 NTU threshold. The on-network diversions – CD and TD – had the highest probability of impairment at 0.1574 and 0.1935, respectively. Given that water quality is often impaired for two years, this corresponds to an impactful wildfire on average once every 10 to 13 years. If either of these were a community's sole water source, they would not meet typical source water reliability standards (e.g., 0.98-0.99). Their high fire exposure is the result of their large watersheds with high proportional coverage of dry forests. In

particular, the CD watershed stands out as exceptionally risky due to the combination of high burn probability, dense forests prone to burning at high severity, and high erosion potential (Figure 3.5). It is possible that long-term risk to TD is underestimated in this study because the fuels data used for both the FSim and FlamMap modeling reflect recent wildfire activity.

Previous work suggests small watersheds may be more prone to wildfire-related impairment due to the greater conditional probability of burning a high proportion of the watershed (Thompson et al. 2013a) and the smaller flows to dilute contaminants (Robinne et al. 2019). The low predicted impairment probabilities for off-network reservoirs in this study diverge from previous findings because these reservoirs have unnaturally high volumes for the local contributing area size, which results in lower sensitivity to suspended sediment inputs. This is especially true for the high-volume terminal reservoirs; TR1 was never impaired at the 100 NTU level and TR2 was impaired only once. The smaller reservoirs were more sensitive to wildfire impacts, but none had 100 NTU exceedance probabilities greater than 0.0167 because most rarely encountered large wildfires (Table 3.2). CR3 is the only on-network reservoir in the study system similar to Strontia Springs Reservoir, which was heavily impacted by the 1996 Buffalo Creek and 2002 Hayman Fires (Moody and Martin 2001; Martin 2016), and motivates much of the regional concern about wildfire risk to water supplies (Jones et al. 2017). CR3 is at moderate risk of impairment (100 NTU exceedance probability = 0.0276) because it is located at higher elevation where burn probability is lower (Figure 3.1) and just over a quarter of the contributing area is mapped as non-burnable due to sparse vegetation in the alpine.

Previous studies largely ignored the system context for water supplies, focusing on at most one or two reservoirs (Elliot et al. 2016; Thompson et al. 2016; Jones et al. 2017). Increasing source water redundancy is often advocated for as a means to mitigate wildfire-water

supply risks (Sham et al. 2013; Murphy et al. 2015; Martin 2016), but without quantitative estimates of the mitigation benefit. Considering covariance in fire exposure across a multi-source water system has been proposed as a means to optimize mitigation decisions using a portfolio investment framework (Warziniack and Thompson 2013). The Monte Carlo simulation methods used here allowed for meaningful characterization of the likelihood that multiple system components will be impaired at the same time (Table 3.5). Our results illustrate two forms of redundancy that are common in many water systems. The first is mitigating uncertainty with a high reliability water source, in this case, a large off network terminal reservoir. Assuming 100% substitutability, TR2 reduced the risk of water supply disruption to practically zero despite frequent impairment to TD (Table 3.5). The second form of redundancy reduces risk of water shortage through alternative conveyance paths. Despite the close proximity of the alternative conveyance paths and the low reliability of path 2, the paths were not always impaired by fire at the same time. The gain in system reliability from alternative sources and conveyance pathways should increase with geographic separation.

Wildfire risk magnification from dependencies has not been widely discussed. For conveyance path 1, we found modest increase in risk from the dependent nature of conveyance infrastructure; the most frequently impacted component was impaired 2.76% of simulation years but at least one component on the conveyance path was impaired in 5.17% of years. This magnification is a result of the increasing watershed area exposed to wildfire. For this assessment, it was assumed the 100 NTU impairment threshold for water treatment also applies to conveyance due to the undesirable effects of sedimentation to intake structures, pipelines, and canals, but it is possible that these components are less sensitive to suspended sediment than treatment infrastructure and therefore the absolute risk is lower. Still, this magnification

approximately doubled the likelihood of a conveyance disruption, so it is important to consider the cumulative exposure for dependent systems. Our simple accounting of co-impairment frequency at the same turbidity threshold was necessary due to limited information on the precise operational constraints of the infrastructure. Assigning an operational performance measure to each component as a function of turbidity and infrastructure characteristics would provide a more accurate accounting of the conditions that would disrupt conveyance beyond a tolerable level.

3.4.1 Analysis Limitations

The limitations of linked fire and watershed modeling systems have been discussed extensively in prior publications (e.g., Elliot et al. 2016; Jones et al. 2017; Chapter 2), but it is worth reiterating that coupling diverse data sources and models has potential for error due to data, model, and model linkage uncertainties. A limitation of the Monte Carlo simulation presented here is the use of current fuel conditions to model both wildfire occurrence with FSim and fire severity with FlamMap. Modeling based on current fuel conditions may not accurately reflect long-term fire potential if recent disturbances have altered fuels from their modal state. These effects could be minimized by modeling fire occurrence and severity based on potential undisturbed fuel conditions instead of current conditions. No attempt was made to account for fire activity under future climates. Wildfire-water supply risks are expected to increase in the short-term in response to increased burning (Sankey et al. 2017), but long-term increases in fire activity may initiate negative fire feedbacks (Hurteau et al. 2019). Current source redundancies may not provide as much disruption protection in the future if population and water demand increase, or water supply decreases.

The watershed modeling in this study also has several limitations. RUSLE is meant for annual erosion prediction (Renard et al. 1997), so the analysis focused on average annual post-storm suspended sediment concentrations. In reality, most erosion is associated with a small number of powerful storms (Wagenbrenner et al. 2006; Robichaud et al. 2013). By averaging the annual load across the number of sediment-generating storms, it is possible to classify a year as unimpaired despite the brief occurrence of impaired water quality after a powerful storm. We also did not account for the potential cumulative impact of storms on subsequent days to raise suspended sediment concentrations in reservoirs above the impairment threshold. The assumption that the sediment load is equally mixed in the average annual reservoir or daily flow volume is also an approximation. Water supply susceptibility to impairment should vary with water body volume due short and long-term trends in precipitation, which also influence fire activity. It is therefore possible that impairment risk is higher than estimated here because waterbody volumes are likely lower than average during periods of high fire activity. The empirical model of hillslope sediment delivery ratio (Wagenbrenner and Robichaud 2014) used to predict the proportion of erosion delivered to streams was developed from plots and catchments burned primarily at moderate and high severity, but many of the smaller fires simulated in this study did not burn entire catchments. Use of this model could overestimate the potential for sediment delivery to streams where wildfire burns only part of a catchment, especially if it is separated from the stream by unburned forest and intact riparian vegetation. As demonstrated by our low and high SDR scenarios, there is also uncertainty in impairment probability magnitude (Table 3.4) due to imperfect understanding of sediment transport processes. Rainfall was treated as a spatially uniform process, but highly localized and intense rainstorms are the norm in this region (Moody and Martin 2009; Murphy et al. 2015; Kampf et

al. 2016). Spatial variability in rainfall might have similar effects as spatial variability in wildfire activity; that is, the probability of intense rainfall encountering a small watershed is probably lower than the probability of intense rainfall encountering a large fire in a large watershed. Therefore, adding spatial variability in rainfall might further decrease risk to water supplies with small contributing areas.

The use of turbidity modeled from suspended sediment as a single metric of water quality is a simplification that seems reasonable in our study region due to past reports of wildfire impacts to municipal water supplies (Sham et al. 2013), but elevated nutrients and heavy metals also impair water (Smith et al. 2011; Abraham et al. 2017). Concerning concentrations of carbon and nitrogen constituents have been detected after past wildfires in Colorado (Rhoades et al. 2011; Murphy et al. 2015). Emelko et al. (2011) presents similar results for the Canadian Rockies and discusses the water treatment implications of elevated post-fire nutrient and metal concentrations. If mobilization and transport of these constituents are tied to surface erosion and storm flows, a similar analysis as presented here, may be possible to assess water supply impairment risk.

3.4.2 Management Implications

The results of this study suggest that, for this system, impairment risk is tolerable for many off-network reservoirs but concerning for on-network diversions and reservoirs with large watersheds. One might interpret these results as suggesting mitigation efforts should be prioritized in the large watersheds serving on-network water supplies to bring them and their parent systems up to desired reliability targets. However, the effectiveness of this strategy will be low if treatments are not well placed and well timed to interact with wildfires. It is possible that focusing instead on reducing fuels around off-network reservoirs would be a cheaper and more

effective means to increase system reliability. Watersheds serving off-network reservoirs are often small, so it may be economical to treat fuels on the majority of the area resulting in meaningful erosion reduction when fire does burn the watershed. Proactively reducing fuels in small watersheds should be straightforward owing to limited options for treatment placement. Spatially explicit hazard or risk measures (e.g., Elliot et al. 2016, Chapter 2) may help to prioritize mitigation in larger watersheds with diverse conditions. Haas et al. (2017) also suggests that fuel treatments aimed at interrupting fire spread paths or facilitating suppression could be designed to restrict fire sizes and subsequent watershed responses to tolerable levels. There is also considerable interest in the use of natural and prescribed fire to expand the pace and scale of fuels reduction. The Monte Carlo simulation system used in this study could be adapted to test the effectiveness of alternative fuel treatment strategies at reducing impairment and system disruption risks. If proactive mitigation is not practical, risk analyses with baseline conditions may help communities prepare for efficient post-fire rehabilitation with mulching (Wagenbrenner et al. 2006; Robichaud et al. 2013; Schmeer et al. 2018).

Unlike sedimentation of on-network reservoirs, there is considerable potential to mitigate water quality impacts with minor infrastructure modifications. The low frequency of rainfall of sufficient intensity to generate sediment (4 to 18 times per year in this region) suggests water quality is likely to be impaired only a small fraction of the time, thus allowing many water sources to be utilized between storms. The actual frequency of impairment can be higher than the frequency of storms when changes in flow resuspend stored sediments (Oropeza and Heath 2013; Miller et al. 2017). Real-time monitoring of stream turbidity can inform water intake closures (Oropeza and Heath 2013; Martin 2016). Pre-sedimentation basins are also an option to reduce sediment concentrations prior to treatment or conveyance (Writer et al. 2014; Martin

2016). Adding several days of raw or treated storage capacity could eliminate much of the hardship from short impairment events. This study also demonstrates that some water systems may already be at low risk of water shortage from wildfire due to existing source water redundancies. Multi-source water systems are common among larger municipalities in Colorado, but small communities often rely on a sole source. In some cases, regional water projects provide the necessary plumbing for inter-community water transfer agreements, which have been discussed as a promising solution to mitigate drought risks (Zeff et al. 2016) and might provide similar protection from wildfire-related water shortages. Communities looking to diversify sources may benefit from analysis of historical or modeled fire activity to identify new sources that are unlikely to be impacted at the same time as their current sources to maximize the benefit of their investments in redundancy.

REFERENCES FOR CHAPTER 3

Abraham J, Dowling K, Florentine S (2017) Risk of post-fire metal mobilization into surface water resources: a review. *Science of the Total Environment* **599-600**, 1740-1755. doi:10.1016/j.scitotenv.2017.05.096

Benavides-Solorio JD, MacDonald LH (2005) Measurement and prediction of post-fire erosion at the hillslope scale, Colorado Front Range. *International Journal of Wildland Fire* **14**, 457-474. doi:10.1071/WF05042

Bivand R, Rundel C (2018) rgeos: Interface to Geometry Engine - Open Source ('GEOS'). R package version 0.4-2 [Software]. Available from https://CRAN.R-project.org/package=rgeos.

Bivand R, Keitt T, Rowlingson B (2019) rgdal: Bindings for the 'Geospatial' Data Abstraction Library. R package version 1.4-3 [Software]. Available from https://CRAN.R-project.org/package=rgdal.

Bradshaw L, McCormick E (2000) FireFamily Plus user's guide, version 2.0. USDA Forest Service, Rocky Mountain Research Station, General Technical Report RMRS-GTR-67WWW. (Ogden, UT, USA)

Buckley M, Beck N, Bowden P, Miller ME, Hill B, Luce C, Elliot WJ, Enstice N, Podolak K, Winford E, Smith SL, Bokach M, Reichert M, Edelson D, Gaither J (2014) Mokelumne watershed avoided cost analysis: why Sierra fuel treatments make economic sense. A report prepared for the Sierra Nevada Conservancy, The Nature Conservancy, and USDA Forest Service. Sierra Nevada Conservancy. (Auburn, CA, USA)

Cannon SH, Gartner JE, Rupert MG, Michael JA, Rea AH, Parrett C (2010) Predicting the probability and volume of post-wildfire debris flows in the intermountain western United States. *Geological Society of America Bulletin* **122**, 127-144. doi:10.1130/B26459.1

Crosby JS, Chandler CC (1966) Get the most from your windspeed observation. *Fire Control Notes* **27**, 12-13.

Elliot WJ, Miller ME, Enstice N (2016) Targeting forest management through fire and erosion modelling. *International Journal of Wildland Fire* **25**, 876-887. doi:10.1071/WF15007

Emelko MB, Silins U, Bladon KD, Stone M (2011) Implications of land disturbance on drinking water treatability in a changing climate: demonstrating the need for "source water supply and protection" strategies. *Water Research* **45**, 461-472. doi:10.1016/j.watres.2010.08.051

ESRI (2015) ArcGIS software, version 10.3 [Software]. Available from https://www.esri.com/en-us/home (Redlands, CA, USA)

Finney MA (2005) The challenge of quantitative risk analysis for wildland fire. *Forest Ecology and Management* **211**, 97-108. doi:10.1016/j.foreco.2005.02.010

Finney M, Grenfell IC, McHugh CW (2009) Modeling containment of large wildfires using generalized linear mixed-model analysis. *Forest Science* **55**, 249-255.

Finney MA, McHugh CW, Grenfell IC, Riley KL, Short KC (2011) A simulation of probabilistic wildfire risk components for the continental United States. *Stochastic Environmental Research and Risk Assessment* **25**, 973-1000. doi:10.1007/s00477-011-0462-z

Finney MA, Brittain S, Seli RC, McHugh CW, Gangi L (2015) FlamMap: fire mapping and analysis system (version 5.0) [Software]. Available from http://www.firelab.org/document/flammap-software.

Frickel DG, Shown LM, Patton PC (1975) An evaluation of hillslope and channel erosion related to oil-shale development in the Piceance basin, north-western Colorado. Colorado Department of Natural Resources, Colorado Water Resources Circular 30. (Denver, CO, USA)

Gannon BM, Wei Y, MacDonald LH, Kampf SK, Jones KW, Cannon JB, Wolk BH, Cheng AS, Addington RN, Thompson MP (2019) Prioritising fuels reduction for water supply protection. *International Journal of Wildland Fire* **28**, 785-803. doi:10.1071/WF18182

Graham RT (2003) Hayman Fire case study. USDA Forest Service, Rocky Mountain Research Station, General Technical Report RMRS-GTR-114. (Ogden, UT, USA)

Haas JR, Calkin DE, Thompson MP (2015) Wildfire risk transmission in the Colorado Front Range, USA. *Risk Analysis* **35(2)**, 226-240. doi:10.1111/risa.12270

Haas JR, Thompson M, Tillery A, Scott JH (2017) Capturing spatiotemporal variation in wildfires for improving post-wildfire debris-flow hazard assessments. In 'Natural hazard uncertainty assessment: modeling and decision support, geophysical monograph 223'. (Eds K Riley, P Webley, M Thompson) pp. 301–317. (John Wiley & Sons: Hoboken, NJ, USA)

Haimes YY (2012) Systems-based guiding principles for risk modeling, planning, assessment, management, and communication. *Risk Analysis* **32(9)**, 1451-1467. doi:10.1111/j.1539-6924.2012.01809.x

Henkle JE, Wohl E, Beckman N (2011) Locations of channel heads in the semiarid Colorado Front Range, USA. *Geomorphology* **129**, 309-319. doi:10.1016/j.geomorph.2011.02.026

Hijmans RJ (2019). raster: Geographic Data Analysis and Modeling. R package version 2.8-19 [Software]. Available from https://CRAN.R-project.org/package=raster.

Hurteau MD, Liang S, Westerling AL, Wiedinmyer C (2019) Vegetation-fire feedback reduces projected area burned under climate change. *Scientific Reports* **9**, 2838. doi:10.1038/s41598-019-39284-1

Jones OD, Nyman P, Sheridan GJ (2014) Modelling the effects of fire and rainfall regimes on extreme erosion events in forested landscapes. *Stochastic Environmental Research and Risk Assessment* **28**, 2015-2025. doi:10.1007/s00477-014-0891-6

Jones KW, Cannon JB, Saavedra FA, Kampf SK, Addington RN, Cheng AS, MacDonald LH, Wilson C, Wolk B (2017) Return on investment from fuel treatments to reduce severe wildfire and erosion in a watershed investment program in Colorado. *Journal of Environmental Management* **198**, 66-77. doi:10.1016/j.jenvman.2017.05.023

Kampf SK, Brogan DJ, Schmeer S, MacDonald LH, Nelson PA (2016) How do geomorphic effects of rainfall vary with storm type and spatial scale in a post-fire landscape? *Geomorphology* **273**, 39-51. doi:10.1016/j.geomorph.2016.08.001

LANDFIRE (2016) *Fuel, topography, existing vegetation type, and fuel disturbance layers* (Version 1.4.0). U.S. Geological Survey. Available from http://landfire.cr.usgs.gov/viewer/.

Larsen IJ, MacDonald LH (2007) Predicting post-fire sediment yields at the hillslope scale: testing RUSLE and disturbed WEPP. *Water Resources Research* **43**, W11412. doi:10.1029/2006WR005560

Larsen IJ, MacDonald LH, Brown E, Rough D, Welsh MJ, Pietraszek JH, Libohova Z, Benavides-Solorio JD, Schaffrath K (2009) Causes of post-fire runoff and erosion: water repellency, cover, or soil sealing? *Soil Science Society of America Journal* **73**, 1393-1407. doi:10.2136/sssaj2007.0432

Martin DA (2016) At the nexus of fire, water and society. Philosophical Transactions of the Royal Society of London. Series B, *Biological Sciences* **371**, 20150172. doi:10.1098/rstb.2015.0172

Miller ME, Elliot WJ, Billmire M, Robichaud PR, Endsley KA (2016) Rapid-response tools and datasets for post-fire remediation: linking remote sensing and process-based hydrological models. *International Journal of Wildland Fire* **25**, 1061-1073. doi:10.1071/WF15162

Miller S, Rhodes C, Robichaud P, Ryan S, Kovecses J, Chambers C, Rathburn S, Heath J, Kampf S, Wilson C, Brogan D, Piehl B, Miller ME, Giordanengo J, Berryman E, Rocca M (2017) Learn from the burn: the High Park Fire 5 years later. USDA Forest Service, Rocky Mountain Research Station, Science You Can Use Bulletin, Issue 25. (Fort Collins, CO, USA)

Moody JA, Martin DA (2001) Initial hydrologic and geomorphic response following a wildfire in the Colorado Front Range. *Earth Surface Processes and Landforms* **26**, 1049-1070. doi:10.1002/esp.253

Moody JA, Martin DA (2009) Synthesis of sediment yields after wildland fire in different rainfall regimes in the western United States. *International Journal of Wildland Fire* **18**, 96-115. doi:10.1071/WF07162

Murphy SF, Writer JH, McCleskey RB, Martin DA (2015) The role of precipitation type, intensity, and spatial distribution in source water quality after wildfire. *Environmental Research Letters* **10**, 084007. doi:10.1088/1748-9326/10/8/084007

NRCS Soil Survey Staff (2016) *Web soil survey*. USDA Natural Resources Conservation Service. Available from https://websoilsurvey.nrcs.usda.gov/.

Nunes JP, Doerr SH, Sheridan G, Neris J, Santín C, Emelko MB, Silins U, Robichaud PR, Elliot WJ, Keizer J (2018) Assessing water contamination risk from vegetation fires: challenges, opportunities and a framework for progress. *Hydrological Processes* **32**, 687-694. doi:10.1002/hyp.11434

Oropeza J, Heath J (2013) Effects of the 2012 Hewlett and High Park Wildfires on water quality of the Poudre River and Seaman Reservoir. City of Fort Collins Utilities Report. (Fort Collins, CO, USA)

Perica S, Martin D, Pavlovic S, Roy I, St. Laurent M, Trypaluk C, Unruh D, Yekta M, Bonnin G (2013) 'NOAA Atlas 14, Volume 8 Version 2, precipitation-frequency atlas of the United States, Midwestern States.' (Silver Spring, MD, USA).

Pietraszek JH (2006) Controls on post-fire erosion at the hillslope scale, Colorado Front Range. Thesis. Colorado State University. (Fort Collins, CO, USA)

R Core Team (2019). R: a language and environment for statistical computing [Software]. R Foundation for Statistical Computing. (Vienna, Austria). Available from http://www.R-project.org/.

Renard KG, Foster GR, Weesies GA, McCool DK, Yoder DC (1997) Predicting soil erosion by water: a guide to conservation planning with the Revised Universal Soil Loss Equation (RUSLE). USDA Agricultural Research Service Agricultural Handbook no. 703. (Washington, DC, USA)

Rhoades CC, Entwistle D, Butler D (2011) The influence of wildfire extent and severity on streamwater chemistry, sediment and temperature following the Hayman Fire, Colorado. *International Journal of Wildland Fire* **20**, 430-442. doi:10.1071/WF09086

Robichaud PR, Wagenbrenner JW, Brown RE, Wohlgemuth PM, Beyers JL (2008) Evaluating the effectiveness of contour-felled log erosion barriers as a post-fire runoff and erosion

mitigation treatment in the western United States. *International Journal of Wildland Fire* **17**, 255-273. doi:10.1071/WF07032

Robichaud PR, Lewis SA, Wagenbrenner JW, Ashmun LE, Brown RE (2013a) Post-fire mulching for runoff and erosion mitigation. Part I: effectiveness at reducing hillslope erosion rates. *Catena* **105**, 75-92. doi:10.1016/j.catena.2012.11.015

Robichaud PR, Wagenbrenner JW, Lewis SA, Ashmun LE, Brown RE, Wohlgemuth PM (2013b) Post-fire mulching for runoff and erosion mitigation. Part II: effectiveness in reducing runoff and sediment yields from small catchments. *Catena* **105**, 93-111. doi:10.1016/j.catena.2012.11.016

Robinne F-N, Bladon KD, Silins U, Emelko MB, Flannigan MD, Parisien M-A, Wang X, Kienzle SW, Dupont DP (2019) A regional-scale index for assessing the exposure of drinking-water sources to wildfires. *Forests* **10**, 384. doi:10.3390/f10050384

Ryan SE, Dwire KA, Dixon MK (2011) Impacts of wildfire on runoff and sediment loads at Little Granite Creek, western Wyoming. *Geomorphology* **129**, 113-130. doi:10.1016/j.geomorph.2011.01.017

Sankey JB, Kreitler J, Hawbaker TJ, McVay JL, Miller ME, Mueller ER, Vaillant NM, Lowe SE, Sankey TT (2017) Climate, wildfire, and erosion ensemble foretells more sediment in western USA watersheds. *Geophysical Research Letters* **44**, 8884-8892. doi:10.1002/2017GL073979

Schmeer SR (2014) Post-fire erosion response and recovery, High Park Fire, Colorado. Thesis. Colorado State University. (Fort Collins, CO, USA.)

Schmeer SR, Kampf SK, MacDonald LH, Hewitt J, Wilson C (2018) Empirical models of annual post-fire erosion on mulched and unmulched hillslopes. *Catena* **163**, 276-287. doi:10.1016/j.catena.2017.12.029

Scott JH, Reinhardt ED (2001) Assessing crown fire potential by linking models of surface and crown fire behavior. USDA Forest Service, Rocky Mountain Research Station, General Technical Research Paper RMRS-RP-29. (Fort Collins, CO, USA)

Scott JH, Thompson MP, Calkin DE (2013) A wildfire risk assessment framework for land and resource management. USDA Forest Service, Rocky Mountain Research Station, General Technical Report RMRS-GTR-315. (Fort Collins, CO, USA)

Shakesby RA, Doerr SH (2006) Wildfire as a hydrological and geomorphological agent. *Earth-Science Reviews* **74**, 269-307. doi:10.1016/j.earscirev.2005.10.006

Sham CH, Tuccillo ME, Rooke J (2013) Effects of wildfire on drinking water utilities and best practices for wildfire risk reduction and mitigation. Water Research Foundation Report 4482. Available from www.waterrf.org.

Short KC, Finney MA, Scott JH, Gilbertson-Day JW, Grenfell IC (2016) Spatial dataset of probabilistic wildfire risk components for the conterminous United States. USDA Forest Service Research Data Archive. (Fort Collins, CO, USA) doi:10.2737/RDS-2016-0034

Singh VP, Jain SK, Tyagi A (2007) Risk and reliability analysis: a handbook for civil and environmental engineers. American Society of Civil Engineers Press. 785 p. (Reston, VA, USA) doi:10.1061/9780784408919

Smith HG, Sheridan GJ, Lane PNJ, Nyman P, Haydon S (2011) Wildfire effects on water quality in forest catchments: a review with implications for water supply. *Journal of Hydrology* **396**, 170-192. doi:j.jhydrol.2010.10.043

Theobald DM, Merritt DM, Norman JB (2010) Assessment of threats to riparian ecosystems in the western U.S. Report to the Western Environmental Threats Assessment Center,

Prineville, OR by the USDA Stream Systems Technology Center and Colorado State University. (Fort Collins, CO, USA)
Thompson MP, Scott J, Kaiden JD, Gilbertson-Day JW (2013a) A polygon-based modeling approach to assess exposure of resources and assets to wildfire. *Natural Hazards* **67**, 627-644. doi:10.1007/s11069-013-0593-2
Thompson MP, Scott J, Langowski PG, Gilbertson-Day JW, Haas JR, Bowne EM (2013b) Assessing watershed -wildfire risks on national forest system lands in the Rocky Mountain region of the United States. *Water* **5**, 945-971. doi:10.3390/w5030945
Thompson MP, Gilbertson-Day JW, Scott JH (2016) Integrating pixel- and polygon-based approaches to wildfire risk assessment: applications to a high-value watershed on the Pike and San Isabel National Forests, Colorado, USA. *Environmental Modeling and Assessment* **21**, 1-15. doi:10.1007/s10666-015-9469-z
Tillery AC, Haas JR, Miller LW, Scott JH, Thompson MP (2014) *Potential post-wildfire debris-flow hazards - a pre-wildfire evaluation for the Sandia and Manzano Mountains and surrounding areas, central New Mexico.* US Geological Survey Scientific Investigations Report 2014-5161. (Albuquerque, NM, USA)
U.S. Environmental Protection Agency (USEPA) and the U.S. Geological Survey (USGS) (2012) National Hydrography Dataset Plus – NHDPlus (Version 2.1). Available from http://www.horizon-systems.com/NHDPlus/index.php.
Wagenbrenner JW, MacDonald LH, Rough D (2006) Effectiveness of three post-fire rehabilitation treatments in the Colorado Front Range. *Hydrological Processes* **20**, 2989-3006. doi:10.1002/hyp.6146
Wagenbrenner JW, Robichaud PR (2014) Post-fire bedload sediment delivery across spatial scales in the interior western United States. *Earth Surface Processes and Landforms* **39**, 865-876. doi:10.1002/esp.3488
Warziniack T, Thompson M (2013) Wildfire risk and optimal investments in watershed protection. *Western Economics Forum* **12(2)**, 19-28.
Wickham H (2011) The split-apply-combine strategy for data analysis. *Journal of Statistical Software* **40(1)**, 1-29. doi:10.18637/jss.v040.i01
Wilson C, Kampf SK, Wagenbrenner JW, MacDonald LH (2018) Rainfall thresholds for post-fire runoff and sediment delivery from plot to watershed scales. *Forest Ecology and Management* **430**, 346-356. doi:10.1016/j.foreco.2018.08.025
Writer JH, Hohner A, Oropeza J, Schmidt A, Cawley KM, Rosario-Ortiz FL (2014) Water treatment implications after the High Park Wildfire, Colorado. *Journal of the American Water Works Association* **106(4)**, 189-199. doi:10.5942/jawwa.2014.106.0055
Zeff HB, Herman JD, Reed PM, Characklis GW (2016) Cooperative drought adaptation: integrating infrastructure development, conservation, and water transfers into adaptive policy pathways. *Water Resources Research* **52**, 7327-7346. doi:10.1002/2016WR018771

CHAPTER 4 – EVALUATING THE POTENTIAL TO MITIGATE SOURCE WATER RISKS WITH IMPROVED CONTAINMENT

4.1 INTRODUCTION

Improved wildfire containment is an attractive strategy to mitigate risk of water supply impairment because of the potential to limit fire sizes and impacts to tolerable levels without completely excluding fire and its benefits from the landscape. Recent efforts to make containment planning more proactive focus on zoning the landscape into fire management units called Potential fire Operational Delineations (PODs) using existing high probability control features such as roads, rivers, and fuel transitions (O'Connor et al. 2016; Thompson et al. 2016a). Beyond the inherent value of engaging managers in the process to identify and critique potential control features, the resulting POD areas become relevant spatial units for pre-fire analysis of endogenous and transmitted wildfire risk to inform response strategies that are appropriate for the predicted direction and magnitude of fire effects to water supplies and other values (Thompson et al. 2016a). While there has been substantial progress engaging managers in the bottom up approach to develop and employ PODs and their associated response strategies (Thompson et al. 2016a, 2018b; Caggiano 2019; Caggiano et al. 2020; Greiner et al. 2020; Dunn et al. 2020; Stratton 2020), less attention has been paid to evaluating the risk mitigation effectiveness of containing wildfire within these units and what functional improvements should be made to the container sizes and spatial arrangement to maximize their protection benefit for water supplies and other resources that depend on the scale of fire activity.

Wildfire is often harmful to water quality because reductions in surface cover and infiltration cause increases in surface runoff and erosion that can mobilize and transport

contaminants into surface water supplies (DeBano et al. 2005; Shakesby and Doerr 2006; Larsen et al. 2009; Smith et al. 2011). While the specific contaminants and concentrations of concern may vary by watershed and water system (Emelko et al. 2011; Smith et al. 2011; Abraham et al. 2017), water quality impairment generally occurs when large quantities of sediment are mobilized by intense rainfall causing contaminant concentrations to exceed thresholds for effective water treatment (e.g., Murphy et al. 2015). Post-fire sediment loads are influenced by fire size and burn severity, topography, soil properties, and rainfall intensity (Benavides-Solorio and MacDonald 2005; Shakesby and Doerr 2006; Schmeer et al. 2018). Previous efforts to account for fire effects on watershed response and water supply impacts account for some of these factors (Omi 1979; Thompson et al. 2013), but the use of relative fire effects measures makes it difficult to evaluate whether a given fire will impair water quality. This shortcoming has been addressed in recent years with increasing use of spatially explicit erosion and sediment transport models to make quantitative predictions of sediment yield from modeled wildfires (e.g., Cannon et al. 2010; Miller et al. 2011, 2016; Sidman et al. 2016). Sediment yield models have been widely used to examine the risk mitigation effectiveness of area-wide fuel treatments meant to reduce burn severity (Elliot et al. 2016; Sidman et al. 2016; Jones et al. 2017; Chapter 2) but they have not yet been used to evaluate the performance of fire containment strategies to reduce area burned.

Some water systems have discrete features, such as terminal reservoirs, that could be targeted for protection within a single POD, but many municipal watersheds in the western U.S. are hundreds to thousands of square kilometers in size and therefore require some level of internal compartmentalization to protect water supplies. In theory, the size and spatial arrangement of PODs could be designed to mitigate the risk of water supply impairment by both

containing fires with potential for large growth and subsequent contaminant loads near their ignition sources and ensuring that within-POD burning does not result in adverse consequence. Managers consider both values at risk and presence of control features when delineating PODs, which often results in smaller PODs near developed areas and larger PODs in the backcountry (Thompson et al. 2016a; Caggiano 2019). It is currently unclear whether the size and configuration of manager-delineated PODs will reduce risk of wildfire-related water impairment. Several attempt have been made to automate the processes of identifying suitable control features and aggregating them into PODs (Thompson et al. 2018a; Wei et al. 2018) using roads, streams, watershed boundaries, and spatial models of suppression difficulty and potential for control (Rodríguez y Silva et al. 2014; O'Connor et al. 2017; Rodríguez y Silva et al. 2020), but data-driven approaches have yet to inform the desired size and spatial configuration of PODs to mitigate a particular risk.

Recognizing the importance of fire size, location, and burn severity for watershed response, several previous studies have employed Monte Carlo wildfire simulation to characterize watershed exposure and water supply risk (Thompson et al. 2013, 2016b; Haas et al. 2017; Chapter 3). Their results suggest that most risk to water supplies is associated with a small subset of total fire activity. Moreover, the source locations of damaging wildfires tend to cluster in certain parts of the landscape, which implies containment benefits will depend strongly on location. Simulated fire ignition locations and fire extents can be intersected with relevant management units to partition fire impacts from burning within the unit of origin and transmission to the surrounding landscape (Haas et al. 2015; Thompson et al. 2016a; Ager et al. 2018). Analyzing risk transmission across a network of PODs could help to identify locations with high source risk that would benefit from increased investment in containment. For example,

fuels could be reduced along POD boundaries to increase containment probability. Areas with fuels conducive to fast fire spread tend to transmit the most fire (Ager et al. 2018), which will result in high water supply risk when adjacent areas have high erosion potential and/or short transport paths to water supplies. Analysis of water supply risk from self-burning could also identify high risk PODs that would benefit from further compartmentalization.

The goal of this study is to provide a proof of concept model to evaluate the effectiveness of a containment network at mitigating risk of water supply impairment. The general approach should also be relevant for assessing risk to other resources that depend on disturbance size. We utilize Monte Carlo wildfire simulation, erosion, and sediment transport modeling to quantify the potential water supply impacts from a set of simulated wildfires with and without containment. We analyze risk and risk mitigation with two measures of water supply impact – total sediment exposure and frequency of exceeding turbidity limits for treatment – to highlight how considering the scale-dependent effects of wildfire changes the perceived mitigation value of fire containment. Risk transmission analysis is used to identify possible improvements to the containment network with measures of transmitted risk highlighting those PODs and POD boundaries that could benefit from activities to improve containment probability and measures of self-burning indicating areas in need of further compartmentalization.

4.2 METHODS

4.2.1 Evaluation framework

The evaluation framework was designed to contrast the water supply impacts of uncontained wildfires and wildfires contained within the POD of origin in terms of total sediment load and average post-storm suspended sediment (Figure 4.1). Total sediment load is

similar to the commonly used net value change measures in risk assessment (Finney 2005; Scott et al. 2013) insomuch as more is interpreted as bad and any marginal reduction decreases risk. However, using change in total sediment load as a measure of risk has the potential to falsely assign mitigation benefit to containment when either the load from the uncontained wildfire is already below a meaningful threshold of water quality impairment or containment reduces erosion but the resulting load is still above the threshold for water impairment. Average post-storm suspended sediment concentration is used here to estimate whether fires will degrade water quality beyond limits for treatment and whether impairment outcomes change with containment. This measure of risk better approximates the threshold-dependent nature of water quality impairment owing to the size of the receiving waterbody and the water system sensitivity to contaminants.

Our evaluation framework focuses on the key uncertainties in wildfire-water impairment risk related to the extent of the watershed burned and post-fire rainfall (Figure 4.1). As further described in following sections, many plausible wildfire perimeters are simulated with the Monte Carlo ignition and spread model RANDIG (Haas et al. 2015), which are then clipped to the PODs of origin to approximate a strategy of improved containment. Post-fire erosion is then simulated for each perimeter using crown fire activity predicted with FlamMap 5.0 (Finney et al. 2015) as a proxy for burn severity to modify the cover and soil variables in the Revised Universal Soil Loss Equation (RUSLE; Renard et al. 2015). We account for uncertainty in post-fire rainfall by modeling erosion for three rainfall scenarios ranging from common to extreme. We estimate annual sediment loads to the water supply based on the predicted proportion of sediment transported off hillslopes and through channels using Sediment Delivery Ratio (SDR) models (Wagenbrenner and Robichaud 2014; Frickel et al. 1975) as described in Chapter 2. Post-

storm suspended sediment concentrations are estimated by assuming average storm sediment loads are diluted in the mean daily flow volume of the river. All analyses were completed with R version 3.5.3 (R Core Team 2019) except where noted otherwise.

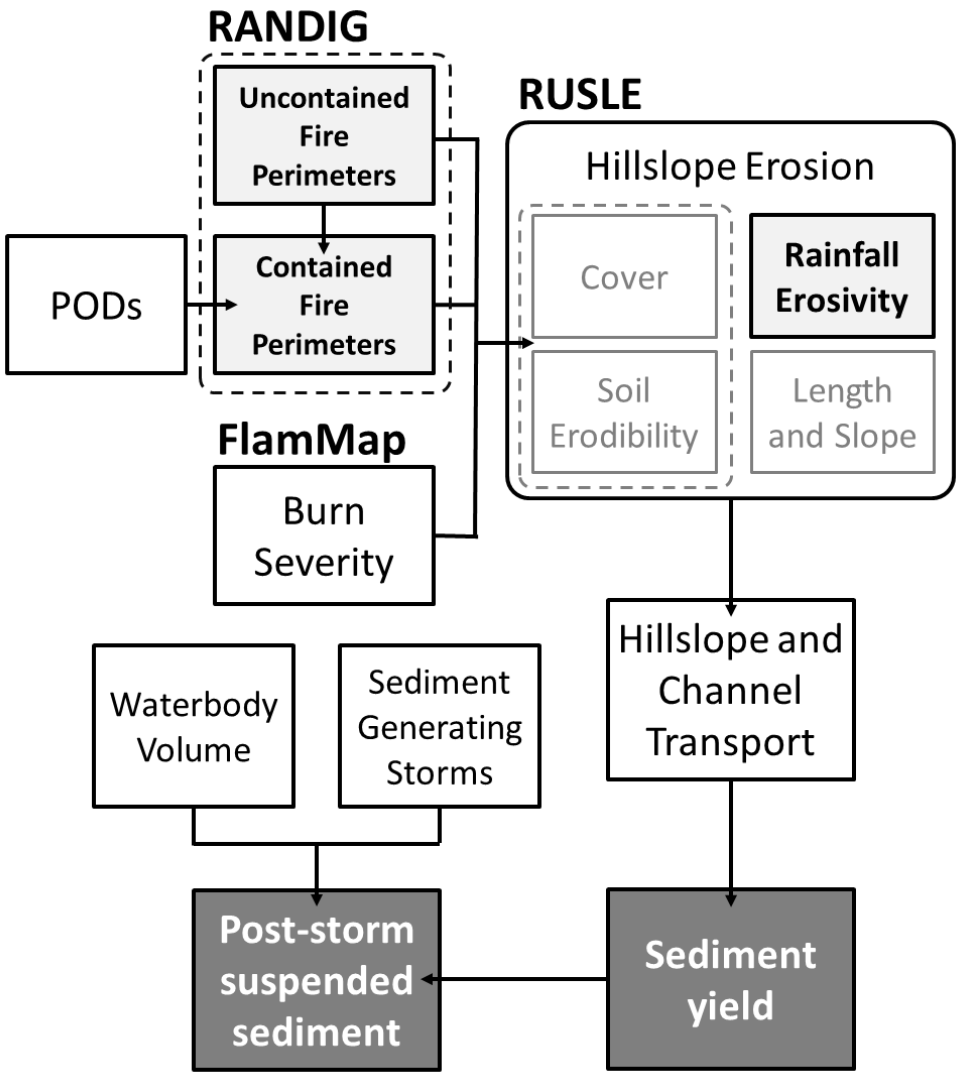

Figure 4.1. Containment evaluation framework

The evaluation framework focuses on total sediment yield and average post-storm suspended sediment as measures of water impairment risk. Variable inputs are in light grey. Stochastically simulated wildfire perimeters are combined with estimates of burn severity to model post-fire erosion and sediment transport to the water supply both with and without containment. Sediment yield is converted to average post-storm suspended sediment concentration using the receiving waterbody volume and the annual frequency of sediment generating storms.

4.2.2 Study area

The study area encompasses 3021 km^2 of the Front Range Mountains in Colorado, USA (Figure 4.2). The Front Range region has a history of large and severe fires that have caused extreme erosion, reservoir sedimentation, and water quality degradation (Moody and Martin 2001; Graham 2003; Wagenbrenner et al. 2006; Oropeza and Heath 2013; Murphy et al. 2015). The names of the focal municipal water supply and other geographic features within the study area are withheld for security reasons. The extent of the study area was defined to include the contributing area to a municipal diversion (1254 km^2) and a network of PODs developed by the local National Forest and their partnering state and local fire management agencies (an additional 1767 km^2). PODs that intersected a 5 km buffer around the watershed were included to analyze fires that spread into the watershed from nearby areas. Elevation ranges from 1559 to 4135 m above sea level across the study area. The climate is continental with warm dry summers and cold winters. Most erosion in this region results from intense convective rainstorms during the summer and early fall (Benavides-Solorio and MacDonald 2005; Moody and Martin 2009). The study area is primarily forest (71.7%) and the remainder is a mix of shrubland (9.0%), sparsely vegetated alpine (8.9%), and grassland (8.7%) (LANDFIRE 2016). Land ownership is split between USFS (55.3%), private (18.8%), NPS (18.1%), local government (6.4%), and state (1.4%).

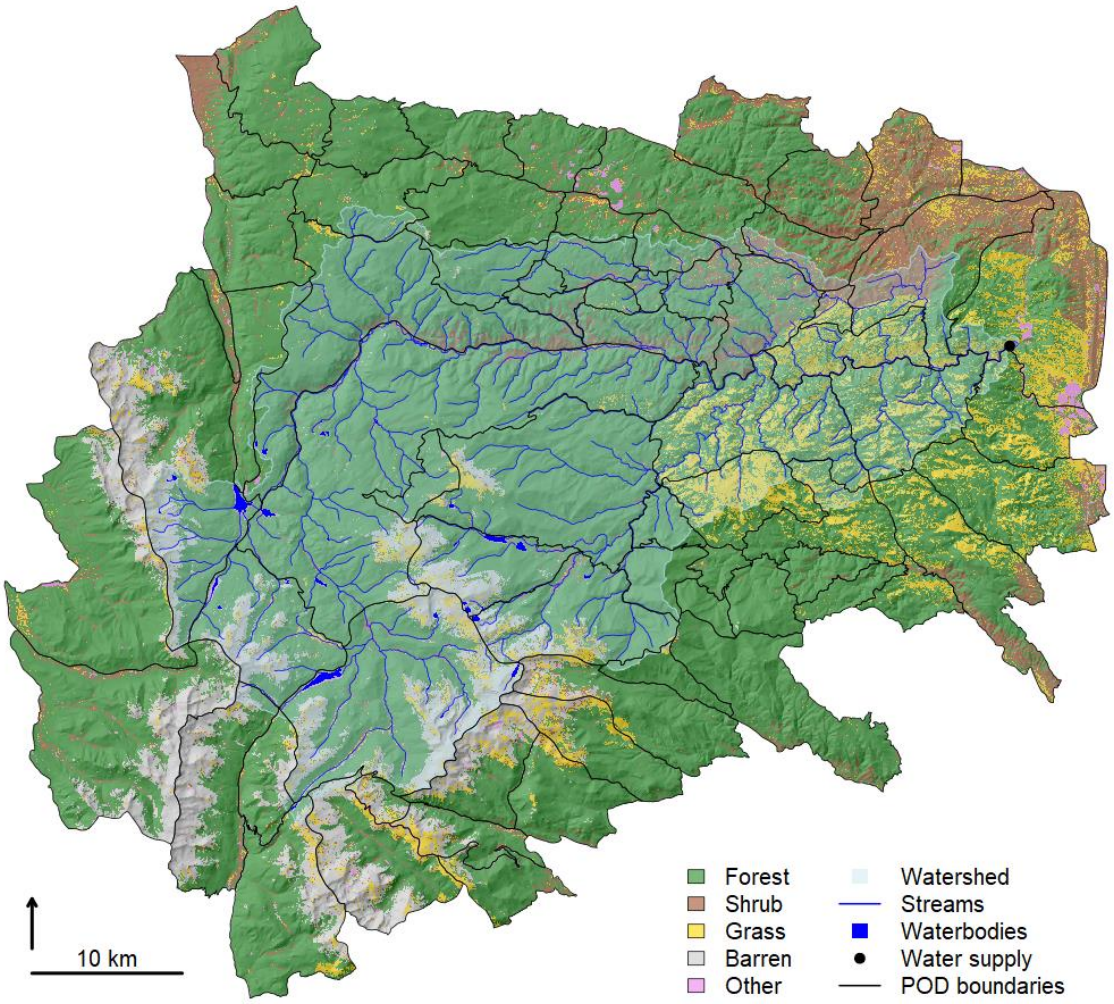

Figure 4.2. Study area

Map of the study area featuring the focal watershed and PODs that intersect a five km buffer around the watershed. Landcover is from LANDFIRE (2016). Barren is mostly sparsely vegetated areas of the alpine.

4.2.3 Potential fire operational delineations

PODs were developed by fire and resource management specialists from the local National Forest and external fire management partners from other federal, state, and local agencies. The PODs range in size from 502 to 23672 ha with a mean of 4316 ha and a median of 3516 ha. The PODs tend to be smallest near human settlements due to both the increased presence of control features and greater need for fire containment around communities. PODs

larger than 10000 ha are clustered in the higher elevation, western portion of the of the study area where much of the land is publicly owned and the transportation network is sparse. PODs also tend to be large along the major river canyon that runs west to east across the study area (Figure 4.2) due to limited presence of high probability control features other than the river and highway in the canyon bottom.

The rugged topography, rocky soils, and dense forests of the study area are major constraints on firefighter and equipment accessibility and operability. Accordingly, managers preferentially chose roads as the control features to bound PODs; of the 1386 km of POD edge, 985 km are roads (71.0%), 167 km are trails (12.0%), 150 km are ridges (10.8%), 46 km are streams (3.3%), and the remaining 40 km are fuel transitions, lakes/reservoirs, or lacking defined control features (2.9%). Many of the trails and ridges selected as control features are in barren or sparsely vegetated areas of the alpine, so roads make up an even larger proportion of POD edges in the fuel types where wildfire transmission is a concern. Numerous observational studies have documented that roads benefit fire control by serving as hard fire breaks that either stop fires passively or in combination with suppression firing or holding activities (Price and Bradstock 2010; Narayanaraj and Wimberly 2011; O'Connor et al. 2017; Yocum et al. 2019; Kolden and Henson 2020). The frequent use of roads in this POD network suggests containment probability should be high along most boundaries under low to moderate fire weather and many boundaries have potential for containment under more extreme conditions with well-coordinated suppression tactics.

4.2.4 Fire occurrence

We used the Monte Carlo fire simulation program RANDIG, which is a command-line version of the FlamMap minimum travel time module (Finney 2006), to model a plausible set of

5000 large fire growth events across the study area. The inputs to RANDIG include raster surfaces of fuels, topography, and ignition density, and a set of fire scenarios describing the fuel moisture, wind speed, wind direction, spotting probability, and burn duration for the simulations and their probabilities of occurrence. The intent of our model parameterization is to approximate the distribution of potential area burned during the initial growth period of large fires owing to variation in wind direction and wind speed. We focused on the early growth period of fires to align with the desire to contain most fires before they leave the POD of origin. Modeling fire growth over longer periods would increase fire size and thus the avoided area burned and water supply impacts but would also introduce greater uncertainty about the final fire extent as more potential containment features are encountered and weather conditions are likely to moderate.

Raster fuels and topography data representing landscape conditions circa 2014 were acquired from LANDFIRE (2016) including canopy cover, canopy bulk density, canopy base height, canopy height, surface fire behavior fuel model (Scott and Burgan 2005), elevation, slope, and aspect. Fuels were adjusted in lodgepole pine (*Pinus contorta* var. *latifolia*) forests by lowering the canopy base height by 20% and changing the fire behavior fuel model to high load conifer litter (TL5 from Scott and Burgan 2005) to better match recent observations of extreme fire behavior in these forests (Moriarty et al. 2019). The other spatial input is a raster surface of ignition density, which influences the relative probability of fire ignition across the modeling domain. Spatial point locations of historical fires from Short (2017) were generalized into a raster surface of ignition density using a kernel density function with a search distance of 10 km in ArcGIS 10.3 (ESRI 2015).

Fuel moisture, wind speed, and wind direction for the fire scenarios (Table 4.1) were informed by data from a Remote Automated Weather Station (RAWS) located in the northern

half of the study area at 2500 m above sea level. Fuel moisture and wind speed percentiles were calculated with FireFamilyPlus 4.1 (Bradshaw and McCormick 2000) and wind speed was converted from a 10-minute to 1-minute average based on Crosby and Chandler (1966). Most large fires in this region occur in early summer during drought years or in late fall when fuel moisture is extremely low. These conditions were approximated using the historical 3rd percentile fire season (April 01-October 31) fuel moistures, which are 2, 3, 6, 30, and 60 percent for the 1-hr, 10-hr, 100-hr, herbaceous, and woody fuels, respectively. Fuel moisture was held constant across all wind scenarios because it exhibits little meaningful variation below the 10th percentile. Wind scenarios were designed to approximate the joint probability distribution of wind speeds and directions that are problematic for fire growth. The 50th, 90th, and 97th percentiles of 1-minute average wind speeds are 19.3, 33.8, and 43.5 kph. We generalized these into three levels of wind speed (16.1, 32.2, and 48.3 kph) and their associated spotting probabilities (0.02, 0.05, and 0.10) that we assigned relative probabilities of occurrence of 0.90, 0.07, and 0.03. Previous large fires in this landscape are associated with strong westerly winds and our analysis of the historical record found that 74.1% of all winds greater than or equal to 16.1 kph were from the northwest, west, or southwest, which have relative probabilities of occurrence equal to 0.29, 0.48, and 0.23. We combined the three levels of wind speed and spotting probabilities with the three variations of wind direction into a total of nine fire scenarios (Table 4.1). Burn duration was set to four hours for all scenarios, which was determined by incrementally adjusting burn duration in 30-minute time steps until the largest simulated fire was within +/- 5% of 20000 ha, which we judge as a reasonable upper bound for fire size during a single burn period in this landscape based on other fires in the region (Graham 2003).

Table 4.1. Fire simulation scenarios

Fire scenarios used to simulate fires in RANDIG. Burn duration was set to 240 minutes and fuel moisture was held constant at the 3rd percentile of the historical record.

Scenario	Wind Speed (kph @ 6 m)	Direction (deg)	Spot Probability	Scenario Probability
1	16.1	225	0.02	0.259
2	16.1	270	0.02	0.431
3	16.1	315	0.02	0.210
4	32.2	225	0.05	0.020
5	32.2	270	0.05	0.034
6	32.2	315	0.05	0.016
7	48.3	225	0.1	0.009
8	48.3	270	0.1	0.014
9	48.3	315	0.1	0.007

4.2.5 Fire behavior and severity

Crown fire activity (Scott and Reinhardt 2001) was modeled as a proxy for burn severity with FlamMap 5.0 (Finney et al. 2015) by mapping surface fire, passive crown fire, and active crown fire to low, moderate, and high severity, respectively. Crown fire activity is commonly used to estimate burn severity for watershed modeling (Tillery et al. 2014; Haas et al. 2017; Chapter 2) because it captures the trend of increasing fire intensity along the gradient of surface to active crown fire behavior. Fuel moisture was set to the same 3rd percentile fuel moisture described in the fire occurrence section. The same topography and modified fuels rasters were also used as the landscape inputs to FlamMap. To simplify the analysis, we modeled burn severity for the middle wind speed scenario (32.2 kph @ 6 m) and used the wind blowing uphill option to represent a consistent worst-case scenario for all aspects.

4.2.6 Post-fire watershed response

Post-fire erosion and sediment transport to the water diversion point was predicted by a system of coupled hillslope erosion, hillslope sediment transport, and channel sediment transport models (Figure 4.1) calibrated for prediction in the study region as detailed in Chapters 2 and 3.

To be brief, only essential details of the methods are repeated here. Model evaluation is reserved for the discussion section of this chapter. Chapter 5 also reviews the limitations of the system of models and highlights potential future improvements. The NHDPlus raster and watershed network products (USEPA and USGS 2012) were used to represent the topological connections between upland sediment sources and the water diversion point via sub-catchment drainage paths to the flowline network and the series of intervening flowlines between each catchment and the diversion. First, gross hillslope erosion was modeled for each fire with a raster Geographic Information System implementation (Theobald et al. 2010) of RUSLE (Renard et al. 1997). Sediment transport to streams was predicted using an empirical model of post-fire hillslope sediment delivery ratio from the western U.S. (Wagenbrenner and Robichaud 2014) to estimate the proportion of sediment generated in each pixel that makes it to the flowline network. Third, the total sediment from each catchment was routed down the flowline network to the diversion point using a simple model of channel sediment delivery ratio (Frickel et al. 1975) adapted for the channel types in the study area.

4.2.6.1 Hillslope Erosion

The GIS implementation of RUSLE predicts gross erosion (Mg ha^{-1} yr^{-1}) as the product of factors for rainfall erosivity (R), soil erodibility (K), length and slope (LS), cover (C), and support practices (P). Rainfall erosivity is calculated as the product of storm maximum rainfall intensity and kinetic energy per unit area (Renard et al. 1997). First year post-fire erosion was modeled at three levels of May to October rainfall erosivity – 403, 887, 5168 MJ mm ha^{-1} hr^{-1} – representing the 2, 10, and 100-year recurrence interval rainfall erosivity for the regional climate (Perica et al. 2013; Wilson et al. 2018; Chapter 2). The May through October period was selected because most post-fire erosion in this climate occurs in response to high intensity summer

rainfall (Benavides-Solorio and MacDonald 2005). LS was calculated from a 30 m resolution digital elevation model (USEPA and USGS 2012) following the methods of Winchell et al. (2008) with a maximum limit on flow accumulation imposed to approximate the original hillslope length guidance in Renard et al. (1997). Baseline K came from the Soil Survey Geographic Database (SSURGO) where available and the State Soil Geographic Database (STATSGO) to fill missing data (NRCS Soil Survey Staff 2016). Post-fire erosion was simulated by modifying the K and C factors based on wildfire extent and burn severity (Larsen and MacDonald 2007; Chapter 2). No support practices were considered to model the unmitigated erosion hazard. Baseline erosion is not a major concern for water quality, so we focused our assessment on the post-fire increase in erosion. First-year post-fire increase in erosion (*A*) was calculated with Eqn 4.1 for each rainfall recurrence interval.

$$A = R \times LS \times [(K_b \times C_b) - (K \times C)] \quad \textbf{Equation 4.1}$$

The subscript *b* indicates the burned condition for K and C factors. We limited hillslope erosion predictions to 100 Mg ha^{-1} yr^{-1} based on the maximum observed values reported in the study region (Moody and Martin 2001, 2009).

4.2.6.2 Hillslope Sediment Transport

An empirical model of post-wildfire hillslope sediment delivery ratio (*hSDR*) from the western U.S. (Wagenbrenner and Robichaud 2014) was used to estimate the proportion of sediment generated in each pixel that makes it to the stream network. The NHDPlus flowlines were first extended to include all pixels with a contributing area greater than 10.8 ha (Henkle et al. 2011) to better approximate the extent of the post-fire channel network. Post-fire *hSDR* was then estimated with the annual length ratio model from Wagenbrenner and Robichaud (2014). We applied this model to predict *hSDR* as a function of the flow path length from each pixel to

the nearest stream channel as the "catchment length" and the flow path length across the pixel as the "plot length" (Eqn 4.2). Flow path length to the nearest channel was calculated from a 30 m digital elevation model (USEPA and USGS 2012) in ArcGIS 10.3 (ESRI 2015). We doubled the predicted *hSDR* to both account for under-sampling of suspended sediment in the model training data and to roughly calibrate our net sediment yield predictions to the small catchment yields from the Hayman Fire in Colorado (Wagenbrenner and Robichaud 2014). This increased the maximum *hSDR* from 0.27 to 0.54 for areas near streams and it increased the minimum *hSDR* from 0.05 to 0.10 for locations furthest from streams. We later compare our modeled gross and net hillslope sediment yields to relevant field observations in the discussion to demonstrate that this assumption is reasonable. Channel pixels were assigned *hSDR* of 1.

$$log(hSDR) = -0.56 - 0.0094 \times \left(\frac{Flow\ path\ length\ to\ nearest\ channel}{Flow\ path\ length\ across\ pixel}\right) \quad \textbf{Equation 4.2}$$

The first-year mass of sediment (Mg) delivered from a catchment to the stream network (TS) was calculated as the sumproduct of the post-fire hillslope erosion (A), the pixel area, and *hSDR* for all burned pixels (N) in the catchment (Eqn 4.3).

$$TS = \sum_{i=1}^{N} A_i \times 0.09 \frac{ha}{pixel} \times hSDR_i \quad \textbf{Equation 4.3}$$

4.2.6.3 Channel Sediment Transport

Sediment was routed through the NHDPlus flowline network to the diversion by adapting the channel sediment delivery ratio (*cSDR*) model of Frickel et al. (1975) to the channel types in the study watershed (Chapter 2). In montane streams of this region, sediment retention is generally highest in low order channels because of high roughness and limited transport capacity and very low in the high order channels with high transport capacity (Moody and Martin 2001). Observations of post-fire sediment transport in a similar watershed in Wyoming suggest transport of fine sediments in suspension should be very efficient in high order channels even

during base flow conditions (Ryan et al. 2011). These trends are approximated in our model by assigning *cSDRs* of 0.75, 0.80, 0.85 and 0.95 per 10 km of stream length to 1st, 2nd, 3rd, and 4th or higher-order streams, respectively. Sediment retention in lakes and reservoirs was accounted for by assigning as a *cSDR* of 0.05 to the terminal flowline in each waterbody. The annual mass of fire-related sediment (Mg) delivered to the water diversion (TD) was calculated as the sum of sediment delivered to streams for all upstream catchments multiplied by the product of *cSDRs* for the intervening flowlines (Eqn 4.4).

$$TD = \sum_{j=1}^{O}(TS_j \times \prod_{k=1}^{P} cSDR_k) \qquad \textbf{Equation 4.4}$$

The subscript *j* is the index for the *O* upstream catchments and the subscript *k* is the index for the *P* intervening flowlines between catchment *j* and the water diversion.

4.2.7 Water supply impacts

The first metric of water supply impact is the total wildfire related sediment delivered to the diversion (Mg). The second metric is the per-fire average post-storm suspended sediment concentration (SSC). Wilson et al. (2018) found that a threshold rainfall intensity of 7 mm h^{-1} best predicts when hillslope erosion will occur in this region. This intensity is exceeded on average four times per year in the study watershed. We make the simplifying assumption the first-year post fire sediment load from the coupled erosion and sediment transport model is divided equally among four storms. Suspended sediment after summer thunderstorms is primarily clay and silt (70-85%) and the remainder is mostly fine-grained organics (Ryan et al. 2011), which differs from the composition of soils mobilized from hillslope erosion. According to Schmeer (2014), clay and silt make up approximately 25% of post-fire sediment mass from hillslope erosion in the region. Combining these two observations, we make a liberal assumption that up to 35% of the hillslope erosion predicted by RUSLE is part of the fine-grained inorganic

and organic components that contribute to suspended sediment. Water quality is usually impaired for short periods (hours to days) following rainstorms in this region (Oropeza and Heath 2013; Sham et al. 2013), so we calculate post-storm suspended sediment concentrations using the average storm load of fine sediment and the daily flow volume past the diversion point, which averages 1.48 x 10^9 liters per day for the May to October period (gage-adjusted estimates from USEPA and USGS 2012). Suspended sediment concentration is rarely monitored directly, so limits for treatment are more commonly expressed in turbidity. For this analysis, we use the high end of 100 Nephelometric Turbidity Units (NTU) reported in the literature (Writer et al. 2014; Murphy et al. 2015) to be conservative in our judgement of impairment. A conversion equation developed from post-fire monitoring of the Fourmile Canyon Fire was used to predict turbidity (NTU) from SSC (mg l^{-1}) (Murphy et al. 2015; Eqn 4.5).

$$NTU = \frac{SSC - 2.84}{1.166} \qquad \textbf{Equation 4.5}$$

4.2.8 Containment effectiveness evaluation and prioritization

To quantify the effectiveness of containment, we focused on the difference between the total water supply impact measures with and without containment including watershed area burned, sediment delivered to the diversion, and number of water quality impairments. The difference between impact measures for the uncontained and contained scenarios is the avoided transmitted risk (Ager et al. 2018). Total sediment load is a continuous value whereas impairment is a binary outcome. Impairment was only considered transmitted when the outcome changes from unimpaired for within POD burning to impaired for the entire fire footprint. To prioritize improvements along the potential control lines that bound PODs, we calculated risk transmission across the POD edges based on their proportional engagement with the fires that originate in their respective PODs; that is, the outcomes associated with fire spreading to the

surrounding landscape were divided among the lines based on their intersected length. It is anticipated that the primary mitigation action would be fuels reduction along the control lines, so transmission risk was normalized by length to compare the relative benefit of hardening control lines.

4.3 RESULTS

4.3.1 Fire occurrence

Historical fire ignitions from the FOD (Short 2017) were concentrated in the lower and middle portions of focal watershed and along the southern boundary of the study area (Figure 4.3a) reflecting both variation in fire season length and human use of the landscape. The 5000 wildfires simulated with RANDIG ranged in size from 0.09 to 20868 ha with a mean of 1961 ha and a median of 1469 ha. We selected the 3040 fires that burned at least part of the focal watershed for futher analysis. Their size distribution did not vary substantially from that of the full simulation set. The excluded fires either did not grow large enough to intercept the focal watershed, or the predominant wind direction caused them to spread away from it. The middle and lower portions of the watershed are predicted to burn most frequently due to both the greater ignition density and the presence of fuel types that promote faster spread (Figure 4.3b). The high elevations in the western half of the study area are predicted to burn infrequently due to low ignition density and the sparse fuels. The southeast corner of the study area near the diversion has low burn probability because the fuels have not yet recovered from a recent wildfire.

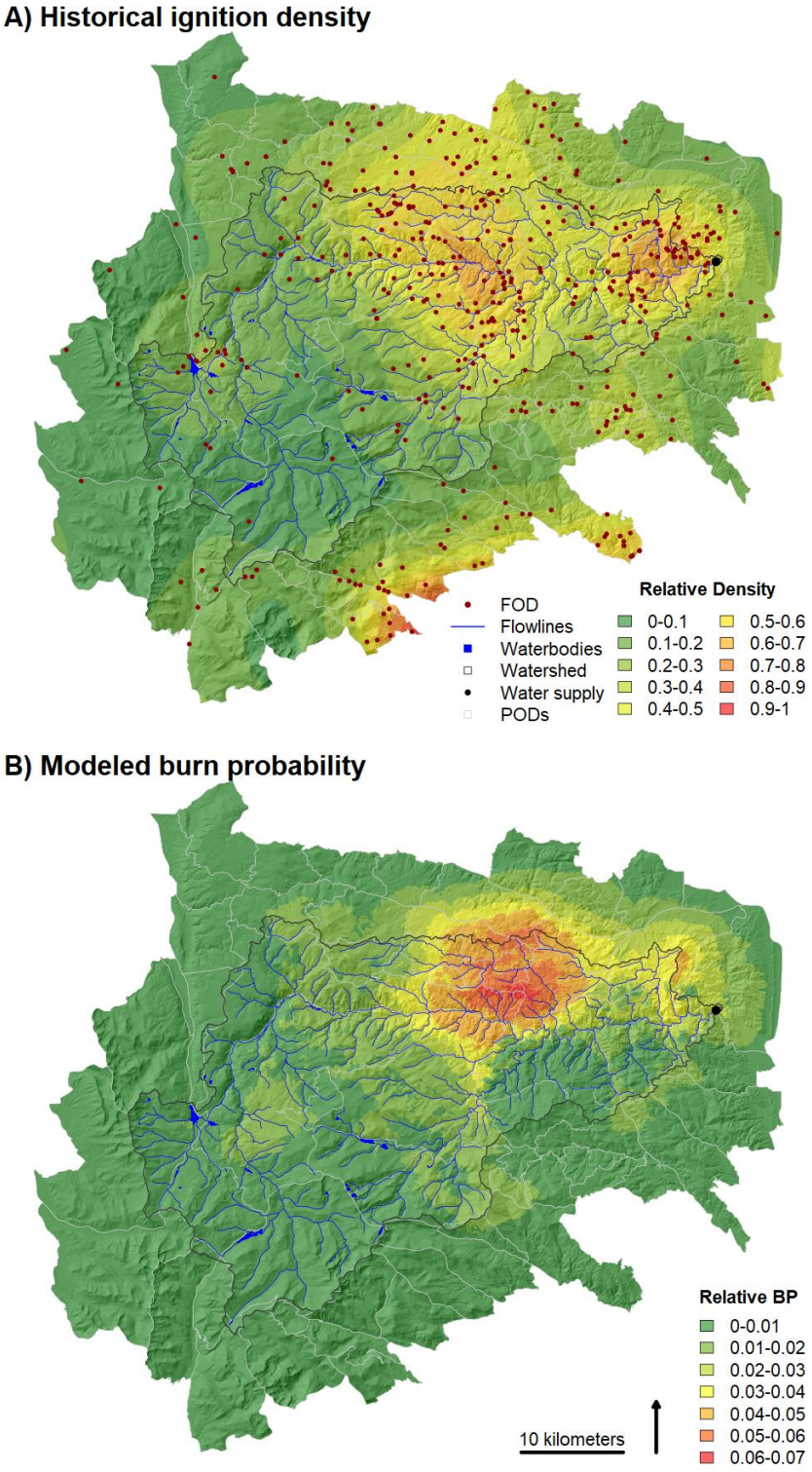

Figure 4.3. Fire simulation results

A) Fire Occurrence Database (FOD) records of historical ignitions and interpolated surface of relative ignition density used in the RANDIG simulations. B) Burn probability from the simulated fires that intercept the study watershed.

4.3.2 Fire behavior and severity

Crown fire activity is predicted to vary across the watershed due to differences in fuels and topography (Figure 4.4a). A notable portion of the alpine and some recently burned areas are mapped as a non-burnable cover type (13.7%). Surface, passive crown, and active crown fire are predicted on 25.9%, 39.3%, and 21.1% of the watershed area, which we use as proxies for low, moderate, and high burn severity. This translates to predictions of low severity effects in grass and shrub fuel types and moderate or high severity effects in most forests. High severity effects are most common in forests with high horizontal and vertical continuity on steep slopes. Our prediction that approximately 60% of the watershed should burn at moderate or high severity is in line with the observed severity of recent large wildfires in Colorado (Sherriff et al. 2014).

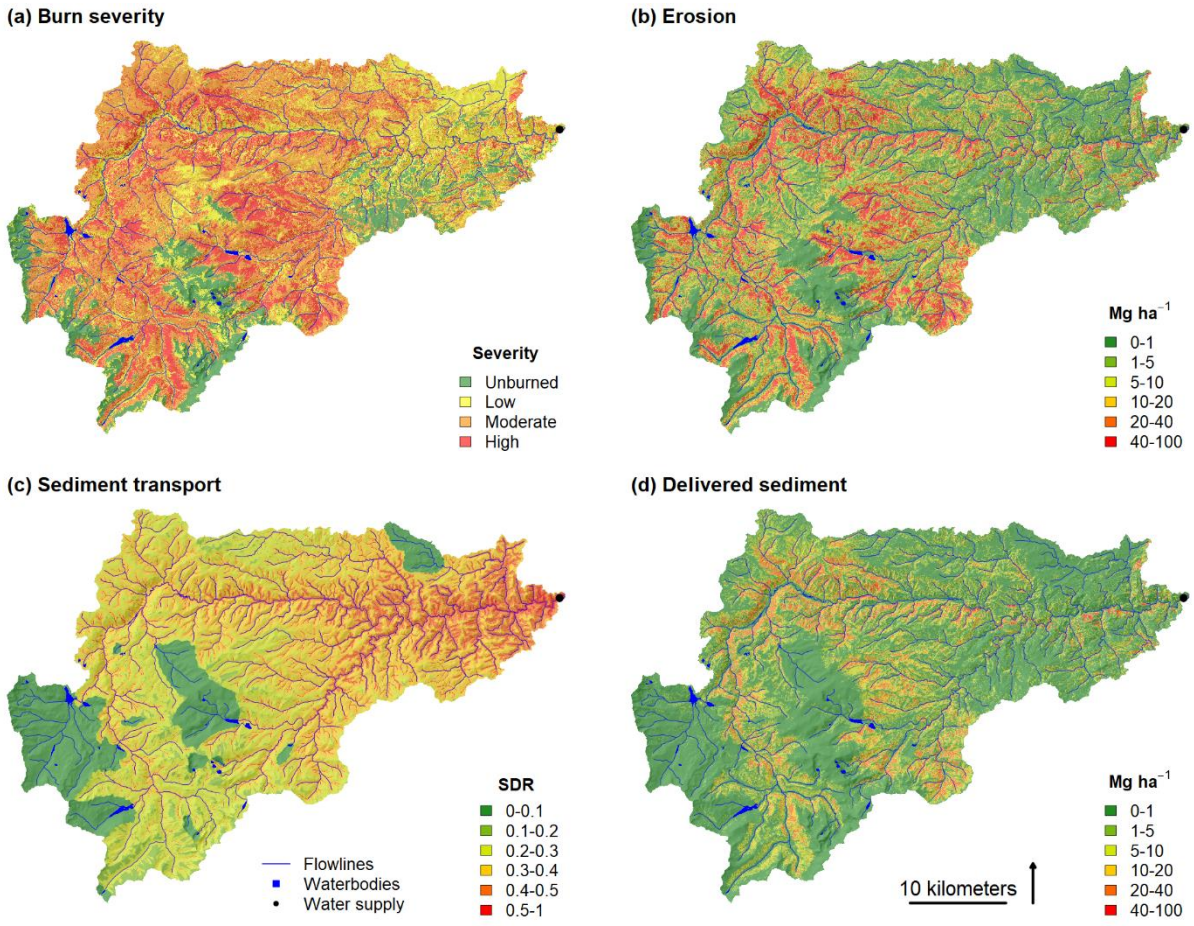

Figure 4.4. Conditional burn severity and watershed effects

A) Predicted burn severity using crown fire activity categories of surface, passive crown, and active crown fire as proxies for low, moderate, and high severity fire. B) Predicted post-fire erosion under the 2-year recurrence interval rainfall erosivity. C) Combined Sediment Delivery Ratio (SDR) accounting for both hillslope and channel transport. D) Predicted sediment delivery to the water supply diversion under the 2-year recurrence interval rainfall erosivity.

4.3.3 Watershed response

Like burn severity, the magnitudes of post-fire erosion and sediment transport vary widely across the watershed owing to variation in topography, soils, and proximity to the diversion. Figure 4.4 illustrates this for the 2-year recurrence interval rainfall erosivity. The greatest sediment hazard is associated with steep terrain near the major channels that is predicted to burn at moderate or high severity. Post-fire erosion and sediment transport potential is generally low in the flatter terrain in the northeast quadrant of the watershed, the high mountains

above major waterbodies, and the recently burned areas. Table 4.2 summarizes the distribution of predicted erosion, sediment delivery to streams, and sediment delivery to the diversion for the 3040 simulated wildfires that burned in the watershed. The predicted mean post-fire gross erosion for the simulated wildfires is 12.3, 20.4, and 46.4 Mg ha^{-1} for the 2, 10, and 100-yr rainfall erosivity, respectively. Much of this sediment should be retained in the watershed, especially where waterbodies interrupt sediment transport (Figure 4c), so delivery to the diversion averages only 4.2, 7.0, and 15.9 Mg ha^{-1} for the 2, 10, and 100-yr rainfall erosivity, respectively.

Table 4.2. Sediment yield across prediction scales

Summary statistics of first-year post fire erosion, sediment delivery to streams, and sediment delivery to the water supply diversion (div.) in Mg ha^{-1} by rainfall erosivity for the simulated wildfires that burned into the watershed. These are total sediment yields including the coarse and fine fractions.

	2-year rainfall erosivity			10-year rainfall erosivity			100-year rainfall erosivity		
Statistic	**Erosion**	**To streams**	**To div.**	**Erosion**	**To streams**	**To div.**	**Erosion**	**To streams**	**To div.**
Lower decile	2.0	1.0	0.4	4.3	2.1	0.9	18.5	9.1	4.3
Lower quartile	5.0	2.6	1.6	9.8	5.0	3.2	32.3	16.5	11.0
Median	9.0	4.7	3.3	16.5	8.6	6.2	45.2	23.4	16.8
Mean	12.3	6.2	4.2	20.4	10.3	7.0	46.4	23.4	15.9
Upper quartile	16.8	8.6	6.0	28.1	14.3	9.9	60.8	30.7	21.5
Upper decile	27.7	13.7	8.7	42.9	20.9	13.6	75.3	36.8	24.7

4.3.4 Avoided watershed area burned

For improved containment at POD boundaries to avoid water supply impacts, the target fires must leave the POD of origin under unmanaged conditions. Of the 3040 simulated wildfires that burned at least part of the focal watershed, 2351 of them (77.3%) burned at least some area outside the origin POD. The remaining 689 fires (22.7%) that did not burn beyond the origin POD have no mitigation benefit in this study. Fires occasionally burned more than ten PODs (Figure 4.5), but of the fires that burned more than one POD, most burned between two and five

PODs (77.9%). This suggests that most fire transmission potential during the initial burn period is between a POD and its adjacent neighbors, but some rare events may burn across multiple POD boundaries.

Containing all fires within their POD of origin would reduce the average watershed area burned from 1361 to 562 ha per fire, a 58.7% reduction (Table 4.3). Containing large fires has the greatest potential to avoid area burned in the watershed; the 1396 fires with more than 1000 ha watershed area burned account for 93.8% of the avoided watershed area burned. The distributions of watershed area burned by fires for the contained and uncontained scenarios are shown in Figure 6a. Containment in the POD of origin would eliminate fires that burn more than 10000 ha in the watershed, which numbered 26 (0.9%) in the uncontained scenario. The percentage of fires burning greater than 5000 ha would be reduced from 4.0 to 0.2.

Impacts from fires that start in PODs that are wholly or mostly outside the watershed should be reduced to negligible levels under the containment scenario, but these PODs account for only a small fraction of watershed area burned when fires are allowed to grow freely (Figure 4.7a). Most fires start in the central and eastern portion of the watershed (Figure 4.3) and the predominant west winds means that PODs in the lower 2/3rds of the watershed are the source of fires that burn the greatest area (Figure 4.7a). All else equal, larger PODs are also a greater source of fire because they have more ignitions. Containment reduced watershed area burned from fires that ignited in 61 of the 70 PODs, but some of the largest PODs still have substantial watershed area burned with containment (Figure 4.7a) because fires have room to grow large before encountering a potential control feature.

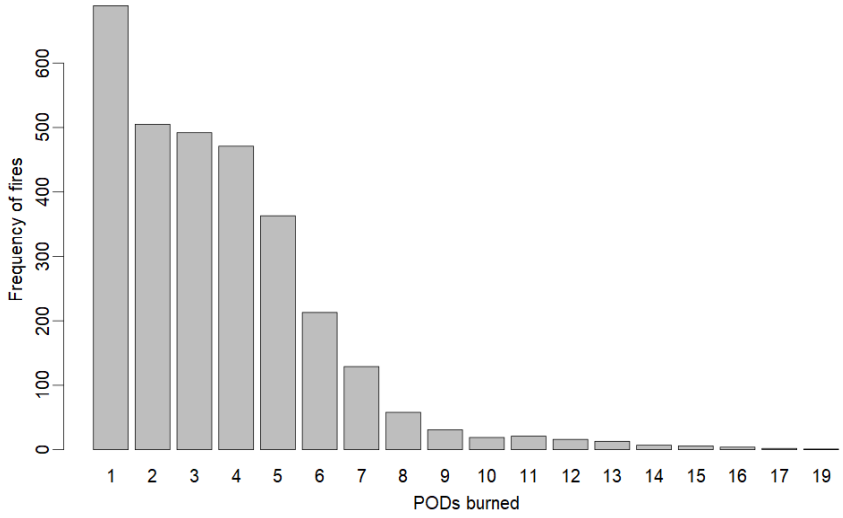

Figure 4.5. PODs encountered by simulated fires

Frequency distribution of PODs encountered by the simulation fires. Any PODs with area greater than 0 ha burned was considered encountered.

Table 4.3. Water supply impacts

Summary of water supply impacts across all fires by containment scenario and rainfall erosivity. A turbidity threshold of 100 NTU was used to compute the number of exceedances.

Watershed area burned (mean ha per fire)				
	Self-burning	**Total**	**Avoided**	**Avoided (%)**
	562	1361	799	58.7
Sediment to diversion (mean Mg per fire)				
Rainfall erosivity	**Self-burning**	**Total**	**Avoided**	**Avoided (%)**
2-yr	3031	6115	3085	50.4
10-yr	4904	10188	5284	51.9
100-yr	10411	23273	12863	55.3
Turbidity exceedances (count of fires)				
Rainfall erosivity	**Self-burning**	**Total**	**Avoided**	**Avoided (%)**
2-yr	1110	1668	558	33.5
10-yr	1503	1910	407	21.3
100-yr	1922	2210	288	13.0

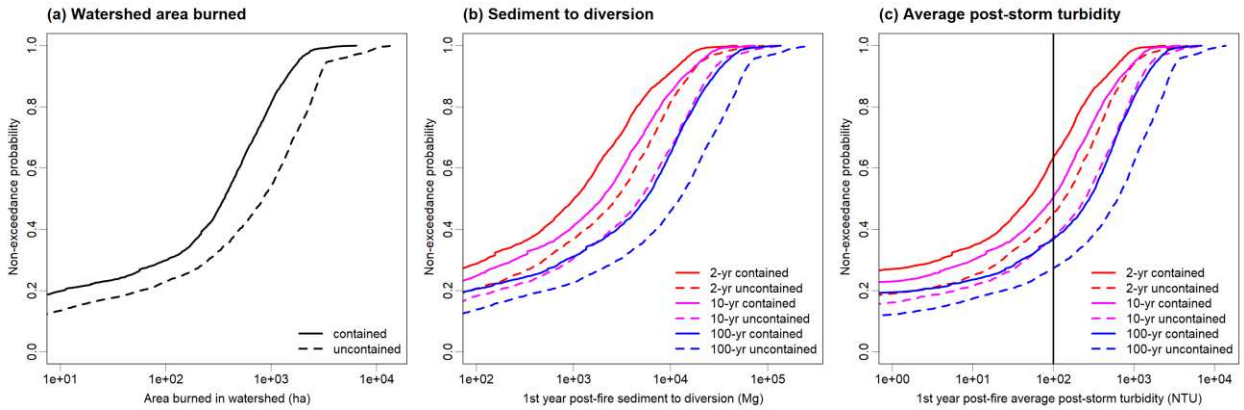

Figure 4.6. Containment effects on impact metric distributions

Summary of containment effects on distribution of fire-level indicators of water supply risk including: A) watershed area burned, B) first-year post-fire sediment to the diversion, and C) first-year post-fire average post-storm turbidity (vertical line marks the 100 NTU standard for treatment).

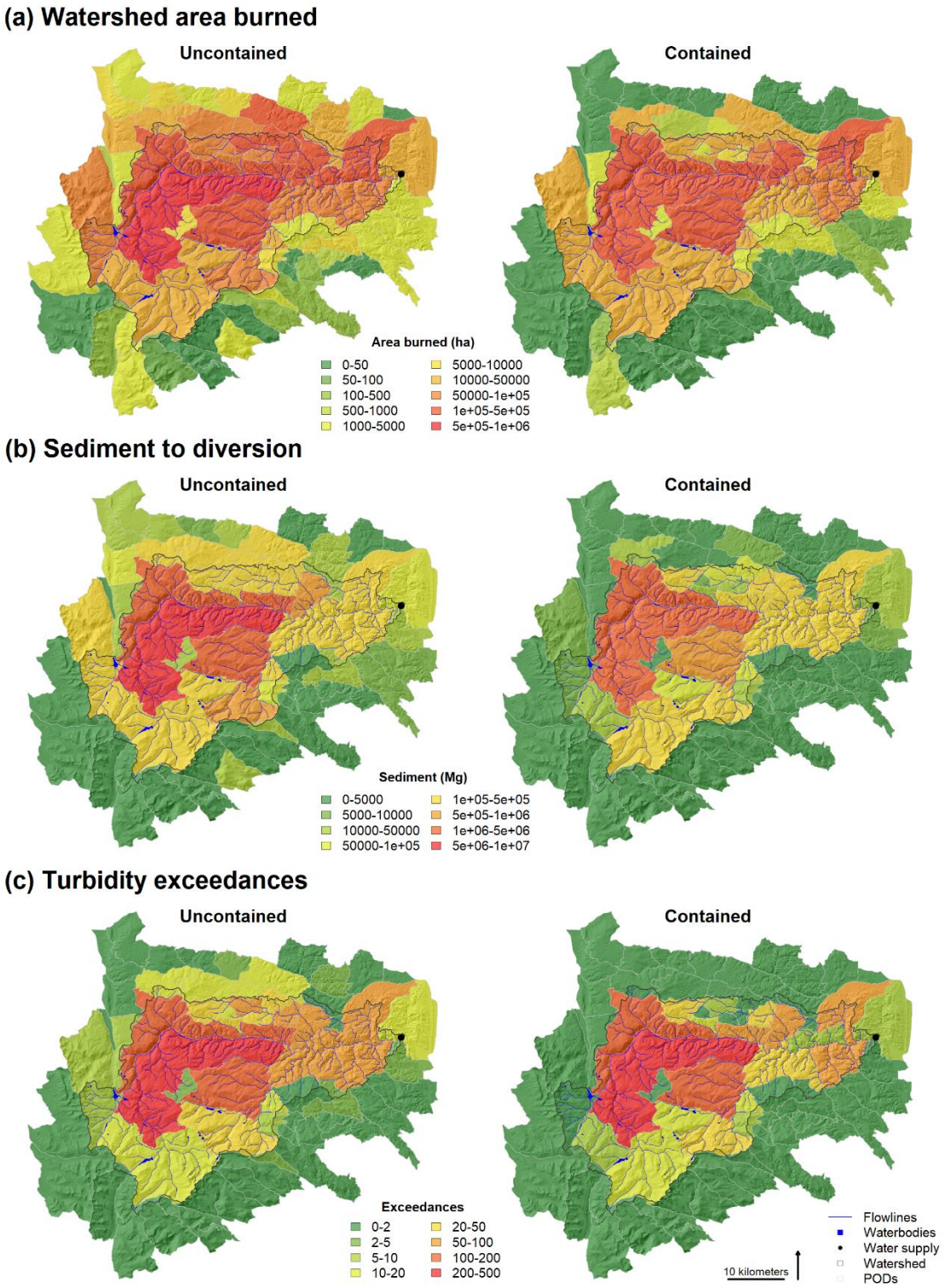

Figure 4.7. Source risk by impact metric

Summary of containment effects on distribution of POD-level indicators of water supply risk including: A) watershed area burned, B) first-year post-fire sediment to the diversion, and C) frequency of turbidity exceedances for fires that originate within each POD. The difference between uncontained and contained scenarios is the transmitted risk.

4.3.5 Avoided sediment

Containment reduced the total sediment load to the pipeline by 50.4-55.3% depending on rainfall erosivity from an average of 6.1-23.2 thousand Mg per fire to an average of 3.1-10.4 thousand Mg per fire (Table 4.3). The fire-level cumulative distributions of sediment delivered to the pipeline for the contained and uncontained scenarios are shown in Figure 4.6b. Sediment loads vary across several orders of magnitude due to differences in fire size, the erosion and sediment transport potential of the burned area, and post-fire rainfall. The effect of containment on sediment load is roughly equivalent to reducing rainfall erosivity one level (Figure 4.6b). The spatial distribution of sediment source risk is similar to that of watershed area burned (Figure 4.7b). PODs that are partially or wholly outside the watershed are a minimal risk to water supplies after containment, but fire activity in the larger PODs situated in the middle of the watershed is still expected to produce substantial sediment.

4.3.6 Avoided water quality impairment

Containment effects on water quality impairment were less substantial than for watershed area burned and total sediment to the diversion (Table 4.3; Figure 4.6c); impairments were reduced by 33.5, 21.3, and 13.0 percent for the 2, 10, and 100-year recurrence interval rainfall erosivity, respectively. With containment, 36.5, 49.4, and 63.2 percent of fires are predicted to exceed the 100 NTU threshold for the 2, 10, and 100-yr rainfall erosivity, respectively. Most fires that caused turbidity to exceed limits for treatment originated in the large PODs in the middle of the watershed (Figure 4.7c). The three PODs with the most turbidity exceedances are all larger than 10000 ha. Containment only reduced the number of turbidity exceedances from these PODs from 640 to 568 (an 11.3% reduction) for the 2-yr rainfall erosivity, and containment offered almost no mitigation benefit (1.0% fewer exceedances) for these PODs under the most

extreme rainfall scenario. In contrast, containment reduced turbidity exceedances by more than 50% in 33 of the 70 PODs under median rainfall conditions. These PODs range in size from 502 to 14153 ha with a mean of 3548 ha. Many of these PODs are mostly or wholly outside the watershed, but some are smaller PODs inside the watershed.

4.3.7 Prioritizing POD network improvements

The impairment analysis results highlight the need to break up the three large PODs with high source risk in the middle portion of the watershed (Figure 4.7c). These three PODs are also the top priorities for further compartmentalization based on watershed area burned and total sediment load from self-burning. With containment, an additional eight PODs were the source of 20 or more impairments under median rainfall conditions. Cumulatively, these top 11 PODs account for 91.4% of all impairments in the contained scenario, so efforts to further reduce fire sizes in these PODs should have high benefit.

Prioritizing improvements along the potential control lines that bound PODs can be informed with measures of risk transmission (Figure 4.8). Total sediment to the diversion was transmitted at the highest rates along POD boundaries in the middle portion of the watershed (Figure 4.8a) where there is high potential for fires to spread into erosion prone terrain near the diversion (Figure 4.3b; Figure 4.4). In contrast, transmitted water impairment was more concentrated along the POD edges associated with the smaller PODs in the north central portion of the watershed (Figure 4.8a). Transmission risk was also high for several control lines in the eastern half of the watershed that are nearly perpendicular to the dominant wind direction. Mitigation priorities differed depending on which metric of transmission risk was used (Figure 4.8; Figure 4.9). The two metrics both identify a similar order of priorities (Spearman's $\rho = 0.89$) but they have moderate disagreement about the magnitudes of potential risk mitigation

(Pearson's $R = 0.71$), especially for the highest-ranking boundaries (Figure 4.9). Most notably, few of the POD edges associated with the three large PODs that are the source of most impairments (Figure 4.7c) are high priorities for mitigating impairment because containment at these locations infrequently changes the impairment outcome despite the potential to avoid large quantities of sediment.

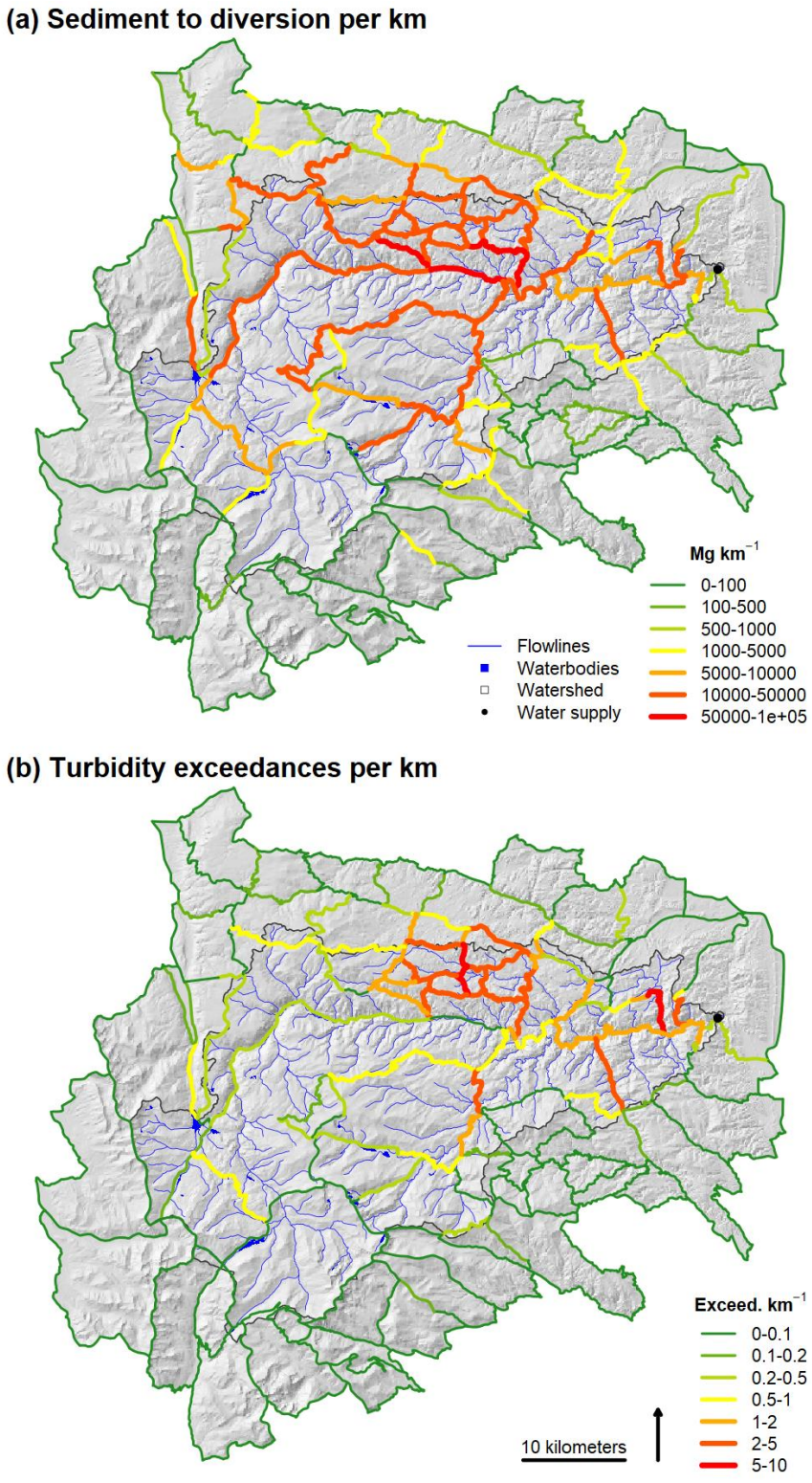

Figure 4.8. Edge risk transmission

Transmitted risk from A) sediment to diversion and B) turbidity exceedances normalized to edge length in kilometers.

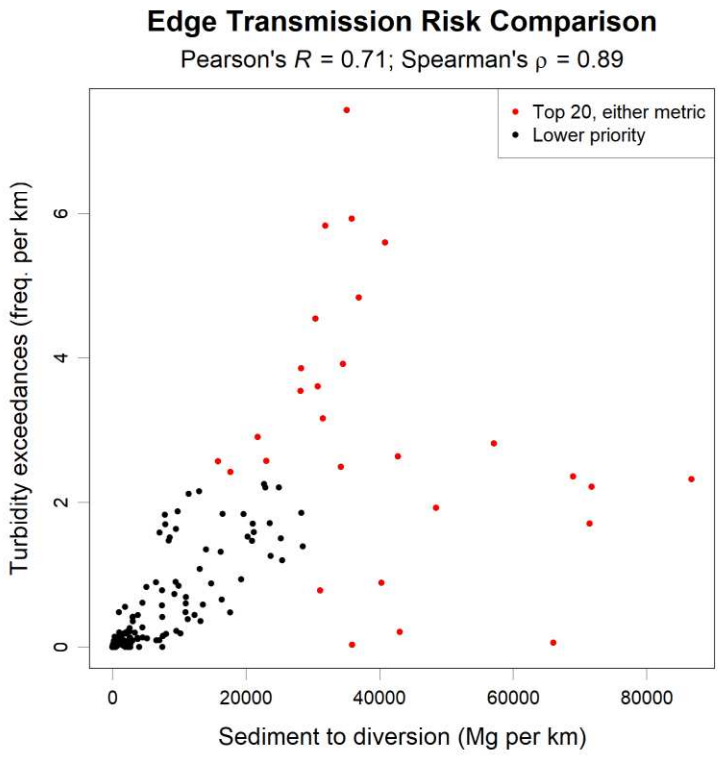

Figure 4.9. Edge risk transmission comparison

Scatterplot of edge transmission metrics (unit is edge). Edges ranked in the top 20 using either metric are colored red.

4.4 DISCUSSION

This proof of concept analysis demonstrates the potential for improved early containment of large fires to lower watershed area burned by 58.7% and to reduce risk to source water between 13.0 and 55.3% depending on impact metric considered. Proportional reductions in total sediment load to the diversion ranged between 50.4 and 55.3%, but the potential to avoid exceeding turbidity limits for treatment was notably lower – varying between 33.5 and 13.0% reduction for the 2- and 100-yr rainfall erosivity, respectively (Table 4.3). The contrasting response of our water impact metrics to increasing rainfall erosivity (Table 4.3) reveals that avoiding large quantities of sediment may not translate to avoiding water impairment if the residual sediment load is still large. The sources of water supply risk and potential mitigation

benefits of fire containment varied widely across the POD network (Figure 4.7) suggesting the potential to further improve mitigation effectiveness with targeted divisions to reduce the size of PODs with high risk from self-burning and fuels reduction to improve containment probability along high transmission boundaries (Figure 4.8).

Our analysis built on previous studies of wildfire-water supply risk and wildfire risk transmission to estimate the avoided water supply impacts from improved fire containment within pre-identified PODs. Omi (1979) approached this issue from the perspective of fuel break construction and maintenance in California using estimates of avoided area burned and a relative damage index to weigh fuel break benefits. Monte Carlo wildfire simulation and watershed effects analyses capture similar information on exposure and impacts with the added benefit of associating fire outcomes with their ignition locations and final extents (Thompson et al. 2016b; Haas et al. 2017). Both of these recent works suggest that improved containment could benefit water supply protection after showing that much of the risk to watershed values is associated with large but infrequent wildfires that would be difficult to mitigate with area-wide fuel treatments due to their rarity in space and time. A recent effort to zone this landscape into PODs (Thompson et al. 2016a) provided the operationally relevant fire containers used in this study to estimate avoided water supply impacts using risk transmission methods (Haas et al. 2015; Ager et al. 2018) like the earlier work of Davis (1965) to estimate the area saved from burning after encountering a control feature. The avoided area burned and sediment load measures we modeled are similar to the impact metrics used to value the benefit of containment in previous studies, but our evaluation of water quality impairment provided a unique opportunity to evaluate whether the sizes and spatial arrangements of the PODs are appropriate to mitigate a scale-dependent risk. Our results suggest POD-based containment could meaningfully reduce risk of

exceeding turbidity limits for treatment (Table 4.3), but the large percentage of unmitigated risk implies that the containment network could be more effective with smaller PODs.

Our estimates of avoided impacts are premised on the simplifying assumption that all fires are contained within their POD of origin and thus are optimistic given the reality that wildfire can breach roads and rivers under extreme weather conditions in this region. We chose not to address the probability of containment in this study because our current understanding of suppressing wildfire at linear control features has not advanced much beyond simple empirical or conceptual models (Wilson 1988; Mees et al. 1993; Agee et al. 2000). It is reasonable to assume that many of the fires we simulated could be contained at the roads that form most POD edges, but probability of success should be lowest under the weather conditions associated with the most damaging fires. Better models of containment probability that incorporate physical characteristics of the control feature, the surrounding fuels and topography, fire behavior, and suppression are critical to refining estimates containment mitigation benefits. We also did not account for suppression burning, which can sometimes substantially increase area burned (Ingalsbee 2015) and thus would dampen the contrast between our containment scenarios.

The post-fire erosion and sediment transport modeling used here has several limitations that are important to acknowledge. First, the linked fire and erosion model system (Figure 4.1) is subject to multiple data, model, and model linkage uncertainties that have potential for prediction error as discussed extensively in previous publications (Elliot et al. 2016; Gannon et al. 2019). Recent work has shown that water quality at the basin scale is sometimes minimally impacted despite modeled increases in hillslope erosion (Blake et al. 2020), emphasizing the need to test and refine erosion and sediment transport models with empirical observations at multiple scales (Moody et al. 2013). Most of our predicted first-year post-fire hillslope erosion yields for the 2-

yr and 10-yr rainfall erosivity scenarios (Table 4.2) are close to the study-wide means of 9.5-22.2 Mg ha^{-1} and range of individual hillslope observations of 0.1-38.2 Mg ha^{-1} from previous fires in the region exposed to moderate rainfall (Wagenbrenner et al. 2006; Larsen et al. 2009; Robichaud et al. 2013a; Schmeer et al. 2018). Many of these studies had hillslope sediment fences fill and overtop, so the reported yields are usually interpreted as a lower bound estimate of the true erosion rate. For the 100-yr rainfall erosivity, only the top decile of modeled fires exceed the 72 Mg ha^{-1} of rill and interrill erosion reported in the first year after the Buffalo Creek Fire in response to similarly extreme rainfall (converted from volume estimates of Moody and Martin [2001] using bulk density of 1.6 Mg m^{-3}). Despite doubling the efficiency of hillslope transport in this study, only the net sediment delivery to streams for the upper decile of fires with 10-yr rainfall erosivity and the upper half of fires with 100-yr rainfall erosivity (Table 4.2) approach the small catchment sediment yields of 22.0-38.6 Mg ha^{-1} observed in the first two years after the Hayman Fire (Robichaud et al. 2008, 2013b). This seems reasonable given the larger size of most catchments in this study. After our rough calibration, our combined hillslope and channel SDR values (Figure 4.4c) are close to SDR values estimated with similar travel time methods (Ferro and Porto 2000; Fernandez et al. 2003). None of the simulated fires at any rainfall level (Table 4.2) are predicted to deliver sediment to the diversion at a rate close to the whole watershed sediment yield of 52.5 Mg ha^{-1} for the first year of the Buffalo Creek Fire (Moody and Martin 2001), likely because we did not account for channel erosion.

Our water quality impairment analysis also layers on additional assumptions that the annual suspended sediment load is evenly divided among the annual average of four sediment-generating storms and the storm sediment load is evenly mixed in the average daily flow volume of the river during the thunderstorm season. Despite these approximations, the resulting

turbidities – which averaged 309, 516, and 1181 NTU for the 2, 10, and 100-yr rainfall erosivity, respectively – align well with common observations in the region of post-fire turbidities between 100 and 1000 NTU and occasional observations >1000 NTU (Rhoades et al. 2011; Oropeza and Heath 2013; Murphy et al. 2015). The assumption that storm load is an equal division of annual load does not account for the substantial intra-annual variability in storm characteristics (Murphy et al. 2015; Kampf et al. 2016) nor the interannual variability in the frequency of storms with sufficient intensity to cause erosion (Wilson et al. 2018; Chapter 3). Similarly, unaccounted for variability in daily flow volume should influence the vulnerability of the water source. Given these simplifications, we have more confidence in our contrasts of containment protection benefits across scenarios than we do in our absolute estimates of impairment risk. Our analysis also focused exclusively on the acute periods of severe water quality degradation after rainstorms in the first year after fire, so it is unclear if containing fires to smaller sizes will avoid elevated carbon, nitrogen, phosphorus, manganese, and suspended solids concentrations that may persist for years after fires in Colorado (Rhoades et al. 2011; Murphy et al. 2015), increasing treatment complexity and cost and raising concerns about the formation of disinfection byproducts (Writer et al. 2014; Hohner et al. 2016). Similar water quality responses and treatment challenges have been observed after wildfires in Canada, Australia, and Europe (Emelko et al. 2011; Smith et al. 2011).

Despite uncertainties in the precise magnitude of risk reduction, improved containment appears promising compared to other mitigation strategies. We found that limiting fires to their POD of origin should reduce the total sediment load from wildfire between 50.4 and 55.3% (Table 4.3). Previous assessments of landscape-scale fuel treatments predict long-term sediment reduction of 19% (Elliot et al. 2016) and up to 34% reduction in long-term sediment costs

(Chapter 2). Based on the narrowest contrast in these figures (34% for fuels reduction and 50.4% for containment), the containment failure rate would have to be greater than 32% for fuels reduction to match the mitigation effectiveness of POD-based containment. Furthermore, compartmentalizing fire in small units of the landscape has the potential to avoid disrupting multi-source water systems by limiting fire impacts to a single source (Chapter 3). The benefit of containing individual wildfires should vary widely (Figure 4.6), as fire encounters with control features and associated impacts beyond the POD of origin depend strongly on where the fire ignites, which is similar to what Buckley et al. (2014) report for fuels reduction effects on fire-level sediment yields. The effect of fuels reduction on post-fire water quality has not been directly evaluated by other studies, but the sediment yields predicted for individual fires in Buckley et al. (2014) and Jones et al. (2017) suggest that fuels reduction may not meaningfully change the water quality outcomes of the largest fires, especially when they combine with extreme post-fire rainfall, despite substantial reductions in sediment loads.

We also demonstrated how risk transmission metrics could inform improvements to the POD network. The small number of PODs with high risk from self-burning should be targeted for further compartmentalization. Fine scale analyses of risk factors within the PODs and containment opportunities would benefit these efforts. If further divisions are not feasible or practical (e.g., because of wilderness or wildlife habitat concerns), these PODs could be candidates for fuels reduction with prescribed fires or managed wildfires for resource benefit. However, the limited control opportunities in these PODs suggests that managed fires may also need to be large, which raises concerns about whether they would impair water quality. The analysis presented here for extreme wildfires could be adapted to evaluate the risk of impairment from fires under more favorable weather conditions. As previously discussed, we did not

estimate the probability of containing wildfire at POD boundaries and how containment probability would change with fuels reduction, but managers are interested in identifying POD boundaries in need of improvements to support safe and effective fire response. Measures of transmission risk across the POD edges (Figure 4.8) highlight where these efforts should be targeted to maximize risk reduction. However, priorities differed depending on the water supply effects measure used (Figure 4.9); most notably, there is greater potential to avoid impairment by improving containment probability around the smaller PODs. Further analyses are needed to evaluate if fuel conditions around these POD edges necessitate treatment for firefighting effectiveness and safety.

4.5 CONCLUSION

Improved wildfire containment has potential to meaningfully reduce wildfire risk to water supplies, but these effects are scale dependent. In our test case, approximately 75% of fires intersected potential control features and, if these fires were contained within their POD of origin, watershed area burned would be reduced by 58.7%, total sediment load to the diversion would be reduced between 50.4 and 55.3%, and water quality impairment would be reduced between 13.0 and 33.5%. Risk mitigation was higher for total sediment load than impairments because containment did not always change water quality outcomes. Moreover, priorities to improve the network design by modifying the size of the PODs or improving containment probability along their edges differ depending on the effects measure used. This highlights the importance of properly defining water supply impacts for wildfire risk assessment and avoided impact analyses. Similar analyses could be applied to other scale-dependent resources at risk of wildfire to inform containment network design.

REFERENCES FOR CHAPTER 4

Abraham J, Dowling K, Florentine S (2017) Risk of post-fire metal mobilization into surface water resources: a review. *Science of the Total Environment* **599-600**, 1740-1755. doi:10.1016/j.scitotenv.2017.05.096

Agee JK, Bahro B, Finney MA, Omi PN, Sapsis DB, Skinner CN, van Wagtendonk JW, Weatherspoon CP (2000) The use of shaded fuelbreaks in landscape fire management. *Forest Ecology and Management* **127**, 55-66. doi:10.1016/S0378-1127(99)00116-4

Ager AA, Palaiologou P, Evers CR, Day MA, Barros AMG (2018) Assessing transboundary wildfire exposure in the southwestern United States. *Risk Analysis* **38(10)**, 2105-2127. doi:10.1111/risa.12999

Benavides-Solorio JD, MacDonald LH (2005) Measurement and prediction of post-fire erosion at the hillslope scale, Colorado Front Range. *International Journal of Wildland Fire* **14**, 457–474. doi:10.1071/WF05042

Blake D, Nyman P, Nice H, D'Souza FML, Kavazos CRJ, Horwitz P (2020) Assessment of post-wildfire erosion risk and effects on water quality in south-western Australia. *Fire* **29**, 240-257. doi:10.1071/WF18123

Bradshaw L, McCormick E (2000) FireFamily Plus user's guide, version 2.0. USDA Forest Service, Rocky Mountain Research Station, General Technical Report RMRS-GTR-67WWW. (Ogden, UT, USA)

Buckley M, Beck N, Bowden P, Miller ME, Hill B, Luce C, Elliot WJ, Enstice N, Podolak K, Winford E, Smith SL, Bokach M, Reichert M, Edelson D, Gaither J (2014) Mokelumne watershed avoided cost analysis: why Sierra fuel treatments make economic sense. A report prepared for the Sierra Nevada Conservancy, The Nature Conservancy, and USDA Forest Service. Sierra Nevada Conservancy. (Auburn, CA, USA)

Caggiano MD (2019) Collaboratively Engaging Stakeholders to Develop Potential Operational Delineations. Colorado Forest Restoration Institute Report CFRI-1908. (Fort Collins, CO, USA)

Caggiano MD, O'Connor CD, Sack RB (2020) Potential Operational Delineations and Northern New Mexico's 2019 Fire Season. Colorado Forest Restoration Institute Report CFRI-2002. (Fort Collins, CO, USA)

Cannon SH, Gartner JE, Rupert MG, Michael JA, Rea AH, Parrett C (2010) Predicting the probability and volume of post-wildfire debris flows in the intermountain western United States. *Geological Society of America Bulletin* **122**, 127-144. doi:10.1130/B26459.1

Crosby JS, Chandler CC (1966) Get the most from your windspeed observation. *Fire Control Notes* **27**, 12-13.

Davis LS (1965) The economics of wildfire protection with emphasis on fuel break systems. California Division of Forestry. 166 p. (Sacramento, CA, USA)

DeBano LF, Neary DG, Ffolliott PF (2005) Soil physical processes. In 'Wildland fire in ecosystems: effects of fire on soils and water'. (Eds DG Neary, KC Ryan, LF DeBano) USDA Forest Service, Rocky Mountain Research Station, General Technical Report RMRS-GTR-42-Vol. 4. (Eds DG Neary, KC Ryan, LF DeBano) p. 29-51. (Ogden, UT, USA)

Dunn CJ, O'Connor CD, Abrams J, Thompson MP, Calkin DE, Johnston JD, Stratton R, Gilbertson-Day J (2020) Wildfire risk science facilitates adaptation of fire-prone social-

ecological systems to the new fire reality. *Environmental Research Letters* **15(2)**, 025001. doi:10.1088/1748-9326/ab6498
Elliot WJ, Miller ME, Enstice N (2016) Targeting forest management through fire and erosion modelling. *International Journal of Wildland Fire* **25**, 876-887. doi:10.1071/WF15007
Emelko MB, Silins U, Bladon KD, Stone M (2011) Implications of land disturbance on drinking water treatability in a changing climate: demonstrating the need for "source water supply and protection" strategies. *Water Research* **45**, 461-472. doi:10.1016/j.watres.2010.08.051
ESRI (2015) ArcGIS (version 10.3) [Software]. Available from https://www.esri.com/en-us/home (Redlands, CA, USA)
Ferro V, Porto P (2000) Sediment Delivery Distributed (SEDD) Model. *Journal of Hydrologic Engineering* **5**, 411-422.
Fernandez C, Wu JQ, McCool DK, Stöckle CO (2003) Estimating water erosion and sediment yield with GIS, RUSLE, and SEDD. *Journal of Soil and Water Conservation* **58**, 128-136.
Finney MA (2005) The challenge of quantitative risk analysis for wildland fire. *Forest Ecology and Management* **211**, 97-108. DOI: 10.1016/j.foreco.2005.02.010
Finney MA (2006) An overview of FlamMap fire modeling capabilities. In 'Fuels Management-How to Measure Success: Conference Proceedings'. 28-30 March 2006; Portland, OR. (Eds. Andrews PL, Butler BW) USDA Forest Service Rocky Mountain Research Station Proceedings RMRS-P-41. p. 213-220 (Fort Collins, CO, USA)
Finney MA, Brittain S, Seli RC, McHugh CW, Gangi L (2015) FlamMap: fire mapping and analysis system (version 5.0) [Software]. Available from http://www.firelab.org/document/flammap-software
Frickel DG, Shown LM, Patton PC (1975) An evaluation of hillslope and channel erosion related to oil-shale development in the Piceance basin, north-western Colorado. Colorado Department of Natural Resources, Colorado Water Resources Circular 30. (Denver, CO, USA)
Gannon BM, Wei Y, MacDonald LH, Kampf SK, Jones KW, Cannon JB, Wolk BH, Cheng AS, Addington RN, Thompson MP (2019) Prioritising fuels reduction for water supply protection. *International Journal of Wildland Fire* **28**, 785-803. doi:10.1071/WF18182
Graham RT (2003) Hayman Fire case study. USDA Forest Service, Rocky Mountain Research Station, General Technical Report RMRS-GTR-114. (Ogden, UT, USA)
Greiner M, Kooistra C, Schultz C (2020) Pre-season planning for wildland fire response: an assessment of the US Forest Service's Potential Operational Delineations (PODs). Public Lands Policy Group at Colorado State University. Practitioner Paper #05. 20 p. (Fort Collins, CO, USA)
Haas JR, Calkin DE, Thompson MP (2015) Wildfire risk transmission in the Colorado Front Range, USA. *Risk Analysis* **35(2)**, 226-240. doi:10.1111/risa.12270
Haas JR, Thompson M, Tillery A, Scott JH (2017) Capturing spatiotemporal variation in wildfires for improving post-wildfire debris-flow hazard assessments. In 'Natural hazard uncertainty assessment: modeling and decision support, geophysical monograph 223'. (Eds K Riley, P Webley, M Thompson) p. 301-317. (John Wiley & Sons: Hoboken, NJ, USA)
Henkle JE, Wohl E, Beckman N (2011) Locations of channel heads in the semiarid Colorado Front Range, USA. *Geomorphology* **129**, 309-319. doi:10.1016/j.geomorph.2011.02.026
Hohner AK, Cawley K, Oropeza J, Summers RS, Rosario-Ortiz FL (2016) Drinking water treatment response following a Colorado wildfire. *Water Research* **105**, 187-198. doi:10.1016/j.watres.2016.08.034

Ingalsbee T (2015) Ecological fire use for ecological fire management: managing large wildfires by design. In 'Proceedings of the large wildland fires conference'. May 19-23, 2014. Missoula, MT. (Eds. Keane RE, Matt J, Parsons R, Riley K) USDA Forest Service Rocky Mountain Research Station Proceedings RMRS-P-73. P. 120-127 (Fort Collins, CO, USA)

Jones KW, Cannon JB, Saavedra FA, Kampf SK, Addington RN, Cheng AS, MacDonald LH, Wilson C, Wolk B (2017) Return on investment from fuel treatments to reduce severe wildfire and erosion in a watershed investment program in Colorado. *Journal of Environmental Management* **198**, 66-77. doi:10.1016/j.jenvman.2017.05.023

Kampf SK, Brogan DJ, Schmeer S, MacDonald LH, Nelson PA (2016) How do geomorphic effects of rainfall vary with storm type and spatial scale in a post-fire landscape? *Geomorphology* **273**, 39-51. doi:10.1016/j.geomorph.2016.08.001

Kolden CA, Henson C (2020) A socio-ecological approach to mitigating wildfire vulnerability in the wildland urban interface: a case study from the 2017 Thomas Fire. *Fire* **2**, 9. doi:10.3390/fire2010009

LANDFIRE (2016) Fuel, topography, existing vegetation type, and fuel disturbance layers, LANDFIRE 1.4.0., U.S. Geological Survey. Available from http://landfire.cr.usgs.gov/viewer/

Larsen IJ, MacDonald LH (2007) Predicting post-fire sediment yields at the hillslope scale: testing RUSLE and disturbed WEPP. *Water Resources Research* **43**, W11412. doi:10.1029/2006WR005560

Larsen IJ, MacDonald LH, Brown E, Rough D, Welsh MJ, Pietraszek JH, Libohova Z, Benavides-Solorio JD, Schaffrath K (2009) Causes of post-fire runoff and erosion: water repellency, cover, or soil sealing? *Soil Science Society of America Journal* **73**, 1393-1407. doi:10.2136/sssaj2007.0432

Mees R, Strauss D, Chase R (1993) Modeling wildland fire containment with uncertain flame length and fireline width. *International Journal of Wildland Fire* **3(3)**, 179-185. doi:10.1071/WF9930179

Miller ME, MacDonald LH, Robichaud PR, Elliot WJ (2011) Predicting post-fire hillslope erosion in forest lands of the western United States. *International Journal of Wildland Fire* **20**, 982-999. doi:10.1071/WF09142

Miller ME, Elliot WJ, Billmire M, Robichaud PR, Endsley KA (2016) Rapid-response tools and datasets for post-fire remediation: linking remote sensing and process-based hydrological models. *International Journal of Wildland Fire* **25**, 1061-1073. doi:10.1071/WF15162

Moody JA, Martin DA (2001) Initial hydrologic and geomorphic response following a wildfire in the Colorado Front Range. *Earth Surface Processes and Landforms* **26**, 1049-1070. doi:10.1002/esp.253

Moody JA, Martin DA (2009) Synthesis of sediment yields after wildland fire in different rainfall regimes in the western United States. *International Journal of Wildland Fire* **18**, 96-115. doi:10.1071/WF07162

Moody JA, Shakesby RA, Robichaud PR, Cannon SH, Martin DA (2013) Current research issues related to post-wildfire runoff and erosion processes. *Earth-Science Reviews* **122**, 10-37. doi:10.1016/j.earscirev.2013.03.004

Moriarty K, Cheng AS, Hoffman CM, Cottrell SP, Alexander ME (2019) Firefighter observations of "surprising" fire behavior in mountain pine beetle-attacked lodgepole pine forests. *Fire* **2**, 34. doi:10.3390/fire2020034

Murphy SF, Writer JH, McCleskey RB, Martin DA (2015) The role of precipitation type, intensity, and spatial distribution in source water quality after wildfire. *Environmental Research Letters* **10**, 084007. doi:10.1088/1748-9326/10/8/084007

Narayanaraj G, Wimberly MC (2011) Influences of forest roads on the spatial pattern of wildfire boundaries. *International Journal of Wildland Fire* **20**, 792-803. doi:10.1071/WF10032

NRCS Soil Survey Staff (2016) Web soil survey. USDA Natural Resources Conservation Service. Available from https://websoilsurvey.nrcs.usda.gov/

O'Connor CD, Thompson MP, Rodríquez y Silva F (2016) Getting ahead of the wildfire problem: quantifying and mapping management challenges and opportunities. *Geosciences* **6(3)**, 35. doi:10.3390/geosciences6030035

O'Connor CD, Calkin DE, Thompson MP. 2017. An empirical machine learning method for predicting potential fire control locations for pre-fire planning and operational fire management. *International Journal of Wildland Fire* **26**, 587-597. doi:10.1071/WF16135

Omi PN (1979) Planning future fuelbreak strategies using mathematical modeling techniques. *Environmental Management* **3(1)**, 73-80. doi:10.1007/BF01867070

Oropeza J, Heath J (2013) Effects of the 2012 Hewlett and High Park Wildfires on water quality of the Poudre River and Seaman Reservoir. City of Fort Collins Utilities Report. (Fort Collins, CO, USA)

Perica S, Martin D, Pavlovic S, Roy I, St. Laurent M, Trypaluk C, Unruh D, Yekta M, Bonnin G (2013) 'NOAA Atlas 14, Volume 8 Version 2, precipitation-frequency atlas of the United States, Midwestern States.' (Silver Spring, MD, USA).

Price O, Bradstock R (2010) The effect of fuel age on the spread of fire in sclerophyll forest in the Sydney region of Australia. *International Journal of Wildland Fire* **19(1)**, 35-45. doi:10.1071/WF08167

R Core Team (2019). R: A language and environment for statistical computing [Software]. R Foundation for Statistical Computing, Vienna, Austria. Available from https://www.R-project.org/

Renard KG, Foster GR, Weesies GA, McCool DK, Yoder DC (1997) Predicting soil erosion by water: a guide to conservation planning with the Revised Universal Soil Loss Equation (RUSLE). USDA Agricultural Research Service Agricultural Handbook no. 703. (Washington, DC, USA)

Rhoades CC, Entwistle D, Butler D (2011) The influence of wildfire extent and severity on streamwater chemistry, sediment and temperature following the Hayman Fire, Colorado. *International Journal of Wildland Fire* **20**, 430-442. doi:10.1071/WF09086

Robichaud PR, Wagenbrenner JW, Brown RE, Wohlgemuth PM, Beyers JL (2008) Evaluating the effectiveness of contour-felled log erosion barriers as a post-fire runoff and erosion mitigation treatment in the western United States. *International Journal of Wildland Fire* **17**, 255-273. doi:10.1071/WF07032

Robichaud PR, Lewis SA, Wagenbrenner JW, Ashmun LE, Brown RE (2013a) Post-fire mulching for runoff and erosion mitigation. Part I: effectiveness at reducing hillslope erosion rates. *Catena* **105**, 75-92. doi:10.1016/j.catena.2012.11.015

Robichaud PR, Wagenbrenner JW, Lewis SA, Ashmun LE, Brown RE, Wohlgemuth PM (2013b) Post-fire mulching for runoff and erosion mitigation. Part II: effectiveness in reducing runoff and sediment yields from small catchments. *Catena* **105**, 93-111. doi:10.1016/j.catena.2012.11.016

Rodríguez y Silva F, Molina Martínez JR, González-Cabán A (2014) A methodology for determining operational priorities for prevention and suppression of wildland fires. *International Journal of Wildland Fire* **23**, 544-554. doi:10.1071/WF13063

Rodríguez y Silva F, Molina Martínez JR, Thompson MP, O'Connor K (2020) Landscape and wildfires seminary: diagnosis and suppression, methodological advances. University of Cordoba, Forest Engineering Department, Forest Fire Laboratory. 47 p. (Cordoba, Spain)

Ryan SE, Dwire KA, Dixon MK (2011) Impacts of wildfire on runoff and sediment loads at Little Granite Creek, western Wyoming. *Geomorphology* **129**, 113-130. doi:10.1016/j.geomorph.2011.01.017

Schmeer SR (2014) Post-fire erosion response and recovery, High Park Fire, Colorado. Thesis. Colorado State University. (Fort Collins, CO, USA.)

Schmeer SR, Kampf SK, MacDonald LH, Hewitt J, Wilson C (2018) Empirical models of annual post-fire erosion on mulched and unmulched hillslopes. *Catena* **163**, 276-287. doi:10.1016/j.catena.2017.12.029

Scott JH, Burgan RE (2005) Standard fire behavior fuel models: a comprehensive set for use with Rothermel's surface fire spread model. USDA Forest Service, Rocky Mountain Research Station, General Technical Report RMRS-GTR-153. (Fort Collins, CO, USA)

Scott JH, Reinhardt ED (2001) Assessing crown fire potential by linking models of surface and crown fire behavior. USDA Forest Service, Rocky Mountain Research Station, General Technical Research Paper RMRS-RP-29. (Fort Collins, CO, USA)

Scott JH, Thompson MP, Calkin DE (2013) A wildfire risk assessment framework for land and resource management. USDA Forest Service, Rocky Mountain Research Station, General Technical Report RMRS-GTR-315. (Fort Collins, CO, USA)

Shakesby RA, Doerr SH (2006) Wildfire as a hydrological and geomorphological agent. *Earth-Science Reviews* **74**, 269-307. doi:10.1016/j.earscirev.2005.10.006

Sham CH, Tuccillo ME, Rooke J (2013) Effects of wildfire on drinking water utilities and best practices for wildfire risk reduction and mitigation. Water Research Foundation Report 4482. Available from www.waterrf.org

Sherriff RL, Platt RV, Veblen TT, Schoennagel TL, Gartner MH (2014) Historical, observed, and modeled wildfire severity in montane forests of the Colorado Front Range. *PLoS One* **9**, e106971. doi:10.1371/journal.pone.0106971

Short KC (2017) Spatial wildfire occurrence data for the United States, 1992-2015 (4th Edition). USDA Forest Service Research Data Archive. (Fort Collins, CO, USA) doi:10.2737/RDS-2013-0009.4

Sidman G, Guertin DP, Goodrich DC, Thoma D, Falk D, Burns IS (2016) A coupled modelling approach to assess the effect of fuel treatments on post-wildfire runoff and erosion. *International Journal of Wildland Fire* **25**, 351-362. doi:10.1071/WF14058

Smith HG, Sheridan GJ, Lane PNJ, Nyman P, Haydon S (2011) Wildfire effects on water quality in forest catchments: a review with implications for water supply. *Journal of Hydrology* **396**, 170-192. doi:10.1016/j.jhydrol.2010.10.043

Stratton RD (2020) The path to strategic wildland fire management planning. *Wildfire Magazine* **29(1)**, 24-31.

Theobald DM, Merritt DM, Norman JB (2010) Assessment of threats to riparian ecosystems in the western U.S. Report to the Western Environmental Threats Assessment Center, Prineville, OR by the USDA Stream Systems Technology Center and Colorado State University. (Fort Collins, CO, USA)

Thompson MP, Scott J, Langowski PG, Gilbertson-Day JW, Haas JR, Bowne EM (2013b) Assessing watershed -wildfire risks on national forest system lands in the Rocky Mountain region of the United States. *Water* **5**, 945-971. doi:10.3390/w5030945

Thompson MP, Bowden P, Brough A, Scott JH, Gilbertson-Day J, Taylor A, Anderson J, Haas JR (2016a) Application of wildfire risk assessment results to wildfire response planning in the Southern Sierra Nevada, California, USA. *Forests* **7(3)**, 64. doi:10.3390/f7030064

Thompson MP, Gilbertson-Day JW, Scott JH (2016b) Integrating pixel- and polygon-based approaches to wildfire risk assessment: applications to a high-value watershed on the Pike and San Isabel National Forests, Colorado, USA. *Environmental Modeling and Assessment* **21**, 1-15. doi:10.1007/s10666-015-9469-z

Thompson MP, Liu Z, Wei Y, Caggiano MD (2018a) Analyzing wildfire suppression difficulty in relation to protection demand. In 'Environmental Risks'. (Eds. Mihai F-C, Grozavu A) doi:10.5772/intechopen.76937

Thompson MP, MacGregor DG, Dunn CJ, Calkin DE, Phipps J (2018b) Rethinking the wildland fire management system. *Journal of Forestry* **116(4)**, 382-390. doi:10.1093/jofore/fvy020

Tillery AC, Haas JR, Miller LW, Scott JH, Thompson MP (2014) Potential post-wildfire debris-flow hazards - a pre-wildfire evaluation for the Sandia and Manzano Mountains and surrounding areas, central New Mexico. US Geological Survey Scientific Investigations Report 2014–5161. (Albuquerque, NM, USA)

US Environmental Protection Agency (USEPA) and the US Geological Survey (USGS) (2012) National Hydrography Dataset Plus - NHDPlus. Version 2.1. Available from http://www.horizon-systems.com/NHDPlus/index.php

Wagenbrenner JW, MacDonald LH, Rough D (2006) Effectiveness of three post-fire rehabilitation treatments in the Colorado Front Range. *Hydrological Processes* **20**, 2989-3006. doi:10.1002/hyp.6146

Wagenbrenner JW, Robichaud PR (2014) Post-fire bedload sediment delivery across spatial scales in the interior western United States. *Earth Surface Processes and Landforms* **39**, 865-876. doi:10.1002/esp.3488

Wei Y, Thompson MP, Haas JR, Dillon GK, O'Connor CD (2018) Spatial optimization of operationally relevant large fire confine and point protection strategies: model development and test cases. *Canadian Journal of Forest Research* **48**, 480-493. doi:10.1139/cjfr-2017-0271

Wilson AAG (1988) Width of firebreak that is necessary to stop grass fires: some field experiments. *Canadian Journal of Forest Research* **18(6)**, 682-687. doi:10.1139/x88-104

Wilson C, Kampf SK, Wagenbrenner JW, MacDonald LH (2018) Rainfall thresholds for post-fire runoff and sediment delivery from plot to watershed scales. *Forest Ecology and Management* **430**, 346-356. doi:10.1016/j.foreco.2018.08.025

Winchell MF, Jackson SH, Wadley AM, Srinivasan R (2008) Extension and validation of a geographic information system-based method for calculating the Revised Universal Soil Loss Equation length-slope factor for erosion risk assessments in large watersheds. *Journal of Soil and Water Conservation* **63**, 105-111. doi:10.2489/jswc.63.3.105

Writer JH, Hohner A, Oropeza J, Schmidt A, Cawley KM, Rosario-Ortiz FL (2014) Water treatment implications after the High Park Wildfire, Colorado. *Journal of the American Water Works Association* **106(4)**, 189-199. doi:10.5942/jawwa.2014.106.0055

Yocum LL, Jenness J, Fulé PZ, Thode AE (2019) Previous fires and roads limit wildfire growth in Arizona and New Mexico, U.S.A. *Forest Ecology and Management* **449**, 117440. doi:10.1016/j.foreco.2019.06.037

CHAPTER 5 – RISK MODEL LIMITATIONS AND POTENTIAL FOR IMPROVEMENT

The risk models used in Chapters 2, 3, and 4 have data, model, and model linkage uncertainties that have potential for considerable prediction error. The models were roughly calibrated for use in the montane watersheds of the Colorado Front Range based on sometimes sparse local or regional observations. Future modelers are cautioned to carefully consider whether these assumptions are appropriate for other locations. Model limitations were only discussed briefly in each chapter, so they will be expanded on here with attention towards possible improvements.

5.1 FIRE MODELING

5.1.1 Fire likelihood and exposure

All three of the research chapters rely on some form of fire ignition and spread modeling to estimate the likelihood of encountering wildfire. Chapters 2 and 3 both used probabilistic wildfire risk components modeled with FSim (Finney et al. 2011; Short et al. 2016). FSim was calibrated in these applications to approximate historical rates of burning and fire size distributions within fire modeling pyromes, which are regions with roughly similar biophysical controls on fire activity. This modeling did not account for spatial variation in ignition density and it did not carefully calibrate burn probability or fire size distributions across biophysical gradients or vegetation types within pyromes (Short et al. 2016). The FSim results suggest fire is far more likely in the lower elevation, warmer and drier forests than the higher elevation, cooler and wetter forests, except where fuels have been reduced by recent wildfire activity (Figure 2.6a; Figure 3.1). The pattern of higher burn probability in lower elevation forests is generally

consistent with the historical ecology of the region (Schoennagel et al. 2004; Sherriff et al. 2014). The fire ignition and spread modeling in Chapter 4 produced similar patterns in burn probability despite adding spatial variation in ignitions and simplifying to a smaller set of problem weather scenarios (Figure 4.3b). Although there is reasonable alignment between modeled patterns of fire occurrence and historical fire regimes, FSim predicts some questionably low burn probabilities in lodgepole pine forests and the wildland urban interface, which could undervalue risk and risk mitigation in these areas. Future risk analyses at a similar sub-regional scale could benefit from calibrating burn probability and fire size distributions across biophysical gradients and vegetation types.

Chapter 2 and 3 both present absolute estimates of risk that depend on the FSim calibration to historical patterns of fire occurrence. As discussed previously, there is potential for error in the spatial distribution of risk if within pyrome variation in fire occurrence is not calibrated. Fire likelihood estimates are also premised on current fuel conditions, including recent fires, so they may not be accurate as landscape conditions change. A significant concern for long-range planning is the potential mismatch between historical and future rates of burning. Studies that project past fire-climate statistical relationships into the future suggest area burned could be approximately two to three times higher over the next half century in the Southern Rockies (Spracklen et al. 2009; Litschert et al. 2012). If these increases are uniform, the estimated risk and risk reduction from Chapters 2 and 3 could be adjusted with a simple scaling factor to account for climate change. An alternative is to run FSim for future climates, like Riley and Loehman (2016), to capture any spatial variability in fire increases. There is some reason to believe there may be larger increases in burning at higher elevations because fire activity is thought to be currently limited by the cooler, wetter climate (Schoennagel et al. 2004). Changes

in human ignitions could also affect the likelihood and patterns of future wildfire activity. If fire activity dramatically increases, there may also be need to better account for the influence of vegetation dynamics on both area burned and fire severity. A recent analysis suggests that fire-fire feedbacks should dampen increases in area burned in the Sierra Nevada Mountains of California by approximately 15% (Hurteau et al. 2019).

In Chapter 2, fire likelihood was represented using a modeled surface of annual burn probability (Short et al. 2016), which was scaled to the probability of encountering fire in each pixel over a 25-year period of fuel treatment effectiveness to estimate treatment-fire encounter rates. This allowed us to report on the change in expected wildfire damages by pixel as if they are certain quantities, yet the modeling presented in Chapters 3 and 4 suggests that there should be high spatial and temporal variability in wildfire occurrence. Hence, the actual treatment-fire encounter rate may be highly variable across multi-decade planning periods. Variability in treatment-fire encounter rates and avoided damages could be better communicated by reporting these measures for multi-decade subsets of perimeters from FSim. For example, Barros et al. (2018) used a similar technique to describe the potential benefits of managing wildfire for resource benefits by reporting managed fire-wildfire encounter rates and change in impacts over many 50-year simulation periods.

In Chapter 2, no fuel treatment effects on burn probability were modeled. This simplification allowed us to estimate treatment benefits independently for each candidate fuel treatment location at the expense of representing neighborhood effects on fire likelihood. Change in burn probability is often quantified for a limited set of fuel treatment scenarios with Monte Carlo fire ignition and spread models (e.g., Thompson et al. 2013b; Scott et al. 2016), but it is not currently practical to run these analyses for many possible treatment unit combinations

across a large landscape. For now, it is probably best to ignore neighborhood effects for prioritization (e.g., Chapter 2) and to quantify them as needed with post-hoc analysis of several planned scenarios. Accounting for off-site reductions in burn probability would increase the risk mitigation value of fuel treatment compared to our estimates.

5.1.2 Fire behavior and burn severity

In Chapters 2, 3, and 4, crown fire activity (CFA) categories of surface, passive crown, and active crown fire were used as proxies for low, moderate, and high burn severity, respectively. Fire severity often increases along the gradient from surface to active crown fire behavior because crown fire initiation depends on surface fire intensity (Scott and Reinhardt 2001) and total fire intensity increases as more fuel is engaged in combustion. Fire intensity or related flame length measures are also commonly used to translate predicted fire behavior into burn severity for watershed effects analyses (Thompson et al. 2013a; Elliot et al. 2016). However, there is limited understanding of what fire behavior metrics best predict soil burn severity (Moody et al. 2013). Soils do not transmit heat efficiently, so intense but short duration surface or crown fire behavior may not always correspond to high soil heating or complete combustion of surface cover (DeBano and Neary 2005). Despite these uncertainties, our predictions of burn severity (Table 2.3; Figure 3.4; Figure 4.4) generally align with our expectations of high severity effects in areas with heavy forest fuels and steep slopes and primarily low severity effects in low density forest and non-forest fuel types. The proportion of area predicted to burn at moderate or high severity is also close to the proportion of area burned at these severity levels by previous large fires in the Colorado Front Range (Sherriff et al. 2014).

CFA will often detect improvements in fire behavior and effects associated with fuel treatments to increase canopy base height and reduce surface fuels (Agee and Skinner 2005;

Reinhardt et al. 2008), but its broad categories and abrupt transitions between classes limit its precision for quantifying fuel treatment effects. Changes to the fire behavior fuel model or canopy attributes will have different effects depending on how close the starting conditions are to a threshold in fire behavior. Assuming that surface fire equates to low burn severity likely underestimates the variability in fire intensity, soil heating, fuel consumption, and burn severity within this category. It also precludes prediction of moderate or high severity effects in non-forest fuels. Our modeled fuel treatments in Chapter 2 were more successful at changing active crown fire to passive crown fire than they were at changing passive crown fire to surface fire because of the low starting canopy base heights and the relatively small proportional effect of treatment (Table 2.1). Canopy base height measurements should be prioritized in field monitoring to validate the baseline data and magnitude of treatment effects. Using CFA as the sole metric to judge fuel treatment effects may sometimes produce questionable results. For example, treatments that drastically raise canopy base height but add surface fuels may successfully avoid crown fire behavior at the expense of increasing the surface fire intensity and severity. It is tempting to instead use a continuous measure, like fire intensity or flame length, to evaluate treatment effects, but this approach will have similar limitations due to the reliance on categorical fire behavior fuel models (Anderson 1982; Scott and Burgan 2005) to represent pre- and post-treatment surface fuels.

Fire behavior and severity were predicted assuming that all areas of the landscape will burn under conditions with very dry fuels and winds blowing upslope at high speeds. The basic fire behavior module in FlamMap further assumes fire spread in the heading direction through each pixel (Finney et al. 2015). This near worst-case scenario is meant to approximate that most area burns in the Colorado Front Range during very dry and windy conditions (Graham 2003;

Haas et al. 2015). However, this scenario does not apply to all fires or burn periods within fires. Fire intensity distributions generated with FSim, which accounts for fire occurrence under a wider range of environmental conditions and tracks spread direction to account for lower intensities from backing and flanking, tend to be far lower than the worst case modeled with FlamMap (Thompson et al. 2016). Accounting for this variability would therefore lower the average fire behavior and associated severity and post-fire erosion. However, whether this is viewed as an improvement depends on whether the aim of the analysis is to characterize the mean effects of all fire or the potential effects of extreme events. From the perspective of quantifying fuel treatment effectiveness in Chapter 2, modeling fire behavior and effects for extreme fire weather conditions presents a conservative estimate of fuel treatment benefits as they are generally most effective under moderate conditions (Kalies and Yocom Kent 2016).

5.2 WATERSHED MODELING

Due to the forward-looking nature of wildfire risk assessment and the many uncertainties in both future fire and post-fire conditions, simple methods were used to model post-fire erosion and sediment transport. The goal for the watershed modeling was to estimate the magnitude of post-fire sediment delivery to water infrastructure in a spatially distributed manner to account for post-fire impacts independently for each unit of the landscape in Chapter 2. This necessarily involved approximations of the physical processes. The following sections discuss the limitations of the three components of the model – hillslope erosion, hillslope transport, and channel transport – and our application of the system in Chapters 3 and 4 to predict water quality impairment.

5.2.1 Hillslope Erosion

Hillslope erosion was modeled with a gridded spatial implementation of the Revised Universal Soil Loss Equation (RUSLE) (Renard et al. 1997; Theobald et al. 2010). RUSLE was developed for agricultural use, so there are questions about how well it can predict post-fire erosion in wildland environments and steep terrain. It is also a gross erosion model meant for prediction in environments where erosion (versus deposition) is the primary process. These limitations warranted several adjustments to calibrate RUSLE for post-fire erosion prediction in montane watersheds of Colorado.

The first modifications focused on the length and slope (LS) factor. Flow accumulation was limited to 0.9 ha when calculating the length and slope factor (LS) per Winchell et al. (2008) to approximate the hillslope length guidance from the original model (Renard et al. 1997). Without this adjustment, RUSLE would predict very high erosion rates where flow concentrates in drainages, which is far from the original intent of the model despite the general agreement of this trend with field observations (Desmet and Govers 1996; Moody and Martin 2001). The final LS value was also limited to the maximum of 72.15 provided in Renard et al. (1997) to control for excessive slope factor values. Similar methods of estimating LS based on stream power (Moore and Burch 1986) can produce lower values depending on how the analyst decides to set the length and slope exponent parameters (e.g., Blake et al. 2020). The LS factor tends to be very high for much of the study area due to the steep terrain. This is because slope contributes to the LS calculation twice: first in the slope factor (Equation 2.9) and second in the length factor exponent (Equations 2.10-2.12). The length factor exponent increases with slope steepness due the prediction that rill erosion becomes increasingly dominant (compared to interrill erosion) with increasing slope (McCool et al. 1989).

There is currently no empirical evaluation of the RUSLE LS factor for erosion prediction in montane watersheds of Colorado, but there are several studies that report on hillslope erosion mechanisms and topographic drivers. Moody and Martin (2001) estimated that interrill erosion was more than two times higher than rill erosion after the Buffalo Creek Fire. An important caveat to this finding is that there is some ambiguity in what constitutes rill, gully, and channel erosion and much of the channel erosion reported by Moody and Martin (2001) came from previously unchannelized low-order drainages that may overlap with some definitions of rilling. In contrast, Pietraszek (2006) found that 63-76% of the total sediment yield from small swales after the Hayman and Schoonover Fires came from rill erosion. Regardless of the precise mechanisms of erosion, it is reasonable to question whether erosion should increase dramatically with slope, as implied by RUSLE, given that slope has not been identified as an important predictor of hillslope erosion in two empirical studies from Colorado (Benavides-Solorio and MacDonald 2005; Schmeer et al. 2018). In contrast to RUSLE, Schmeer et al. (2018) found a negative relationship between hillslope length and sediment yield for plots ranging in length between 48 to 266 m. Hayman Fire results from Pietraszek (2006) instead show constant per unit area sediment yields across plot sizes ranging between 0.02 and 0.5 ha. Validating the LS factor for use in steep, complex terrain will likely continue to be a challenge given the difficulty of controlling for variability in other factors. Future field studies could improve understanding of length and slope influences on erosion by stratifying their sampling across a gradient in LS while keeping burn severity and soil properties as constant as possible.

The cover (C) and soil erodibility (K) factors were both manipulated in our model to simulate post-fire increases in erosion by burn severity and vegetation type (Table 2.2). Fire effects on forests were mainly informed by Larsen and MacDonald (2007), who reported on both

the mean post-fire C factor by burn severity and the approximate proportional increase in K factor for high burn severity. We adopted the same approach used by Schmeer (2014) to generalize the Larsen and MacDonald (2007) result into K factor increases of 50, 75, and 100 percent for low, moderate, and high burn severity, respectively. The C factor changes in non-forest vegetation types were estimated using proportional adjustment factors given the limited information of how fire effects these vegetation types locally. Table 2.2 shows increases for these cover types for moderate and high severity burning, but they were generally not candidates to burn at these levels due to the lack of tree canopy to support passive or active crown fire activity. It is likely that the predictive performance of the model could be improved by representing fire effects on a continuous gradient instead of three levels of burn severity like the measures of percent surface cover or its inverse that are used in empirical models (Benavides-Solorio and MacDonald 2005; Larsen et al. 2009; Schmeer et al. 2018). However, moving towards continuous measures of severity raises the need for equivalent improvements to the fire behavior and severity modeling and field research to characterize C and K factor responses at higher resolution.

Numerous studies document that rainfall is an important and highly variable control on post-fire erosion in Colorado (Wagenbrenner et al. 2006; Larsen et al. 2009; Moody and Martin 2009; Moody et al. 2013; Robichaud et al. 2013a, 2013b; Murphy et al. 2015; Kampf et al. 2016; Schmeer et al. 2018; Wilson et al. 2018). Different techniques were used to account for rainfall variability in each of the research chapters. The spatial risk assessment and fuel treatment planning in Chapter 2 was based on a median rainfall scenario. Uncertainty in avoided risk was communicated for a range of annual rainfall erosivity percentiles as a simple method to convey that the realized treatment effects could vary widely. The Monte Carlo analysis in Chapter 3

improved upon this by representing rainfall erosivity as a time varying factor that was combined with space and time varying wildfire occurrence to estimate their joint impacts on risk. Water supply impacts in Chapter 4 were reported for three percentiles of annual rainfall erosivity – ranging from common to extreme – to convey the approximate probabilities of experiencing the modeled impacts.

All three research chapters relied on a historical rainfall data set (Perica et al. 2013) that was processed into rainfall erosivity for a later study of rainfall thresholds for erosion (Wilson et al. 2018). Historical records from 11 representative stations of the Colorado Front Range were combined as a means to represent the spatial and temporal variability in annual rainfall erosivity across the region (Figure 2.4). In practice, no spatial variability in rainfall erosivity was modeled within years. This approximation likely dampens the variability in risk estimates compared to the reality that rainfall meaningfully varies within years due to the highly localized nature of intense rainfall events in this region (Wagenbrenner et al. 2006; Moody and Martin 2009; Moody et al. 2013; Murphy et al. 2015; Kampf et al. 2016). Rainfall erosivity is calculated as the product of total storm energy and maximum 30-minute intensity (MJ mm ha^{-1} hr^{-1}). The rainfall data used for this analysis had 15-minute resolution, but some studies suggest that peak intensities measured over shorter durations (e.g., 10 minutes) are better predictors of erosion (Robichaud et al. 2013a, 2013b). Despite the potential to improve erosion prediction with higher resolution rainfall data, local studies have demonstrated that rainfall erosivity calculated with the maximum 30-minute intensity is a strong predictor of post-fire hillslope erosion (Benavides-Solorio and MacDonald 2005; Schmeer et al. 2018). Therefore, this component of the model is likely sufficient but could be marginally improved by incorporating intra-annual spatial variability.

In general, the gridded spatial implementation of RUSLE predicts hillslope erosion rates that are similar to field observations when averaged across small watersheds (Figure 2.5), which is similar to the evaluation made by Larsen and MacDonald (2007). Pixel-level estimates do have the potential to exceed plausible erosion rates when extreme values of LS, C, and K overlap (Chapter 2). Unrealistic erosion rates were controlled for in Chapters 3 and 4 by limiting erosion to the approximate regional maximum of 100 Mg ha^{-1} yr^{-1} (Moody and Martin 2009). Functionally, this could represent sediment supply limitations on steep slopes. The resulting fire-wide mean erosion predictions align reasonably well with regional field observations (Table 3.3 and Table 4.2). Without adjustments to constrain our erosion values, RUSLE predictions can far exceed those made with alternative models like WEPP or KINEROS2 (Kampf et al. 2020). However, it should be noted that our net sediment delivery to streams predictions are closer to what these models predict. Using a more physically-based erosion model like WEPP or KINEROS2 will avoid extreme erosion predictions, but there is little evidence that these models are more accurate than RUSLE, especially if the goal is only to identify relative levels of erosion hazard across a watershed (Larsen and MacDonald 2007; Kampf et al. 2020). Meaningful improvements in post-fire erosion modeling are largely dependent on increased data collection to calibrate and evaluate models including field experiments or stratification of observational studies to better isolate topography, cover, and soil controls.

5.2.2 Hillslope Transport

Hillslope transport was represented using an empirical model of annual Sediment Delivery Ratio (SDR) developed from wildfires in the western U.S. (Wagenbrenner and Robichaud 2014) with a rough calibration to align predicted catchment net sediment yields with regional field observations. The model uses the length ratio of the nested sub-unit to the larger

catchment to represent how per-unit area sediment yields decline between the two scales of measurement (Eqns 2.14-15). This model was applied in a spatially distributed manner by treating each pixel as a smaller sub-unit and its flow path distance to the nearest stream as the length of the larger catchment. This represents the general tendency for the transport efficiency of upland sediment sources to decrease within increasing distance from streams (Walling 1983), but the model ignores other important factors that influence sediment transport like runoff depth, slope steepness, and surface roughness.

The empirical SDR model has several limitations for estimating net sediment yield in Colorado. First, there is considerable variability in annual SDR not explained by the model (Wagenbrenner and Robichaud 2014 figure 7), which is based on limited data from only three wildfires in Washington, Utah, and Arizona. These sites were selected for model development because the nested sampling structure provides stronger evidence for scaling relationships than disjointed sampling. In a separate analysis, Wagenbrenner and Robichaud (2014) reported that sediment yield increased slightly with catchment area at the Hayman Fire, in contrast to all other sites where sediment yield declined with increasing catchment size. Sediment yields declined with increasing catchment size at the Bobcat Fire, also in Colorado, but the largest plots at Bobcat were smaller in size than at Hayman. SDR is normally interpreted as a tool to scale gross erosion to net sediment yield to account for transport and storage processes (Walling 1983; de Vente et al. 2007), but Wagenbrenner and Robichaud (2014) also observed increasing evidence of sediment generation from fluvial erosion processes with increasing catchment size, which is consistent with post-fire observations from the Buffalo Creek Fire in Colorado (Moody and Martin 2001). Their model is also presented as a bedload SDR model in acknowledgement that sediment fences do not capture suspended sediment with high efficiency, especially in storms

that cause flows to overtop fences. As implied by other SDR models (e.g., Lu et al. 2006), it is likely that the suspended fraction transports with higher efficiency than the bedload component, so the whole soil SDR should be higher than predicted by the empirical model.

In Chapters 2 and 3, it was demonstrated that doubling the predicted SDR better aligned our net sediment yield predictions with the small catchment sediment yields from the Hayman Fire (Robichaud et al. 2008, 2013b). A higher precision adjustment was not pursued given the sparse observations and potential differences in watershed and rainfall characteristics. This approximate calibration increased the maximum SDR for near stream areas from 0.27 to 0.54, which is still low compared to the maximum SDR modeled by others in similar environments (Fernandez et al. 2003; Hamel et al. 2015). There is some uncertainty as to whether doubling the hillslope transport efficiency accurately represents the physical processes at play if gully and channel erosion add new sources of sediment with increasing catchment size. Sediment yields tend to peak in disturbed watersheds at the scales where the dominant erosion processes occur (Ostercamp and Toy 1997; de Vente et al. 2007), which may be small catchments in Colorado where concentrated flows after fires incise previously unchannelized drainages (Moody and Martin 2001, 2009). In some basins, SDR may peak at even larger scales due to changes in land use or geology, thus causing a reversal in the expected decline in sediment yield with basin area (de Vente et al. 2007). SDR models that account for travel time, peak discharge, particle size, upstream contributing area, and resisting factors along the downstream flow path (e.g., Ferro and Porto 2001; Lu et al. 2005; Borselli et al. 2008) might improve SDR estimates (Vigiak et al. 2012) but generally require data to inform parameter adjustments. For example, the InVest sediment retention model (Hamel et al. 2015) uses the SDR model of Vigiak et al. (2012) with an assumed maximum SDR of 0.8 and the need to set a sigmoidal curve shape parameter to

determine how SDR scales with the connectivity index. Until more sediment yield observations are available from larger catchments to inform these calibrations, it is unlikely that these models will offer significant improvements.

Increasing SDR to account for greater transport efficiency of fine sediments is also justified on the theoretical basis that these particles should transport more efficiently than the coarser particles that are preferentially trapped in sediment fences. Ryan et al. (2011) observed increased suspended sediment yields after a wildfire in Wyoming while bedload transport did not significantly increase. Rathburn et al. (2017) showed that more intense rainstorms tend to generate higher suspended sediment concentrations, but suspended sediment concentrations after most storms in the first year after the High Park Fire reached concerning levels for water treatment. This suggests that suspended sediment transport capacity is not likely to be a limiting factor for storms that generate surface runoff. Therefore, it is possible that the efficiency of suspended sediment transport is underestimated in Chapters 3 and 4 by assuming the bedload-centric model of Wagenbrenner and Robichaud (2014) applies to the clay and silt fractions. Even after doubling the modeled SDR, our highest values are in the low end of the SDR ranges predicted by Lu et al. (2006) for clay and silt in the mountainous portion of their study watershed in Australia. Higher efficiency transport of fine sediment would increase the risk of water quality impairment compared to our estimates. Representing hillslope transport with an annual SDR model also ignores the considerable inter-storm variability in SDR owing to the pulsed nature of erosion and transport (Walling 1983; Wagenbrenner and Robichaud 2014). Obscuring inter-storm SDR variability with the annual average is a minor concern for gaging the long-term impacts of reservoir sedimentation, but it could affect evaluations of water quality impairment if most sediment is transported during a small proportion of storms.

5.2.3 Channel Transport

Channel transport was modeled using is a very conceptual adaptation of the simple SDR model proposed by Frickel et al. (1975) for channel types in the Piceance Basin of western Colorado. The original model emphasizes stream order and the presence of raw gullies (channels) as evidence of high flow conditions that should efficiently transport sediment. Discontinuous gullies are expected to transport sediment less efficiently. Ungullied drainages with vegetation and evidence of deposition should retain the most sediment. In our model, we used Strahler stream order as a rough proxy for flow and channel conditions that influence sediment transport. We assigned channel SDRs per 10 km of stream length of 0.75, 0.80, 0.85, and 0.95 to 1st, 2nd, 3rd, and 4th or higher order streams, respectively. This captures the general tendency for sediment transport to be less efficient in the lower order channels due to smaller and often ephemeral or intermittent flows and the greater influence of riparian vegetation on roughness compared to higher order channels (e.g., Manning's n values from Chow 1959). However, this simple approach ignores significant intra-order variation in factors such as channel slope, bed material, form, and floodplain connectivity that influence sediment storage opportunities and the potential for channel erosion to contribute new sources of sediment.

Stream order is not a perfect indicator of transport efficiency, but it likely captures the general trend in SDR across our study watersheds. Moody and Martin (2001) observed that Buffalo Creek, a third order stream with a slope of 1.6% and an estimated annual mean discharge of 42.3 cfs (USEPA and USGS 2012), was efficiently transporting post-fire sediment even during base flow conditions. In contrast, Spring Creek, a first order stream with a slope of 4.7% and an estimated annual mean discharge of 1.9 cfs (USEPA and USGS 2012), primarily transported sediment during storm flow conditions. The much higher proportion of sediment

transported in Buffalo Creek during base flow conditions (85%) than in Spring Creek (33%) suggests that the lower order streams are more limited by transport capacity than higher order streams. Rathburn et al. (2017) noted similar trends in low order channels monitored after the High Park Fire. Higher intensity storms caused sediment deposition in ephemeral channels, whereas lower intensity storms caused degradation. This suggests that large pulses of sediment from upland sources will often exceed the transport capacity of low order channels despite their association with increased flows. There is less definitive evidence of higher transport capacity in the major channels, but qualitative observations that the South Fork of the Poudre contributed more sediment than expected to downstream water supplies after the High Park Fire suggest that major channels are generally efficient transport pathways (Miller et al. 2017)

Channel transport could be modeled more accurately with process-based models that account for channel and flow characteristics. Empirical bedload sediment transport models based on excess shear stress or stream power (e.g., Meyer-Peter and Mueller 1948; Ashida and Michiue 1972; Martin and Church 2000; Wong and Parker 2006) all predict increasing transport rates with increasing channel bed slope and flow depth. Slope does not vary consistently with stream order so it is possible that such an approach would alter our connectivity measures. Discharge increases consistently with stream order, so these models would still predict very efficient sediment transport in higher order channels. Bedload transport models would provide the ability to assess whether increased post-fire flows should cause channel erosion, assuming bedload composition and flow conditions can be appropriately characterized. Taking a sediment balance routing approach to account for upland and channel sources and storage could be accomplished for individual wildfires (e.g., Chapters 3 and 4) but this technique is not compatible with the

approach used in Chapter 2 to estimate water supply consequences independently for each unit of the landscape.

Potential for sediment storage in lakes and reservoirs was represented in our model by assigning them low SDRs, but no effort was made to account for bank and floodplain storage. SDR should be very high for channels with limited storage opportunities, such as steep mountain streams in v-shaped valleys (de Vente et al. 2007), but it may be lower for channels that connect to floodplains during post-fire storm flows. Moody and Martin (2001) observed substantial sediment storage in floodplains after the Buffalo Creek Fire that is likely to have a long residence time. In the first year after the High Park Fire, sediment mobilized from early storms was deposited primarily on the channel banks, where it was later remobilized by higher flows (Oropeza and Heath 2013; Miller et al. 2017). This short duration bank storage could affect storm-level SDR estimates but it probably has negligible impacts on SDR at annual or longer time scales. Sediment can also be stored in alluvial fans at the base of steep drainages. The residence time for alluvial fan storage should be short when delivered to confined valleys, but it may have longer residence times when delivered to unconfined valleys far from the main channel (Rathburn et al. 2007). The current SDR model could be refined to using morphological indicators of storage potential such as valley confinement to reduce SDR in reaches with high storage potential. It would be difficult to accurately model storage processes without rainfall-event level predictions of runoff and erosion to identify where excess supply will be stored in channels and to identify the reaches and flow conditions that are likely to deposit sediment in floodplains.

The lack of post-fire sediment yield observations from larger watersheds remains a barrier to improving hillslope and channel transport modeling. Our predicted whole watershed

sediment yields for the first year after fire (Figure 2.5; Table 4.2) are mostly below the first year yield of 52.5 Mg ha^{-1} observed by Martin and Moody (2001) in response to extreme rainfall after the Buffalo Creek Fire (converted reservoir input volume using 1.6 Mg m^{-3} bulk density). The combined hillslope and channel SDR models represent the general trend for sediment yield to decline with increasing watershed size, but as discussed previously, it is questionable whether these scaling relationships accurately reflect transport efficiency given the likely sediment contributions from channel erosion. More accurate budgeting of sediment sources is needed to isolate the effects of transport and storage mechanisms.

5.2.4 Water Impairment

The water quality impairment evaluation used in Chapters 3 and 4 is a first approximation of how annual sediment loads translate into storm-level water quality outcomes. The annual time scale of the erosion estimates and similar limitations with the sediment transport models preclude accurate predictions of individual storm outcomes. For this reason, we focused on the average annual post-storm suspended sediment concentrations and turbidities as indicators of whether sediment loads should be high enough in a given year to impair water quality. Several key assumptions needed to bridge the gap between annual sediment loads and storm-level suspended sediment concentrations and turbidities warrant further evaluation and improvement.

RUSLE is an annual erosion model, which required an assumption of how the annual load is distributed among storms. We made the simplifying assumption that the annual load is equally divided among the frequency of storms exceeding a threshold intensity for hillslope erosion (Wilson et al. 2018). There is some uncertainty associated with this threshold, which can affect the number of storms the load is divided among. A larger issue with this assumption is that it does not represent inter-storm variability in erosion. Previous studies from this region

demonstrate that most erosion occurs in response to a few powerful storms (Wagenbrenner et al. 2006; Robichaud et al. 2013b). Impairment probabilities would be higher using the annual maximum storm loads. This component of the model could be improved by using an erosion model meant for storm level prediction, which would require equivalent revisions to how potential future rainfall conditions are represented.

We also made a gross approximation that 35% of the sediment generated by hillslope erosion should contribute to the suspended sediment load. This figure was arrived at by combining post-fire observations of suspended load particle sizes and composition from a similar watershed in Wyoming with observations of hillslope erosion sediment from one of the study watersheds. Ryan et al. (2011) observed that silt and clay accounted for 70-85% of post-fire suspended load during summer storm flows and the remainder was mostly fine organics. Schmeer (2014) reported that approximately 25% of the mineral component of hillslope sediment after the High Park Fire was in the clay and silt size classes but did not report on the organic component. Hence, we assumed that a similar proportion of fine organics observed by Ryan et al. (2011) could accompany the mineral sediment from our watersheds, boosting our estimate to a maximum of 35%. These assumptions could be improved in two ways. Spatial soils data from the Soil Survey Geographic Database (SSURGO) could be used to represent differences in hillslope sediment composition across the watershed instead of assuming it is constant. Second, estimates of ash load could be incorporated as models of ash production and transport improve. Ash production is highly variable and difficult to predict because it depends on space and time varying factors such as fuel composition and load and burning conditions (Bodí et al. 2014).

Suspended sediment transport and mixing are also greatly simplified in our model. As discussed previously, it is likely that the suspended load transports more efficiently than bedload, which means suspended loads may be underestimated. To estimate suspended sediment concentrations, it was assumed that the average storm load was perfectly mixed in the receiving reservoir storage volume or stream mean daily flow volume. In reality, perfect mixing is not achieved in either waterbody type. In reservoirs, much of the sediment should settle out of suspension before mixing and thus will be a minor threat to water quality at the outlet unless the reservoir is small, or the input points are near the outlet. For streams, it was assumed that the storm load would be diluted in the mean daily flow volume, which may dampen peak storm suspended sediment concentrations that occur at finer time steps. Inspection of storm-level hyetographs, hydrographs, and turbidity time series could help refine the time frame used to define the dilution volume. This could also help to evaluate whether the mean seasonal discharge is a reasonable representation of post-storm flows, or if there is need to increase it for the concentration calculations.

Another limitation is our use of an empirical equation (Eqn 3.5) from a different watershed (Murphy et al. 2015) to convert from suspended sediment concentration to turbidity for ease of comparison with documented water quality thresholds for treatment (Writer et al. 2014; Murphy et al. 2015). Suspended sediment-turbidity relationships can vary between watersheds and even between transport events within watersheds owing to differences in sediment composition. Ideally, water managers would express their treatment limits in the more fundamental metric – suspended sediment concentration – so this conversion step would be unnecessary. The potential error from this source is likely minor given that many of the years or fires with predicted water quality impairment far exceed the 100 NTU threshold used in Chapters

2 and 3. Decreasing or increasing the impairment threshold by a factor of ten to account for the many uncertainties in the analysis doesn't radically alter the results (Table 3.4; Figure 3.7), especially the relative impairment risk among the water supplies. Similarly, our focus on the relative reduction in impairment risk in Chapter 4 should be robust to moderate changes in the absolute magnitude of risk.

5.3 COMBINED RISK MODELING

The coupled design of our risk models has the potential to magnify uncertainties from the component models. It is difficult to precisely estimate how uncertainty propagates through the system without intensive simulation due to the spatial nature of the data and models. For this reason, intermediate results were featured in each chapter and compared to available field observations to evaluate system performance. As discussed in the previous sections, our estimates of burn severity, post-fire erosion, watershed sediment yields, and post-storm water quality measures were close to regional field observations with the exception of a few questionable departures that are highlighted again below. The implications of uncertainty differ for spatial prioritization and estimating risk magnitudes.

For spatial prioritization, the greatest concern is whether the component models accurately reflect the spatial variation in wildfire and post-fire hazards across the landscape. Burn probability modeling is critical for wildfire risk assessment, but there is widely recognized need to evaluate the quality of predictions and a lack of consensus on how best to do so (Parisien et al. 2019). Similarly, pre-fire burn severity modeling is largely untested except in terms of the modeled proportions of burn severity compared to previous fires (Elliot et al. 2016; Chapter 4). Although there is some epistemic uncertainty with the wildfire hazard components, the aleatory

uncertainty is probably much greater owing to randomness in ignition locations and weather conditions. The greatest uncertainty with the post-fire watershed modeling is whether erosion and sediment transport mechanisms are properly represented. RUSLE erosion predictions were most sensitive to the LS factor, yet there is limited local evidence that hillslope erosion increases dramatically with slope length and steepness. If erosion rates are less sensitive to LS, risk may be more evenly distributed across the watershed. The spatial implementation of RUSLE likely captures some channel erosion (Desmet and Govers 1996), but it would be better to model channel erosion separately to understand if its magnitude and spatial distribution shifts risk to different parts of the landscape. Uncertainties with the hillslope and sediment transport components raise similar concerns. Risk would be more concentrated near water supplies with less efficient transport and more dispersed across large watersheds with more efficient transport.

For estimating risk magnitudes, the biggest concern is whether the quantities of intermediate and final impact measures are reasonable. Modeled estimates of burn probability and severity aligned well with regional trends in fire activity from the recent past (Short et al. 2016; Chapter 4). There is some potential for error in risk estimation from the fire hazard components if their spatial patterns are not calibrated within the study watersheds. Several adjustments were necessary to align the watershed model predictions with regional field observations. These calibration steps improve confidence that the sediment yield predictions are reasonable for the region (Figure 2.5), but it is possible that some of the regional observations are not representative of the study watersheds due to differences in soils, topography, climate, or erosion mechanisms. It is reassuring that the economic risk estimates from Chapter 2 were close to the results of a similar study in California (Elliot et al. 2016). The water quality impairment analyses in Chapters 3 and 4 employed coarse approximations of erosion, transport, and dilution

processes at finer time scales, which implies there is considerable uncertainty in the absolute impairment probabilities. However, varying the water quality impairment threshold by a factor of ten in either direction (Table 3.4) did not qualitatively change our conclusions about which water supplies were low or high risk.

Resolving epistemic uncertainties with any of the model components could improve confidence in risk maps, fuel treatment priorities, and risk magnitudes. Yet, these improvements are unlikely to meaningfully improve our ability to forecast wildfire-water supply impacts given the high aleatory uncertainty from spatial and temporal variability in wildfire and rainfall (Jones et al. 2014; Chapter 3). Reducing uncertainty in the watershed model components would be more valuable in the context of post-fire hazard assessment where the watershed model components account for more of the total uncertainty after fire extent and severity are fixed.

REFERENCES FOR CHAPTER 5

Agee JK, Skinner CN (2005) Basic principles of forest fuel reduction treatments. *Forest Ecology and Management* **211**, 83-96. doi:10.1016/j.foreco.2005.01.034

Anderson HE (1982) Aids to determining fuel models for estimating fire behavior. USDA Forest Service, Intermountain Forest and Range Experiment Station, General Technical Report INT-122. (Ogden, UT, USA)

Ashida K, Michiue M (1972) Hydraulic resistance of flow in an alluvia bed and bed load transport rate. *Proceedings of Japan Society of Civil Engineers* **206**, 59-69.

Benavides-Solorio JD, MacDonald LH (2005) Measurement and prediction of post-fire erosion at the hillslope scale, Colorado Front Range. *International Journal of Wildland Fire* **14**, 457-474. doi:10.1071/WF05042

Barros AMG, Ager AA, Day MA, Krawchuk MA, Spies TA (2018) Wildfires managed for restoration enhance ecological resilience. *Ecosphere* **9(3)**, e02161. doi:10.1002/ecs2.2161

Blake D, Nyman P, Nice H, D'Souza FML, Kavazos CRJ, Horwitz P (2020) Assessment of post-wildfire erosion risk and effects on water quality in south-western Australia. *Fire* **29**, 240-257. doi:10.1071/WF18123

Bodí MB, Martin DA, Balfour VN, Santín C, Doerr SH, Pereira P, Cerdà A, Mataix-Solera J (2014) Wildland fire ash: production, composition and eco-hydro-geomorphic effects. *Earth-Science Reviews* **130**, 103-127. doi:10.1016/j.earscirev.2013.12.007

Borselli L, Cassi P, Torri D (2008) Prolegomena to sediment and flow connectivity in the landscape: a GIS and field numerical assessment. *Catena* **75**, 268-277. doi:10.1016/j.catena.2008.07.006

Chow VT (1959) Open-channel hydraulics. McGraw-Hill. 680 p. (New York, NY, USA)

Desmet PJJ, Govers G (1996) A GIS procedure for automatically calculating the USLE LS factor on topographically complex landscape units. *Journal of Soil and Water Conservation* **51(5)**, 427-433.

de Vente J, Poesen J, Arahkhedri M, Verstraeten G (2007) The sediment delivery problem revisited. *Progress in Physical Geography* **31(2)**, 155-178. doi:10.1177/0309133307076485

Elliot WJ, Miller ME, Enstice N (2016) Targeting forest management through fire and erosion modelling. *International Journal of Wildland Fire* **25**, 876-887. doi:10.1071/WF15007

Graham RT (2003) Hayman Fire case study. USDA Forest Service, Rocky Mountain Research Station, General Technical Report RMRS-GTR-114. (Ogden, UT, USA)

Fernandez C, Wu JQ, McCool DK, Stöckle CO (2003) Estimating water erosion and sediment yield with GIS, RUSLE, and SEDD. *Journal of Soil and Water Conservation* **58(3)**, 128-136.

Ferro V, Porto P (2000) Sediment Delivery Distributed (SEDD) Model. *Journal of Hydrologic Engineering* **5(4)**, 411-422.

Finney MA, McHugh CW, Grenfell IC, Riley KL, Short KC (2011) A simulation of probabilistic wildfire risk components for the continental United States. *Stochastic Environmental Research and Risk Assessment* **25**, 973-1000. doi:10.1007/s00477-011-0462-z

Finney MA, Brittain S, Seli RC, McHugh CW, Gangi L (2015) FlamMap: fire mapping and analysis system (version 5.0) [Software]. Available from http://www.firelab.org/document/flammap-software

Frickel DG, Shown LM, Patton PC (1975) An evaluation of hillslope and channel erosion related to oil-shale development in the Piceance basin, north-western Colorado. Colorado Department of Natural Resources, Colorado Water Resources Circular 30. (Denver, CO, USA)

Haas JR, Calkin DE, Thompson MP (2015) Wildfire risk transmission in the Colorado Front Range, USA. *Risk Analysis* **35(2)**, 226-240. doi:10.1111/risa.12270

Hamel P, Chaplin-Kramer R, Sim S, Mueller C (2015) A new approach to modeling the sediment retention service (InVEST 3.0): case study of the Cape Fear catchment, North Carolina, USA. *Science of the Total Environment* **524-525**, 166-177. doi:10.1016/j.scitotenv.2015.04.027

Hurteau MD, Liang S, Westerling AL, Wiedinmyer C (2019) Vegetation-fire feedback reduces projected area burned under climate change. *Scientific Reports* **9**, 2838. doi:10.1038/s41598-019-39284-1

Jones OD, Nyman P, Sheridan GJ (2014) Modelling the effects of fire and rainfall regimes on extreme erosion events in forested landscapes. *Stochastic Environmental Research and Risk Assessment* **28**, 2015-2025. doi:10.1007/s00477-014-0891-6

Kalies EL, Yocum Kent LL (2016) Tamm review: are fuel treatments effective at achieving ecological and social objectives? A systematic review. *Forest Ecology and Management* **375**, 84-95. doi:10.1016/j.foreco.2016.05.021

Kampf SK, Brogan DJ, Schmeer S, MacDonald LH, Nelson PA (2016) How do geomorphic effects of rainfall vary with storm type and spatial scale in a post-fire landscape? *Geomorphology* **273**, 39-51. doi:10.1016/j.geomorph.2016.08.001

Kampf SK, Gannon BM, Wilson C, Saavedra F, Miller ME, Heldmyer A, Livneh B, Nelson P, MacDonald L (2020) PEMIP: post-fire erosion model inter-comparison project. *Journal of Environmental Management* **268**, 110704. doi:10.1016/j.jenvman.2020.110704

Larsen IJ, MacDonald LH (2007) Predicting post-fire sediment yields at the hillslope scale: testing RUSLE and disturbed WEPP. *Water Resources Research* **43**, W11412. doi:10.1029/2006WR005560

Larsen IJ, MacDonald LH, Brown E, Rough D, Welsh MJ, Pietraszek JH, Libohova Z, Benavides-Solorio JD, Schaffrath K (2009) Causes of post-fire runoff and erosion: water repellency, cover, or soil sealing? *Soil Science Society of America Journal* **73**, 1393-1407. doi:10.2136/sssaj2007.0432

Litschert SE, Theobald DM, Brown TC (2014) Effects of climate change and wildfire on soil loss in the Southern Rockies ecoregion. *Catena* **118**, 206-219. doi:10.1016/j.catena.2014.01.007

Lu H, Moran CJ, Sivapalan M (2005) A theoretical exploration of catchment-scale sediment delivery. *Water Resources Research* **41**, W09415. doi:10.1029/2005WR004018

Lu H, Moran CJ, Prosser IP (2006) Modelling sediment delivery ratio over the Murray Darling Basin. *Environmental Modelling & Software* **21**, 1297-1308. doi:10.1016/j.envsoft.2005.04.021

Martin Y, Church M (2000). Re-examination of Bagnold's empirical bedload formulae. *Earth Surface Processes and Landforms* **25**, 1011-1024. doi:10.1002/1096-9837(200008)25:9<1011::AID-ESP114>3.0.CO;2-H

McCool DK, Foster GR, Mutchler CK, Meyer LD (1989) Revised slope length factor for the Universal Soil Loss Equation. *Transactions of the American Society of Agricultural Engineers* **32**, 1571-1576. doi:10.13031/2013.31192

Meyer-Peter E, Müller R (1948) Formulas for bed-load transport. *Proceedings of the International Association for Hydraulic Structures Research – Second Meeting, Stockholm*, 39-64.

Miller S, Rhodes C, Robichaud P, Ryan S, Kovecses J, Chambers C, Rathburn S, Heath J, Kampf S, Wilson C, Brogan D, Piehl B, Miller ME, Giordanengo J, Berryman E, Rocca M (2017) Learn from the burn: the High Park Fire 5 years later. USDA Forest Service, Rocky Mountain Research Station, Science You Can Use Bulletin, Issue 25. (Fort Collins, CO, USA)

Moody JA, Martin DA (2001) Initial hydrologic and geomorphic response following a wildfire in the Colorado Front Range. *Earth Surface Processes and Landforms* **26**, 1049-1070. doi:10.1002/esp.253

Moody JA, Martin DA (2009) Synthesis of sediment yields after wildland fire in different rainfall regimes in the western United States. *International Journal of Wildland Fire* **18**, 96-115. doi:10.1071/WF07162

Moody JA, Shakesby RA, Robichaud PR, Cannon SH, Martin DA (2013) Current research issues related to post-wildfire runoff and erosion processes. *Earth-Science Reviews* **122**, 10-37. doi:10.1016/j.earscirev.2013.03.004

Moore ID, Burch GJ (1986) Physical basis of the length-slope factor in the Universal Soil Loss Equation. *Soil Science Society of America Journal* **50**, 1294-1298. doi:10.2136/sssaj1986.03615995005000050042x

Murphy SF, Writer JH, McCleskey RB, Martin DA (2015) The role of precipitation type, intensity, and spatial distribution in source water quality after wildfire. *Environmental Research Letters* **10**, 084007. doi:10.1088/1748-9326/10/8/084007

DeBano LF, Neary DG (2005) Soil physical processes. In 'Wildland fire in ecosystems: effects of fire on soils and water'. (Eds DG Neary, KC Ryan, LF DeBano) USDA Forest Service, Rocky Mountain Research Station, General Technical Report RMRS-GTR-42-Vol. 4. (Eds DG Neary, KC Ryan, LF DeBano) p. 21-27. (Ogden, UT, USA)

Oropeza J, Heath J (2013) Effects of the 2012 Hewlett and High Park Wildfires on water quality of the Poudre River and Seaman Reservoir. City of Fort Collins Utilities Report. 33 p. (Fort Collins, CO, USA)

Ostercamp WR, Toy TJ (1997) Geomorphic considerations for erosion prediction. *Environmental Geology* **29(3/4)**, 152-157. doi:10.1007/s002540050113

Parisien M-A, Dawe DA, Miller C, Stockdale CA, Armitage OB (2019) Applications of simulation-based burn probability modeling: a review. *International Journal of Wildland Fire* **28**, 913-926. doi:10.1071/WF19069

Perica S, Martin D, Pavlovic S, Roy I, St. Laurent M, Trypaluk C, Unruh D, Yekta M, Bonnin G (2013) 'NOAA Atlas 14, Volume 8 Version 2, precipitation-frequency atlas of the United States, Midwestern States.' (Silver Spring, MD, USA).

Pietraszek JH (2006) Controls on post-fire erosion at the hillslope scale, Colorado Front Range. Thesis. Colorado State University. (Fort Collins, CO, USA)

Rathburn S, Shahverdian SM, Ryan SE (2017) Post-disturbance sediment recovery: implications for watershed resilience. *Geomorphology* **305**, 61-75. doi:10.1016/j.geomorph.2017.08.039

Reinhardt ED, Keane RE, Calkin DE, Cohen JD (2008) Objectives and considerations for wildland fuel treatment in forested ecosystems of the interior western United States. *Forest Ecology and Management* **256**, 1997-2006. doi:10.1016/j.foreco.2008.09.016

Renard KG, Foster GR, Weesies GA, McCool DK, Yoder DC (1997) Predicting soil erosion by water: a guide to conservation planning with the Revised Universal Soil Loss Equation (RUSLE). USDA Agricultural Research Service Agricultural Handbook no. 703. (Washington, DC, USA)

Riley KL, Loehman RA (2016) Mid-21st-century climate changes increase predicted fire occurrence and fire season length, Northern Rocky Mountains, United States. *Ecosphere* **7(11)**, e01543. doi:10.1002/ecs2.1543

Robichaud PR, Wagenbrenner JW, Brown RE, Wohlgemuth PM, Beyers JL (2008) Evaluating the effectiveness of contour-felled log erosion barriers as a post-fire runoff and erosion mitigation treatment in the western United States. *International Journal of Wildland Fire* **17**, 255-273. doi:10.1071/WF07032

Robichaud PR, Lewis SA, Wagenbrenner JW, Ashmun LE, Brown RE (2013a) Post-fire mulching for runoff and erosion mitigation. Part I: effectiveness at reducing hillslope erosion rates. *Catena* **105**, 75-92. doi:10.1016/j.catena.2012.11.015

Robichaud PR, Wagenbrenner JW, Lewis SA, Ashmun LE, Brown RE, Wohlgemuth PM (2013b) Post-fire mulching for runoff and erosion mitigation. Part II: effectiveness in reducing runoff and sediment yields from small catchments. *Catena* **105**, 93-111. doi:10.1016/j.catena.2012.11.016

Ryan SE, Dwire KA, Dixon MK (2011) Impacts of wildfire on runoff and sediment loads at Little Granite Creek, western Wyoming. *Geomorphology* **129**, 113-130. doi:10.1016/j.geomorph.2011.01.017

Schoennagel T, Veblen TT, Romme WH (2004) The interaction of fire, fuels, and climate across Rocky Mountain Forests. *BioScience* **54(7)**, 661-676. doi:10.1641/0006-3568(2004)054[0661:TIOFFA]2.0.CO;2

Schmeer SR (2014) Post-fire erosion response and recovery, High Park Fire, Colorado. Thesis. Colorado State University. (Fort Collins, CO, USA.)

Schmeer SR, Kampf SK, MacDonald LH, Hewitt J, Wilson C (2018) Empirical models of annual post-fire erosion on mulched and unmulched hillslopes. *Catena* **163**, 276-287. doi:10.1016/j.catena.2017.12.029

Scott JH, Burgan RE (2005) Standard fire behavior fuel models: a comprehensive set for use with Rothermel's surface fire spread model. USDA Forest Service, Rocky Mountain Research Station, General Technical Report RMRS-GTR-153. (Fort Collins, CO, USA)

Scott JH, Reinhardt ED (2001) Assessing crown fire potential by linking models of surface and crown fire behavior. USDA Forest Service, Rocky Mountain Research Station, General Technical Research Paper RMRS-RP-29. (Fort Collins, CO, USA)

Scott JH, Thompson MP, Gilbertson-Day JW (2016) Examining alternative fuel management strategies and the relative contribution of National Forest System land to wildfire risk adjacent to homes – a pilot assessment on the Sierra National Forest, California, USA. *Forest Ecology and Management* **362**, 29-37. doi:10.1016/j.foreco.2015.11.038

Sherriff RL, Platt RV, Veblen TT, Schoennagel TL, Gartner MH (2014) Historical, observed, and modeled wildfire severity in montane forests of the Colorado Front Range. *PLoS One* **9**, e106971. doi:10.1371/journal.pone.0106971

Short KC, Finney MA, Scott JH, Gilbertson-Day JW, Grenfell IC (2016) Spatial dataset of probabilistic wildfire risk components for the conterminous United States. USDA Forest Service Research Data Archive. (Fort Collins, CO, USA) doi:10.2737/RDS-2016-0034. (Fort Collins, CO)

Spracklen DV, Mickley LJ, Logan JA, Hudman RC, Yevich R, Flannigan MD, Westerling AL (2009) Impacts of climate change from 2000 to 2050 on wildfire activity and carbonaceous aerosol concentrations in the western United States. *Journal of Geophysical Research* **114**, D20301. doi:10.1029/2008JD010966.

Theobald DM, Merritt DM, Norman JB (2010) Assessment of threats to riparian ecosystems in the western U.S. Report to the Western Environmental Threats Assessment Center, Prineville, OR by the USDA Stream Systems Technology Center and Colorado State University. (Fort Collins, CO, USA)

Thompson MP, Scott J, Langowski PG, Gilbertson-Day JW, Haas JR, Bowne EM (2013a) Assessing watershed -wildfire risks on national forest system lands in the Rocky Mountain region of the United States. *Water* **5**, 945-971. doi:10.3390/w5030945

Thompson MP, Vaillant NM, Haas JR, Gebert KM, Stockmann KD (2013b) Quantifying the potential impacts of fuel treatments on wildfire suppression costs. *Journal of Forestry* **111**, 49-58. doi:10.5849/jof.12-027

Thompson MP, Gilbertson-Day JW, Scott JH (2016) Integrating pixel- and polygon-based approaches to wildfire risk assessment: applications to a high-value watershed on the Pike and San Isabel National Forests, Colorado, USA. *Environmental Modeling and Assessment* **21**, 1-15. doi:10.1007/s10666-015-9469-z

US Environmental Protection Agency (USEPA) and the US Geological Survey (USGS) (2012) National Hydrography Dataset Plus - NHDPlus. Version 2.1. Available online at: http://www.horizon-systems.com/NHDPlus/index.php

Vigiak O, Borselli L, Newham LTH, McInnes J, Roberts AM (2012) Comparison of conceptual landscape metrics to define hillslope-scale sediment delivery ratio. *Geomorphology* **138**, 74-88. doi:10.1016/j.geomorph.2011.08.026

Wagenbrenner JW, MacDonald LH, Rough D (2006) Effectiveness of three post-fire rehabilitation treatments in the Colorado Front Range. *Hydrological Processes* **20**, 2989-3006. doi:10.1002/hyp.6146

Wagenbrenner JW, Robichaud PR (2014) Post-fire bedload sediment delivery across spatial scales in the interior western United States. *Earth Surface Processes and Landforms* **39**, 865-876. doi:10.1002/esp.3488

Walling DE (1983) The sediment delivery problem. *Journal of Hydrology* **65**, 209-237. doi:10.1016/0022-1694(83)90217-2

Wilson C, Kampf SK, Wagenbrenner JW, MacDonald LH (2018) Rainfall thresholds for post-fire runoff and sediment delivery from plot to watershed scales. *Forest Ecology and Management* **430**, 346-356. doi:10.1016/j.foreco.2018.08.025

Winchell MF, Jackson SH, Wadley AM, Srinivasan R (2008) Extension and validation of a geographic information system-based method for calculating the Revised Universal Soil Loss Equation length-slope factor for erosion risk assessments in large watersheds. *Journal of Soil and Water Conservation* **63**, 105-111. doi:10.2489/jswc.63.3.105

Wong M, Parker G (2006) Reanalysis and correction of bed-load relation of Meyer-Peter and Müller using their own database. *Journal of Hydraulic Engineering* **132(11)**, 1159-1168. doi:10.1061/(ASCE)0733-9429(2006)132:11(1159)

Writer JH, Hohner A, Oropeza J, Schmidt A, Cawley KM, Rosario-Ortiz FL (2014) Water treatment implications after the High Park Wildfire, Colorado. *Journal of the American Water Works Association* **106(4)**, 189-199. doi:10.5942/jawwa.2014.106.0055

CHAPTER 6 – SUMMARY AND CONCLUSIONS

6.1 RESEARCH SUMMARY

This dissertation presented two models to assess wildfire-water supply risks. The first model, introduced in Chapter 2, built on the framework of earlier avoided cost assessments (Buckley et al. 2014; Elliot et al. 2016; Jones et al. 2017) to quantify and map sediment-related risks to three interconnected community water systems, each with multiple reservoirs and diversions that differ in their sensitivity to sediment and importance for system function. The second model, used in Chapters 3 and 4, quantified the risk of wildfire impairing water quality beyond turbidity limits for treatment by modeling average storm sediment loads from stochastically simulated wildfires. Chapter 3 further explored how impairment of individual water supplies influences the potential for disrupting raw water supply in multi-source water systems. Chapters 2 and 4 applied these risk models to estimate the potential effectiveness of mitigating water supply risks with proactive fuels reduction and improved fire containment. The results suggest efforts to limit fire severity and size should meaningfully reduce sediment loads, but mitigation may be less effective at reducing the frequency of water quality impairment because the residual sediment loads from many fires may still be high enough to degrade water quality. Chapter 3 examined the mitigation benefit of source redundancies. We found that redundancy increased system reliability, but gains depended on the impairment risk of the alternative water supplies and their geographic separation. The collective results suggest that water supplies have widely varying wildfire risk and associated opportunities for effective mitigation with fire management or engineering solutions.

6.2 WILDFIRE-WATER SUPPLY RISK ASSESSMENT

The two risk models used in this dissertation have different strengths and limitations worth noting for their application in future studies. The sediment impact cost model proved useful for mapping the source of wildfire-water supply risk across broad landscapes, but valuing sediment impacts to non-reservoir infrastructure was difficult. Water managers did not have a clear means to translate a mass or volume of sediment into costs, so we resorted to estimating the base impact cost to diversions at half that of reservoirs because of the greater flexibility afforded by diversions and managers' perception that water impairment is less costly due to existing source water redundancies. For example, Fort Collins and Greeley experienced degraded water quality in the Cache la Poudre River following the 2012 High Park Fire, but both communities were able to meet water demands with alternative sources (Oropeza and Heath 2013; Writer et al. 2014). The most concerning scenario for these communities is wildfire(s) disrupting raw water supply by impairing multiple sources at the same time. This led us to develop an alternative model, used in Chapters 3 and 4, to evaluate whether discrete wildfire events will impair water supplies using the common risk and reliability framework (Singh et al. 2007) with turbidity as the environmental forcing and turbidity limits for treatment as the impairment threshold. The watershed modeling for this analysis required several approximations related to the frequency and duration of erosion and sediment transport events that warrant further refinement in future studies – ideally by using erosion and sediment transport models meant for storm-level prediction – but still managed to predict storm-level turbidities that are comparable to field observations. We also simplified the analysis by assuming all water supplies have the same impairment threshold, but it is more likely that conveyance infrastructure can tolerate higher turbidity than terminal reservoirs or diversions. The model could be improved with more detailed

accounting of water yield or other performance measures to accurately translate component impairments into system consequences (Haimes 2012).

The two risk models used in this dissertation send mixed messages about the magnitude of risk and need for mitigation. In Chapter 1, we found that wildfire-related sediment costs should amount to only 11.5 million USD over a 25-year period assuming wildfires are followed my median rainfall conditions. The moderate economic risk of fire-generated sediment in our study is due to low to moderate burn probability and stakeholder-informed sediment impact costs. The modern fire regime of the Colorado Front Range is characterized by large, but still relatively infrequent wildfires (Graham 2003; Sherriff et al. 2014). Based on the National FSim results (Short et al. 2016), only 6.6% of the landscape (317 km^2) is expected to burn over our assessment period. This level of fire activity and associated post-fire erosion does not translate to extreme economic risk given sediment impact costs ranging between 1.6 to 37.5 USD Mg^{-1}. In contrast, the Monte Carlo wildfire and rainfall simulation presented in Chapter 3 indicates that water supplies with large watersheds, particularly on-network stream diversions, may experience water quality impairment in nearly 20% of years. Water utilities have very low tolerance for raw water supply disruption; for example, many communities in Colorado plan for firm water yield up to a 100-year recurrence interval drought. Assuming this common reliability standard represents water utility tolerance for supply disruption in 1% of years, risk of wildfire-related water quality impairment is unacceptably high for some water supplies. In some cases, source redundancies reduce the risk of water supply disruption to an acceptable level, but some water systems with no or few redundancies may be unacceptably vulnerable to wildfire-related water quality disruption under current conditions.

Neither of our risk models accounted for potential increases in fire activity due to changing climate and ignition sources, so our risk estimates are likely conservative. Studies that project current fire-climate relationships into the future suggest area burned in the Southern Rockies could increase as much as 50-175% in coming decades (Spracklen et al. 2009; Litschert et al. 2012). The growing influence of anthropogenic ignitions (Cattau et al. 2020) also suggests that area burned could increase due to the increasing population and recreational activity. Risk in the sediment cost model will increase linearly with area burned assuming the gains in fire activity are roughly uniform across the landscape. If large fires become more frequent, so should the risks of water quality impairment and system supply disruption. In Chapter 3, we made the simplifying assumptions that water yield and waterbody volume are constant, but like fire activity, they both respond to interannual precipitation variability. Considering the correlation among these factors would likely increase the risk of impairment because waterbody size should be lower than average during large wildfire years and the lower water yield from alternative sources during dry years will provide less ability to buffer system consequences. Increasing water demand from a growing population may also reduce the mitigation effectiveness of redundancies. Future risk assessments would improve their utility for long term planning by incorporating these factors.

6.3 RISK MITIGATION EFFECTIVENESS

Precise estimates of risk and risk mitigation are not required to identify areas of a landscape that would benefit from mitigation, but they are increasingly sought by watershed collaboratives and water utilities to make the financial case for proactive mitigation and to report transparent measures of program outcomes (Buckley et al. 2014; Ozment et al. 2016; Jones et al.

2017). The studies that established the avoided cost framework used in Chapter 2 (Buckley et al. 2014; Elliot et al. 2014; Jones et al. 2017) all focused on avoiding reservoir sedimentation by proactively treating fuels to reduce burn severity and post-fire erosion. In Chapter 2, we found a highly negative return on investment from fuels reduction in our study watersheds to avoid sediment costs, which closely aligns with the estimate that 68 million USD of fuel treatment would avoid only 1 million USD of reservoir sedimentation costs in the Mokelumne Watershed in California (Buckley et al. 2014). The narrow accounting of wildfire-related sediment impacts in both our studies likely underestimate the true value of mitigation for water utilities, but other costs would have to be many times larger than we currently estimate in order to break even. The only study to suggest a positive return on investment from fuels reduction to avoid sediment (Jones et al. 2017) assumed that all fuel treatments will be burned by wildfire followed by extreme but rare rainfall (10 to 100-year recurrence intervals). Although this combination of wildfire and rainfall has occurred in Colorado (Moody and Martin 2001), the combined probability of extreme wildfire and extreme rainfall is very low, so avoided cost estimates for these extreme scenarios are probably not representative of the average fuel treatment effects.

The risk mapping and fuel treatment optimization presented in Chapter 2 can help target fuels reduction towards the most cost-effective treatment types and locations, but we estimate that the maximum feasible risk reduction from proactively treating fuels is between one third and one half in this landscape with an unlimited budget. This is because treating fuels reduces but does not eliminate risk to water supplies and not all areas of the landscape can be managed with forest fuels treatments. It is unclear whether this level of risk reduction, whether expressed in absolute costs or percent reduction, meets water manager and stakeholder objectives. I suspect that the outcomes of landscape-scale fuel treatment are desirable to water stakeholders, but it will

be difficult to justify funding the majority of the work since their return on investment is low. Most avoided costs from fuels reduction in our study watersheds are projected to come from reduced damage to private property and reduced suppression costs (Talberth et al. 2013) like similar assessments from California and southwest Colorado (Buckley et al. 2014; Quantified Ventures 2019). Watershed investment programs may have better success engaging water-focused funders with this framework if they can attract funds from other investors in proportion to their projected benefits.

Our fuel treatment optimization model in Chapter 2 primarily selected a thinning only treatment despite the greater effectiveness of the combined thinning and prescribed fire treatment and the greater cost-effectiveness of using prescribed fire alone. This is partially the result of the fuel treatment and fire behavior modeling limitations that are discussed in Chapters 2 and 5, but it also reflects that we mapped only a small portion of the landscape as suitable for prescribed fire as a first entry treatment. Since our initial discussions with managers to define prescribed fire constraints in our model, the local National Forest has ramped up their prescribed fire program focusing on large broadcast burn units (USDA Forest Service 2020) and has plans to further expand the use of prescribed fire in many areas we currently map as infeasible (Arapahoe and Roosevelt National Forests 2019). These plans are currently still conceptual in nature and optimistic compared to a recent analysis of broadcast burning opportunity in the Colorado Front Range (Addington et al. 2020), but they suggest a commitment towards cost-effective treatment at scale on public lands. Monitoring from these efforts will also help to refine our understanding of local prescribed fire effects, which we suspect are more substantial than in the study we used to parameterize our model (Stephens and Moghaddas 2005). The cost-effectiveness of mitigating

risk with fuels reduction could dramatically improve compared to our estimates if prescribed fire is both more effective and more widely implemented.

The water quality impairment risk model introduced in Chapter 3 facilitated our evaluation of the risk mitigation effectiveness of fire containment in Chapter 4. Proactive investments in fire containment have historically focused on constructed fuel breaks (Omi 1979), but modern efforts have shifted towards zoning the landscape into Potential fire Operational Delineations (PODs) based primarily on existing control features such as roads and rivers (O'Connor et al. 2016, 2017; Thompson et al. 2016). We estimated that containing all wildfires within their POD of origin would reduce area burned in the study watershed by 58.7% and total sediment load by 50.4-55.3%. These figures are conditional on successful fire containment, but high enough to suggest that containment will compare favorably to fuels reduction as long as the containment failure rate is less than 32%. However, we found that containment should only reduce the frequency of water quality impairment at the focal diversion by 33.5% if fires are followed by median rainfall and by 13.0% if fires are followed by extreme (100-year return interval) rainfall. This suggests that avoided area burned and sediment load do not translate directly into reduced incidents of water quality impairment. Much of the unmitigated risk under median rainfall conditions was concentrated in a few PODs, so there is potential to improve the effectiveness of the containment network by further compartmentalizing these areas of the watershed. The cost-effectiveness of improved fire containment depends on the actions taken to implement it. Most effort is currently focused on low-cost planning to identify candidate control features, aggregate them into PODs, and develop response strategies (Thompson et al. 2016). Fuels reduction along the POD boundaries to improving firefighter safety and probability of success would carry a higher price tag but the cost should still be far lower than the area-wide

fuels reduction evaluated in Chapter 2 because treatment would be concentrated in a smaller area along roads. Furthermore, our transmission risk analysis in Chapter 4 suggests that control feature hardening could be prioritized in a few high-risk areas of the network. Improved fire containment models are needed to rigorously evaluate the cost effectiveness of these actions.

The primary focus of this dissertation was evaluating the mitigation effectiveness of land and fire management solutions, but our results from Chapter 3 validate that raw water supply reliability could substantially improve by adding or enhancing source water redundancies as advocated for by other researchers (Sham et al. 2013; Murphy et al. 2015; Martin 2016). Source redundancy is attractive for its ability to mitigate contamination impacts from wildfire and other disturbances and for providing additional drought protection, but it likely carries a steep price tag given that the most traded water rights in Northern Colorado are selling at close to 30000 USD per acre-foot (Runyon 2018). Although it may be costly and impractical for every community to acquire alternative sources, there could be opportunity for a regional water sharing agreement similar to that explored to mitigate drought impacts in North Carolina to make use of neighboring communities' excess water supplies in time of need (Zeff et al. 2016). There may also be potential for other low or moderate cost engineering solutions such as such as constructing sediment basins to protect vulnerable conveyance infrastructure (Martin 2016) or adding raw or treated water storage to weather the often brief periods of degraded water quality following storms (Oropeza and Heath 2013; Murphy et al. 2015). Source water protection plans in Colorado have started to consider engineering solutions alongside traditional watershed management approaches (RESPEC 2019). It will be interesting to see how different communities decide to invest in pre-fire mitigation and how it allocated among "green" and "grey" infrastructure solutions.

6.4 MANAGEMENT IMPLICATIONS

The discrepancy we found between sediment cost and water quality impairment risk models highlights the need for watershed and water managers to explicitly discuss water supply vulnerabilities and select appropriate tools to assess risk. Combining a solid baseline understanding of risk with clear water supply reliability goals will help communities evaluate if pre-fire mitigation is needed and what combination of actions should be part of their mitigation strategy. Of the mitigation strategies we examined, source water redundancy offered the greatest benefit, but it may not be practical for every community to develop a fully substitutable and high-reliability alternative water supply. Landscape-scale fuels reduction and improved fire containment are expected to lower wildfire risks between 13.0-55.3% depending on impact metric considered. It is likely that the residual risk after one or both of these pre-fire mitigation approaches is still high enough that some fires will require significant response and recovery actions to safeguard drinking water such as temporarily shutting down intakes, emergency rehabilitation, monitoring, maintenance, changes to treatment processes, and/or investments in new infrastructure (Martin 2016). To better prepare communities, source water protection planning should consider both watershed and infrastructure solutions at pre-fire, response, and recovery time scales.

Many of the results presented in this dissertation are highly context-dependent and may not translate well to different watersheds and water systems. Still, several general principles emerged from our research. A common theme is that wildfire-water supply risks are not uniform across large watersheds, so efforts should be made to characterize the spatial distribution of risk and exploit this information to prioritize mitigation. A simple checklist for prioritizing fuel

treatment is to aim for locations with high probability of burning at high severity, high erosion potential, and high connectivity to water supplies. Improved containment efforts should be prioritized in areas with high ignition density and potential for fires to spread into erosion prone terrain with high connectivity to water supplies. In our assessment of impairment risk, wildfire exposure was a key determinant of risk. Whenever possible, water supply exposure should be minimized with off-network storage and alternative sources should be geographically dispersed to avoid simultaneous exposure. Water quality impairment is a threshold dependent process, so accurate assessment of risk and mitigation effectiveness needs to consider not only what contaminant loads are avoided but also whether the residual loads are problematic. Fuels reduction or containment actions that only marginally reduce contaminant loads are unlikely to change the water quality outcomes of large fires, so mitigation should be designed explicitly to limit fire size and/or severity below critical thresholds for impairment for a given watershed and water supply.

REFERENCES FOR CHAPTER 6

Addington RN, Tavernia BG, Caggiano MD, Thompson MP, Lawhon JD, Sanderson JS (2020) Identifying opportunities for the use of broadcast prescribed fire on Colorado's Front Range. *Forest Ecology and Management* **458**, 117655. doi:10.1016/j.foreco.2019.117655

Arapaho and Roosevelt National Forests and Pawnee National Grassland (ARP) (2019) Northern Front Range Collaborative Watershed Resilience Project. USDA Joint Chiefs' Award FY2019 Accomplishment Report. Available from www.fs.usda.gov/detail/arp/home/?cid=FSEPRD640139 4 p. (Fort Collins, CO, USA)

Buckley M, Beck N, Bowden P, Miller ME, Hill B, Luce C, Elliot WJ, Enstice N, Podolak K, Winford E, Smith SL, Bokach M, Reichert M, Edelson D, Gaither J (2014) Mokelumne watershed avoided cost analysis: why Sierra fuel treatments make economic sense. A report prepared for the Sierra Nevada Conservancy, The Nature Conservancy, and USDA Forest Service. Sierra Nevada Conservancy. (Auburn, CA, USA)

Cattau ME, Wessman C, Mahood A, Balch JK (2020) Anthropogenic and lightning-started fires are becoming larger and more frequent over a longer season length in the U.S.A. *Global Ecology and Biogeography* **29**, 668-681. doi:10.1111/geb.13058

Elliot WJ, Miller ME, Enstice N (2016) Targeting forest management through fire and erosion modelling. *International Journal of Wildland Fire* **25**, 876-887. doi:10.1071/WF15007

Graham RT (2003) Hayman Fire case study. USDA Forest Service, Rocky Mountain Research Station, General Technical Report RMRS-GTR-114. (Ogden, UT, USA)

Haimes YY (2012) Systems-based guiding principles for risk modeling, planning, assessment, management, and communication. *Risk Analysis* **32(9)**, 1451-1467. doi:10.1111/j.1539-6924.2012.01809.x

Jones KW, Cannon JB, Saavedra FA, Kampf SK, Addington RN, Cheng AS, MacDonald LH, Wilson C, Wolk B (2017) Return on investment from fuel treatments to reduce severe wildfire and erosion in a watershed investment program in Colorado. *Journal of Environmental Management* **198**, 66-77. doi:10.1016/j.jenvman.2017.05.023

Runyon L (2018) Price of key Northern Colorado Water Supply reaches new peak. KUNC radio story. May 29, 2018. Available from https://www.kunc.org/post/price-key-northern-colorado-water-supply-reaches-new-peak#stream/0

Litschert SE, Brown TC, Theobald DM (2012) Historic and future extent of wildfires in the Southern Rockies Ecoregion, USA. *Forest Ecology and Management* **269**, 124-133. doi:10.1016/j.foreco.2011.12.024

Martin DA (2016) At the nexus of fire, water and society. Philosophical Transactions of the Royal Society of London. Series B, *Biological Sciences* **371**, 20150172. doi:10.1098/rstb.2015.0172

Moody JA, Martin DA (2001) Initial hydrologic and geomorphic response following a wildfire in the Colorado Front Range. *Earth Surface Processes and Landforms* **26**, 1049-1070. doi:10.1002/esp.253

Murphy SF, Writer JH, McCleskey RB, Martin DA (2015) The role of precipitation type, intensity, and spatial distribution in source water quality after wildfire. *Environmental Research Letters* **10**, 084007. doi:10.1088/1748-9326/10/8/084007

O'Connor CD, Thompson MP, Rodríquez y Silva F (2016) Getting ahead of the wildfire problem: quantifying and mapping management challenges and opportunities. *Geosciences* **6(3)**, 35. doi:10.3390/geosciences6030035

O'Connor CD, Calkin DE, Thompson MP. 2017. An empirical machine learning method for predicting potential fire control locations for pre-fire planning and operational fire management. *International Journal of Wildland Fire* **26**, 587-597. doi:10.1071/WF16135

Omi PN (1979) Planning future fuelbreak strategies using mathematical modeling techniques. *Environmental Management* **3(1)**, 73-80. doi:10.1007/BF01867070

Oropeza J, Heath J (2013) Effects of the 2012 Hewlett and High Park Wildfires on water quality of the Poudre River and Seaman Reservoir. City of Fort Collins Utilities Report. (Fort Collins, CO, USA)

Ozment S, Gartner T, Huber-Stearns H, Difrancesco K, Lichten N, Tognetti S (2016) Protecting drinking water at the source: lessons learned from watershed investment programs in the United States. World Resources Institute Report. (Washington, DC, USA)

Quantified Ventures (2019) The SW Colorado Wildfire Mitigation Environmental Impact Fund (EIF): an outcomes-based financing approach to scale forest health treatments in Southwest Colorado. Available from https://static1.squarespace.com/static/5d5b210885b4ce0001663c25/t/5d94e93fe6a11c31748bb183/1570040136503/SW+Colorado+Wildfire+Mitigation+EIF+Feasibility+Assessment.pdf

RESPEC (2019) Fish Creek critical community wildfire watershed protection plan (CWP)^2. Report prepared for the City of Steamboat Springs and Mount Werner Water & Sanitation District. Available from http://co-steamboatsprings.civicplus.com/DocumentCenter/View/20031/FishCreek_CWP2 92 p. (Steamboat Springs, CO, USA)

Sham CH, Tuccillo ME, Rooke J (2013) Effects of wildfire on drinking water utilities and best practices for wildfire risk reduction and mitigation. Water Research Foundation Report 4482. 119 p. Available from www.waterrf.org

Sherriff RL, Platt RV, Veblen TT, Schoennagel TL, Gartner MH (2014) Historical, observed, and modeled wildfire severity in montane forests of the Colorado Front Range. *PLoS One* **9**, e106971. doi:10.1371/journal.pone.0106971

Short KC, Finney MA, Scott JH, Gilbertson-Day JW, Grenfell IC (2016) Spatial dataset of probabilistic wildfire risk components for the conterminous United States. USDA Forest Service Research Data Archive. (Fort Collins, CO, USA) doi:10.2737/RDS-2016-0034. (Fort Collins, CO)

Singh VP, Jain SK, Tyagi A (2007) Risk and reliability analysis: a handbook for civil and environmental engineers. American Society of Civil Engineers Press. 785 p. (Reston, VA, USA) doi:10.1061/9780784408919

Spracklen DV, Mickley LJ, Logan JA, Hudman RC, Yevich R, Flannigan MD, Westerling AL (2009) Impacts of climate change from 2000 to 2050 on wildfire activity and carbonaceous aerosol concentrations in the western United States. *Journal of Geophysical Research* **114**, D20301. doi:10.1029/2008JD010966.

Stephens SL, Moghaddas JJ (2005) Experimental fuel treatment impacts on forest structure, potential fire behavior, and predicted tree mortality in a California mixed- conifer forest. *Forest Ecology and Management* **215**, 21-36. doi:10.1016/j.foreco.2005.03.070

Talberth J, Mulligan J, Bird B, Gartner T (2013) A preliminary green–-gray analysis for the Cache la Poudre and Big Thompson watersheds of Colorado's Front Range. Center for Sustainable Economy and World Resource Institute Report. 21 p.

Thompson MP, Bowden P, Brough A, Scott JH, Gilbertson-Day J, Taylor A, Anderson J, Haas JR (2016) Application of wildfire risk assessment results to wildfire response planning in the Southern Sierra Nevada, California, USA. *Forests* **7(3)**, 64. doi:10.3390/f7030064

USDA Forest Service (2020) Hazardous fuel treatment polygons. Available from https://data.fs.usda.gov/geodata/edw/datasets.php

Writer JH, Hohner A, Oropeza J, Schmidt A, Cawley KM, Rosario-Ortiz FL (2014) Water treatment implications after the High Park Wildfire, Colorado. *Journal of the American Water Works Association* **106(4)**, 189-199. doi:10.5942/jawwa.2014.106.0055

Zeff HB, Herman JD, Reed PM, Characklis GW (2016) Cooperative drought adaptation: integrating infrastructure development, conservation, and water transfers into adaptive policy pathways. *Water Resources Research* **52**, 7327-7346. doi:10.1002/2016WR018771